Lipid vesicles in pulsed electric fields

Fundamental principles of the membrane response and its biomedical applications

Perrier, Dayinta L.; Rems, Lea; Boukany, Pouyan E.

DOI
10.1016/j.cis.2017.04.016

Publication date
2017

Document Version
Accepted author manuscript

Published in
Advances in Colloid and Interface Science

Lipid vesicles in pulsed electric fields: fundamental principles of the membrane response and its biomedical applications

Dayinta L. Perrier, Lea Rems, and Pouyan E. Boukany*
Department of Chemical Engineering, Delft University of Technology, Delft, 2629HZ, The Netherlands

*) Author to whom correspondence should be addressed. Electronic mail: P.E.Boukany@tudelft.nl

Abstract

The present review focuses on the effects of pulsed electric fields on lipid vesicles ranging from giant unilamellar vesicles (GUVs) to small unilamellar vesicles (SUVs), from both fundamental and applicative perspectives. Lipid vesicles are the most popular model membrane systems for studying biophysical and biological processes in living cells. Furthermore, as vesicles are made from biocompatible and biodegradable materials, they provide a strategy to create safe and functionalized drug delivery systems in health-care applications. Exposure of lipid vesicles to pulsed electric fields is a common physical method to transiently increase the permeability of the lipid membrane. This method, termed electroporation, has shown many advantages for delivering exogenous molecules including drugs and genetic material into vesicles and living cells. In addition, electroporation can be applied to induce fusion between vesicles and/or cells. First, we discuss in detail how research on cell-size GUVs as model cell systems has provided novel insight into the basic mechanisms of cell electroporation and associated phenomena. Afterwards, we continue with a thorough overview how electroporation and electrofusion have been used as versatile methods to manipulate vesicles of all sizes in different biomedical applications. We conclude by summarizing the open questions in the field of electroporation and possible future directions for vesicles in the biomedical field.

Keywords

lipid vesicle, electroporation, electrofusion, artificial cell, microreactor, drug delivery vehicle

Abbreviations

AC, alternating current; CARS, Coherent Anti-Stokes Raman Scattering; DC, direct current; DIC, differential interference contrast; DOPC, dioleoyl-phosphatidylcholine; DOPG, dioleoyl-phospatidylglycerol; DPhPC, diphytanoyl-phosphatidylcholine; DPPC, dipalmitoyl-phosphatidylcholine; EDTA, ethylenediaminetetraacetic acid disodium salt dehydrate; Egg PC, L-α-phosphatidylcholine from egg yolk; EV, extracellular vesicle; GUV, giant unilamellar vesicle; LUV, large unilamellar vesicle; MD, molecular dynamics; MLV, multilamellar vesicle; MNP, magnetic nanoparticle; PDMS, polydimethylsiloxane; PEG, polyethylene glycol; PC, phosphatidylcholine; PE, phosphatidylethanolamine; PG, phospatidylglycerol; POPC, palmitoyl-oleoyl-phosphatidylcholine; POPE, palmitoyl-oleoyl-phosphatidylethanolamine; SUV, small unilamellar vesicle.

Contents

1. Introduction

Biological cells are soft microscopic entities corresponding to a class of active colloidal systems. These living systems exhibit rich mechanical responses in the presence of external forces as a result of far-from-equilibrium interactions between the cells and their surrounding environment. Many of the paramount functions of living cells are governed by the cell membrane, which encloses the cell and separates its "inside" from the "outside". Traditionally, biologists put tremendous efforts to explain how the cell membrane contributes to the cellular shape, trafficking, motility, and communication by employing top-down approaches [1-3]. In contrast to this classical strategy, biophysicists have succeeded in developing minimal model membrane systems that decipher how cellular membranes behave and interact with intra/extracellular components ranging from nanoparticles, DNA, to proteins such as cytoskeleton [4-7]. In fact, much of our current understanding about cell biology has emerged from such simple model studies [3, 8].

Understanding of the cellular phenomena using fundamental (colloidal) laws based on soft matter physics is still far away. To overcome this issue, lipid vesicles are used as an idealized system to study fundamental biophysical and biochemical cell processes [9]. Lipid vesicles can be prepared in a variety of sizes ranging from tens of nanometres to tens of micrometres, which corresponds to the smallest membrane-enclosed intracellular organelles and to dimensions of almost any type of prokaryotic and eukaryotic cells [10-12]. Based on their size and lamellarity, the vesicles are categorized into four different groups: small unilamellar vesicles (SUVs) with diameters of ~10–100 nm, large unilamellar vesicles (LUVs) with diameters of ~100–1000 nm, giant unilamellar vesicles (GUVs) with diameters >1 µm, and multilamellar vesicles (MLVs) containing multiple bilayers [13]. Various types and mixtures of lipids can be used to prepare the vesicles [14, 15]. Moreover, several techniques are being developed for embedding proteins into the membrane, as well as for encapsulating a wide variety of materials inside the vesicle's aqueous core [16-22]. The versatile character of vesicles in terms of their size, surface functionality, and vesicle interior makes them attractive as simple cell models and ultrasmall biomimetic reactors [23-28]. Furthermore, as lipid vesicles are made from biocompatible and biodegradable materials, they provide a strategy to create safe and functionalized drug delivery systems in health-care applications [29, 30].

Cells and lipid vesicles are also characterized by heterogeneous electrical properties, for which they can be manipulated in electric field. By subjecting cells or vesicles to DC pulses, an electric potential difference (i.e. voltage) builds across the membrane, causing various phenomena. At weak pulses these membrane structures can deform under the influence of the induced electric stresses. At strong pulses, transient pores form in the lipid bilayer, which dramatically increases the membrane permeability. This phenomenon, called electroporation or electropermeabilisation, is nowadays becoming a platform technology for enhancing the transmembrane transport of drugs, genetic material, and other molecules in the areas of medicine, food processing, and in some environmental applications [31-33]. Additionally, electroporation of two cells or vesicles, which are in close proximity, can lead to fusion of the two bodies, allowing one to create hybrid cell-cell, vesicle-vesicle, or cell-vesicle fusion products [34, 35].

In this review, we discuss the responses of lipid vesicles in pulsed electric fields and their biomedical applications. In the first part of the review, we describe how vesicles respond to electric pulses based on theoretical and experimental work on GUVs, concluding with a section about the possibilities to improve the GUV as a model of cell electroporation. The first part complements the previous reviews

[36-39] and covers the recent insights. In the second part of the review, we provide a thorough overview on the use of electric pulses to manipulate GUVs, LUVs, and SUVs in applications related to fundamental biomedical research and clinical medicine.

2. Vesicles as simple models of cells in pulsed electric fields

2.1 The basic principles of membranes in electric fields

2.1.1 Induced transmembrane voltage

The amphiphilic structure of the lipid bilayer makes lipid membranes practically impermeable to ions. In addition, the hydrophobic core of the lipid bilayer is weakly polarizable in an external electric field. Thus, the lipid membrane can be viewed as a thin dielectric layer characterized by practically negligible electrical conductivity and low dielectric permittivity as compared to the surrounding aqueous solutions [40]. The theoretical models, considering the lipid membrane as a thin dielectric layer, have provided an explanation for different phenomena observed in low AC fields including electrorotation, electrodeformation, and dielectrophoretic movement of vesicles/cells [41-44]. Additionally, the models have provided insights into electroporation and electrofusion, both observed when exposing cells or vesicles to strong DC electric pulses [42].

To understand how electric pulses act on a lipid vesicle, first consider an isolated, spherical vesicle exposed to a homogeneous DC electric field (see Fig. 1). The electric field electrophoretically drives the charged particles (ions) in the internal and external solutions, for which the membrane becomes charged similarly as a capacitor. The build-up of charges along the membrane leads to an induced transmembrane voltage (U_m). After a step increase in the electric field intensity E, U_m increases with time according to the Schwan's equation [45]:

$$U_m = 1.5\, ER\cos\theta\left(1 - \mathrm{e}^{-t/\tau_{chg}}\right) \tag{1}$$

Note that U_m is proportional to the vesicle radius R and varies with the angle position θ on the membrane, as shown in Fig. 1, such that it reaches the highest absolute value at the areas facing the electrodes. The characteristic charging time τ_{chg} of the membrane depends on the vesicle radius, membrane capacitance ($C_m \approx$ 0.7 μF/cm [43, 46]), and the conductivities of the internal (λ_i) and external (λ_e) solutions:

$$\tau_{chg} = RC_m\frac{2\lambda_e + \lambda_i}{2\lambda_e\lambda_i} \tag{2}$$

[Here Fig. 1]

If the duration of the exposure to the electric field (*i.e.* the duration of the electric pulse) is longer than the charging time, $t_{pulse} \gg \tau_{chg}$, U_m reaches a steady state, $U_m = 1.5\, ER\cos\theta$. Otherwise, the membrane remains in the charging phase throughout the duration of the electric pulse. In typical experiments with GUVs, where the aqueous solutions consist of dissolved sucrose and glucose ($\lambda_i \approx \lambda_e \approx$ 5 μS/cm [47]), the charging time for a vesicle with radius of 20 μm is about 420 μs. When such GUVs are exposed to electric pulses with duration on the order of 100 μs, the membrane remains in

the charging phase. Upon addition of ions into aqueous solutions, the charging time considerably decreases.

Note that equations (1–2) are valid only for a spherical, nondeformed vesicle, and until the membrane can be considered as electrically nonconductive, i.e., before the membrane becomes electroporated [48, 49]. Furthermore, the equations are valid as long as the dielectric permittivities of the external (ε_e) and internal (ε_i) aqueous solution can be neglected, i.e., for pulse duration considerably longer than the Maxwell-Wagner polarization time $\tau_{MW} = (2\varepsilon_e + \varepsilon_i)/(2\lambda_e + \lambda_i)$ [50]. To determine U_m on deformed or electroporated vesicles, often numerical calculations need to be employed.

2.1.2 Theoretical background on electroporation

Natural pores can be nucleated spontaneously in the lipid membrane due to thermal fluctuations of the lipid molecules. But as the free energy for pore nucleation is much higher than the thermal energy kT (where k is the Boltzmann's constant and T is the absolute temperature), spontaneous occurrence of pores is a very rare event. This free energy can be reduced either by applying lateral (stretching) tension on the membrane or by exposing the membrane to an electric field [51, 52]. Since the bilayer behaves as a dielectric shell, the electric field induces electric stresses on the membrane, which act similarly to a lateral tension, as proposed in different models based on continuum theories [53-55]. If the decrease in the free energy for pore nucleation is governed by electric stresses, the rate of pore nucleation can be written as [56]

$$\nu = A\exp\left(-\frac{\delta_c}{kT} + \frac{BU_m^2}{kT}\right) \tag{3}$$

where δ_c is the nucleation free energy in the absence of U_m, A is a pre-exponential factor and B is a proportionality constant. The free energy δ_c has been estimated to be ~45 kT based on measurements on planar lipid bilayers, however it is expected to depend on the composition of the lipid bilayer [57]. After pore nucleation, the Maxwell stress expands the pores further [58]. Once the electric field is removed, the edge tension (the energy of the pore edge per unit length of the pore circumference) tends to close the pores [59, 60].

During the last decade, molecular dynamics (MD) simulations have provided an additional insight into the molecular mechanisms of pore formation [61]. When the bilayer is exposed to an electric field, the pore nucleation is initiated by formation of a water column spanning the bilayer, which (in typical zwitterionic phospholipid bilayer) is followed by migration of lipid head groups into the wall of the pore [62]. (An example of the pore nucleation sequence taken from MD simulations is shown in Fig. 6.) The average lag time before the onset of pore nucleation is a stochastic variable, but on average the nucleation rate increases exponentially with an increase in U_m [63, 64]. Although in a broader sense, the insights from MD agree with earlier theoretical predictions [65], MD suggest that the pore nucleation is predominantly mediated by the electric-field-driven reorientation of the water dipoles at the water-bilayer interface, and not by tensile electric stresses [64, 66].

Both continuum models and MD simulations indicate that U_m influences the rate of pore nucleation. Hence, it is impossible to theoretically define an absolute critical U_m above which electroporation of the lipid membrane takes place. However, as the nucleation rate increases exponentially with U_m,

electroporation experimentally appears as a threshold-like phenomenon [67]. Thus, it is possible to define a relative threshold as the critical value $U_{m,crit}$ above which electroporation can be detected in a given amount of time and under the given experimental conditions. Additionally, since electroporation is generally detected through a dramatic increase in the membrane permeability and associated molecular transport across the membrane, it is important to note that the pulse parameters influence the growth of the pores, and thus directly control the transmembrane molecular flux. As such, the determined $U_{m,crit}$ depends on the size of the molecular probe and the sensitivity of the detection system [68]. A well-known technique for detecting $U_{m,crit}$ of GUVs is through determining the contrast loss from sucrose-filled GUVs in a glucose environment. Using sucrose in the interior and glucose in the exterior of the GUV leads to a contrast difference when using phase-contrast optical microscopy. However, the presence of the pores allows the sugar molecules to exchange across the membrane, which diminishes the contrast difference after electroporation. Using of this technique $U_{m,crit}$ of fluid phase GUVs is found to be around 1 V [60]. Another method to detect $U_{m,crit}$, recently established by Mauroy et al., is based on detecting the transmembrane transport of manganese ions [68]. With this novel technique they have been able to measure a significantly lower $U_{m,crit}$ of about 6 mV for the same type of GUVs. This extremely low $U_{m,crit}$ is assigned to the small size of the manganese ions, which thus require only small defects in order to cross the bilayer. Moreover, $U_{m,crit}$ of ~650 mV is found for similar type of GUVs by tracking Ca^{2+} influx [69]. It is further worth mentioning that $U_{m,crit}$ is generally determined based on calculating the maximum absolute U_m reached at $\theta = 0$ and π from equation (1). This equation is valid only for a spherical vesicle and does not take into account the shape deformations, which are induced by electric stresses (see Section 2.2.1).

Besides these parameters, that can unintentionally change the measured $U_{m,crit}$, it has also shown that $U_{m,crit}$ can be tuned intentionally. Since both mechanical tension and electric stresses promote pore formation, $U_{m,crit}$ can be reduced by mechanically increasing the lateral tension of the membrane, e.g. by aspirating part of the GUV into a micropipette [54]. For this reason, GUVs which have some initial tension, i.e., GUVs which do not exhibit any visible thermal undulations, electroporate at lower $U_{m,crit}$ [47]. In addition, different membrane compositions influence $U_{m,crit}$. MD simulations showed that $U_{m,crit}$ is to some extent correlated with the thickness of the bilayer [70], though in general, it greatly depends on the detailed architecture of both the lipid head groups and the lipid tails, as well as the lipid phase and the temperature [71-73]. The parameter, on which $U_{m,crit}$ appears to depend predominantly, is the local pressure profile in both the head group and the tail group region, which could affect the mobility of water molecules inside the bilayer [72, 74]. Furthermore, the strong influence of the lipid architecture was also found in MD calculations of the pore nucleation free energy in the absence of the electric field (δ_c in equation (3)) [75, 76]. This shows that the ability of a bilayer to resist poration is an intrinsic property of its constituting lipids. The effect of the lipid composition on the electroporation of GUVs is discussed in greater detail in Section 2.2.3.

2.2 Responses of GUVs in pulsed electric fields

Due to the micrometre size of GUVs, their responses to electric pulses can be monitored and investigated at the microscopic level. In particular, the development of high-speed imaging has dramatically increased the knowledge on the dynamic behaviour of GUVs during and after the

exposure to electric pulses. The basic responses have been determined on GUVs made from zwitterionic phospholipids in the fluid phase such as Egg PC [47, 77, 78] and DOPC [69, 79, 80]. These experiments revealed details on the electrodeformation of the GUVs (Section 2.2.1), which is in high electric fields accompanied by the formation of macropores and lipid loss (associated with electroporation) (Section 2.2.2). Experiments on GUVs made from different lipids and lipid mixtures provided further insights into the effect of the lipid composition on electroporation and the stability of GUVs in an electric field (Section 2.2.3). These observations are outlined below. For completeness we review recent reports together with older data. More comprehensive reviews on this topic (conducted until 2012) can be found in [36-38].

2.2.1 Electrodeformation

The exposure of a GUV to an electric field induces an electrical tension on the membrane, given by the Maxwell stress tensor, which can cause deformation and stretching of the GUV. Depending on the intensity and the duration of the electric pulse, as well as the conductivity of the inner and outer solutions, the shape and the degree of GUV deformation can be significantly varied [36]. Deformation of the GUV is accompanied by an increase in the projected membrane area, which can be categorized into two regimes. For small deformations (low tension), the projected area increases as the weak electric stresses flatten the thermal undulations of the membrane. This regime is often referred to as the entropic regime and is governed by the bending rigidity of the membrane. For stronger deformations (high tension), where all membrane undulations are flattened, the electric stresses lead to elastic stretching of membrane, increasing the area-per-lipid in the bilayer [81, 82]. This regime is governed by the elastic stretching modulus of the membrane. The first studies on GUV electrodeformation were conducted in AC electric fields, which induced ellipsoidal deformations, as predicted by theory [83-88] (see Dimova et al. [36, 37] for reviews). Depending on the frequency of the applied AC field and the ratio between the conductivity of the internal and the external aqueous solutions ($\chi = \lambda_i/\lambda_e$), the GUV can deform into either a prolate or an oblate ellipsoid, with the long axis aligned either parallel or perpendicular to the direction of the electric field, respectively. By measuring electrodeformations of GUVs in AC field, it is possible to extract the information on the mechanical properties of the membrane, such as the bending rigidity [89], and the electrical properties, such as capacitance [46].

Unlike in continuous AC fields, the electrodeformation induced by DC pulses are transient and the GUVs relax back into their spherical shape rapidly after the end of the pulse; therefore, these deformations are experimentally difficult to capture with conventional cameras having a temporal resolution in the millisecond range. The first experimental observations of GUV electrodeformation induced by a 1.2 ms-long pulse were reported by Kinosita et al. [90]. They imaged fluorescently labelled GUVs using a pulsed-laser fluorescence imaging system with a temporal resolution of 100 µs. They observed that, similarly as in AC field, the shape of the deformed GUV depends on the ratio χ; if the internal conductivity is higher than the external conductivity ($\chi > 1$), the GUV deforms into a prolate shape, whereas for $\chi < 1$ the GUV deforms into an oblate shape. These observations were qualitatively corroborated by theoretical work of Hyuga et al. [91, 92]. Later, Riske and Dimova [47, 77] studied the electrodeformation of GUVs exposed to 50–300 µs pulses (where $t_{pulse} < \tau_{chg}$) with a time resolution down to 33 µs, using phase-contrast microscopy and a high-speed digital camera. They observed a similar dependence of the GUV shape on χ, but also highlighted the influence of ions in the external solution. In the absence of ions, the GUVs were deformed into prolate ellipsoids

for $\chi > 1$ [47]. Upon addition of ions, the GUVs were transiently deformed into peculiar cylindrical shapes, again depending on the ratio χ (Fig. 2) [77]. For $\chi > 1$ tube-like shapes were observed analogous to prolate ellipsoids, for $\chi \approx 1$ square-like deformations were reported, and for $\chi < 1$ disk-like deformations were observed comparable to oblate shapes. Such "squaring" of the GUV shape was also noted in the presence of gold nanoparticles [36]. Moreover, Riske and Dimova [47, 77] measured the degree of deformation by determining the aspect ratio a/b of the deformed GUVs (Fig. 2c). They demonstrated that the degree of deformation increases with the increasing electric field strength and/or the pulse duration, while it also depends on the initial tension of the GUV. Sadik et al. [78] further studied the prolate deformations by systematically varying χ (between 1.92 and 53.0). At constant χ the aspect ratio scaled quadratically with the electric field strength, confirming the dominant role of the electric stresses in driving the deformations. With increasing χ at a constant electric field strength, the aspect ratio asymptotically approached a maximum value. Note that in the experiments described above, the electrodeformations were often accompanied by macroporation of the GUV membrane (see Section 2.2.2).

[Here Fig. 2]

Analytical modelling results based on balancing the stresses acting on the GUV membrane (electric, hydrodynamic, bending, and tension) demonstrated that the shape of deformation during an electric pulse relates to the different charging kinetics on the external and internal side of the membrane (see Fig. 3) [93]. If $\chi > 1$, the charges accumulate faster on the internal side and the resulting electric stresses tend to elongate the GUV along the direction of the electric field inducing a prolate deformation (Fig. 3a). On the contrary, if $\chi < 1$, a transient oblate deformation can occur during the charging phase of the membrane, since the charges accumulate faster on the external side, and the electric stresses tend to compress the GUV in the direction of the electric field (Fig. 3b). Once the membrane is fully charged, the accumulated charges on the internal and external sides are balanced, the electric field is expelled from the interior, and the GUV is deformed into a prolate ellipsoid (Fig. 3c). Hence, under the condition $\chi > 1$, the shape deformation can only be prolate, as corroborated by experiments [47, 78]. Under the condition $\chi < 1$, an oblate-to-prolate shape transition is predicted [93]. However, the oblate-to-prolate transition is difficult to observe experimentally, as explained by Salipante and Vlahovska [79]. On one hand, the GUV can attain an oblate shape only during the charging phase of the membrane, $t < \tau_{chg}$. On the other hand, significant deformation can only occur for times longer than the characteristic time in which the electric stresses can deform the GUV during the pulse [93]

$$\tau_{el} = \frac{\mu_e\left(1 + \mu_i/\mu_e\right)}{\varepsilon_0 \varepsilon_e E^2} \tag{4}$$

where μ_e and μ_i are the viscosities of the external and internal solution, respectively. In low electric field, where $\tau_{el} > \tau_{chg}$, the deformation occurs after the membrane is fully charged and only a prolate shape can be observed. In a high electric field, where $\tau_{el} < \tau_{chg}$, the deformation occurs while the membrane is still charging. However, in typical experimental conditions, such an electric field strength leads to electroporation and the associated increase in the membrane conductivity. If the membrane becomes conductive, theory predicts that the GUV can remain oblate when $\chi < 1$ [91, 92, 94]. To demonstrate experimentally the oblate-to-prolate transition, Salipante and Vlahovska [79] used a double-pulse protocol consisting of a strong 20 µs pulse followed by a longer 50 ms pulse

with a lower intensity. The first pulse was strong enough to induce an oblate deformation but short enough to avoid electroporation, whereas the second pulse allowed full charging of the membrane leading to a prolate deformation. More complex numerical models based on electrohydrodynamic principles further corroborated the predicted oblate-to-prolate transition, and in addition revealed more complicated shapes of GUVs, including the squared shapes [94-97], resembling those observed by Riske and Dimova [77]. In summary, electrodeformation of a GUV during the pulse is dynamic and depends on the pulse duration, strength, presence of ions in the external solution, conductivity ratio χ, and membrane electroporation. As it is challenging to model the highly nonlinear dependence of pore nucleation and pore growth on U_m and associated tensile stresses, as well as the ionic and fluid exchanges across the pores, current models of GUV electrodeformation are either limited to treatment of a nonconductive membrane and are strictly valid only before the onset of electroporation [93-97], or consider a simplified case of a completely conductive membrane and are based on semi-empirical treatment of the hydrodynamic forces [78, 91, 92].

[Here Fig. 3]

After the exposure of a GUV to an electric pulse, which leads to electrodeformation, the GUV relaxes back to the spherical shape (in the absence of electric field). Provided that the GUV has not been electroporated, the characteristic relaxation time depends on the stretching regime attained by the membrane during the pulse. Relaxation of an elastically stretched GUV proceeds with a characteristic time on the order of 100 μs [47], whereas relaxation of membrane undulations strongly depends on the initial (pre-pulse) tension of the GUV. Yu et al. [98] theoretically analysed relaxation of GUVs deformed in the second (entropic) regime and showed that such analysis can be applied to measure the bending rigidity and the initial membrane tension of GUVs.

2.2.2 Electroporation: macropores and lipid loss

When applying weak electric pulses, a GUV can be electrodeformed in the absence of detectable electroporation, as discussed above. By increasing the intensity and/or duration of the electric pulse, electrodeformation becomes accompanied by electroporation of the GUV membrane. Experiments on GUVs have shown two interesting phenomena associated with electroporation, which are not observed in living cells: the creation of micrometre-sized pores (macropores) and the expel of lipids from the GUV membrane [47, 69, 77, 80, 90]. Kinosita et al. [90] reported that formation of macropores was preceded by a measurable increase in the membrane conductivity, indicating the presence of optically-undetectable nanoscale pores. Thus they postulated that macropores could arise from growth or coalescence of smaller pores, or as a consequence of electrodeformation. In the following studies, the formation of macropores was linked to the increase in the membrane tension caused by the electric field [47, 60]. As inferred from the measurements on GUVs aspirated into a micropipette, when the membrane tension exceeds a critical value called the lysis tension, the bilayer ruptures due to unlimited growth of unstable pore(s) [99]. Unlike in the aspiration experiments where the tension imposed on the membrane is controlled by the micropipette, the tension induced by an electric field relaxes as the pores grow and the fluid leaks out from the GUV [60, 100]. Therefore, large macropores can form without disintegrating the membrane. The value of the lysis tension depends on the lipid composition and varies roughly between 3 and 10 mN/m for phospholipid fluid GUVs [54, 101], although it also depends on the time and rate at which the tension is imposed [99, 102, 103]. To compare the electric tension σ_{el} induced on the membrane at given U_m with the lysis tension σ_{lys} Needham and Hochmuth proposed a simple derivation [54]

$$\sigma_{el} = \frac{1\varepsilon_m}{2h_e}\left(\frac{h}{h_e}\right) U_m{}^2 \quad (5)$$

where ε_m and h_e represent the dielectric permittivity and the thickness of the hydrohobic lipid core, respectively, whereas h represents the total thickness of the membrane. By inserting typical values for fluid phospholipids ε_m = 2·10^{-11} F/m, h_e = 2.8 nm, and h = 3.9 nm, the lysis tension of 5 mN/m is reached at $U_m \approx$ 1 V [54]. This was corroborated by the experimental observation of macropores at $U_m \approx$ 1 V when exposing GUVs to an electric pulse with a duration in the order of 100 µs [47, 54].

Under the conditions which lead to prolate deformation of a GUV, macropores are generally formed near the poles of the GUV, where the highest U_m and largest electrical tension are predicted based on theory [47, 78, 95]. Compared with non-macroporated GUVs, macroporated GUVs attain a higher aspect ratio during the pulse and relax more slowly back to spherical shape after the pulse [47]. The post-pulse relaxation of the GUV shape is governed by the closure of macropores, which takes about 10 ms to few 100 ms, depending on the size of the macropores and the residual membrane tension [47, 60]. The velocity of pore closure is determined by the interplay between the edge tension of the pore and the leak-out of the internal fluid from the GUV [47, 59, 60]. The analysis of the closure kinetics of macropores thus provides a method for measuring the edge tension in GUVs with different lipid compositions [60]. Additionally, since the leak out of the internal fluid depends on the viscosity of this fluid, the pore closure can be slowed down by increasing the viscosity, e.g. by adding glycerol to water [100].

When cylindrical deformations occurred, Riske and Dimova observed macropores at the corners of the deformed membrane (as indicated in Fig. 2 with white arrows) [77]. McConnell et al. [94, 95, 104] attempted to theoretically understand this observation by numerically calculating the time-dependent evolution of the induced membrane tension (Fig. 4). The results showed that when the GUV deforms into a cylindrical shape, the highest positive (stretching) tension is induced at the corners of the deformed GUV (Fig. 4c), which is expected to promote formation and growth of pores in these regions. If the membrane does not porate at this point of time, the highest tension shifts to the poles of the GUV (Fig. 4d-e). Indeed, Portet and Dimova [60] used similar experimental conditions as in Fig. 2b, but they exposed the GUVs to longer 5 ms pulses with lower intensity and captured macropores at the poles of the GUVs towards the end of the pulse. Note that the tension shown in Fig. 4 is not equal to the one in equation (5), but was determined numerically by a more rigorous calculation of the electric and hydrodynamic stresses acting on the membrane. More specifically, the tension in Fig. 4 corresponds to the Lagrange multiplier that enforces incompressibility of the membrane area [94].

[Here Fig. 4]

Several reports further showed an asymmetric pattern of the pore distribution [60, 69, 80, 90]. Kinosita et al. [90] reported that macropores in asolectin (soybean phospholipid) GUVs formed preferentially on the side facing the positive electrode (anode). In contrast, Tekle et al. [69] observed that macropores preferentially formed on the side facing the negative electrode (cathode) in DOPC GUVs. Macropores were rarely found on the anodic hemisphere, but the results suggested that the anodic side is permeabilized by a greater number of smaller (optically undetectable) pores [69]. Preferential macroporation of the cathodic side was also observed by Portet et al. in DOPC and Egg PC vesicles [60, 80]. Furthermore, both Tekle et al. [69] and Portet et al. [60, 80] detected

macropores in combination with a reduced size of the GUVs after the pulse. The size reduction can be attributed to the expel of lipids in the form of small vesicles and/or tubules, as reported by Portet et al. [80] based on imaging of fluorescently-labelled GUVs (Fig. 5). In some cases, multiple pulses were applied to detect visible lipid ejection, and by increasing the number of pulses, the size of the GUVs progressively decreased [80]. Mauroy et al. [105] showed similar lipid ejection by use of CARS microscopy, confirming that lipid loss is not an artefact of membrane labelling. Moreover, they demonstrated that lipid loss is controlled by the pulse duration and can be detected at a significantly lower electric field when GUVs are exposed to 5 ms pulses compared to 100 µs pulses. Portet et al. [80] assumed that the amount of ejected lipids is proportional to the permeabilized membrane area, showing good agreement with the experimental results, whereas Sadik et al. [78] reported a correlation between the post-pulse reduction in the membrane area and the aspect ratio attained by GUVs during electrodeformation. However, the mechanisms responsible for the asymmetric distribution of pores and lipid ejection are not yet completely understood. It also remains unclear whether electroporation and lipid loss are either coincident or interrelated phenomena. For instance, tubule formation can also be observed in GUVs exposed to non-electroporating AC fields [106]. Theoretical works on the instability of a lipid membrane in an electric field suggested that a bilayer can undergo undulations with an increasing amplitude [107-111], which may eventually lead to tubulation and loss of lipids. When the membrane is separating fluids with an equal conductivity and permittivity, such a membrane instability could result from ionic currents in the electric double layer next to the membrane surface [108, 109]. When the membrane is separating fluids with asymmetric electrical properties, particularly different conductivities, such an instability could also be a consequence of the transient mismatch between the ionic accumulation at the two sides of the membrane [110, 111]. These instabilities were predicted both for a nonconducting and a conducting (electroporated) membrane.

[Here Fig. 5]

2.2.3 Influence of membrane composition on electroporation

One of the main advantages of using vesicles is that the membrane composition can be controlled and thus the mechanical properties can be tuned. So far, the lipids of all systems discussed in this review have been in the fluid phase (or liquid-disordered phase), where the lipids possess high mobility and chain disorder. Lowering the temperature below the transition temperature of a lipid, brings the lipid in the so-called gel phase (or solid-ordered phase), where the lipids are tightly packed and exhibit low mobility. The transition temperature varies with different types of lipids, whereby some lipids exist in the fluid and others in the gel phase at room temperature [112]. Therefore, a simple method to change the mechanical properties of the membrane is to select a lipid with a different phase or create a two-phase system with both liquid and gel domains. The addition of cholesterol to fluid phase lipids brings the lipids in an intermediate phase, the liquid-ordered phase. Cholesterol organizes the hydrophobic core of the membrane causing ordering of the lipids while maintaining the lateral mobility [113]. Mixing cholesterol in a binary mixture of lipids induces a two-phase liquid system of liquid-ordered, containing saturated lipids and cholesterol, and liquid-disordered domains, containing unsaturated lipids and possibly a low level of cholesterol. Below, we discuss the influence of altering the lipid composition of the membrane on the critical U_m at which electroporation is detected (i.e. $U_{m,crit}$). This influence has been studied both at the molecular level by the use of MD simulations, and at the microscopic level by the use of GUVs.

Both MD simulations and experiments on GUVs demonstrated that $U_{m,crit}$ in fluid phase lipids depends on the structure of the lipid tails as well as the head groups. MD simulations indicated that for lipids with a PC head group, $U_{m,crit}$ increases with the chain length of the lipid tails [70]. In contrast with simulations, Mauroy et al., studied GUVs from different PC lipids experimentally, showing no influence of the hydrophobic chain length on $U_{m,crit}$ [68]. Apart from the influence of the chain length, MD simulations also demonstrated a considerate effect of methyl branches in the lipid tails, as well as the type of linkage between the head group and the carbonyl region [73]. Polak et al. observed that $U_{m,crit}$ increases, respectively, in linear-chained DPPC lipids, methyl-branched DPhPC with ester linkages, and DPhPC with ether linkages, all in the fluid phase. Based on their analysis, they proposed that the presence of methyl branches could reduce the mobility of water molecules in the hydrophobic core and hence increase $U_{m,crit}$. Additionally, Polak et al. also studied $U_{m,crit}$ of archaeal lipids, which have the same tail structure as DPhPC-ether lipids, whereas the archaeal head groups are formed by large sugar moieties [72]. Compared with DPhPC-ether, archaeal lipids exhibit higher $U_{m,crit}$, associated with stronger interactions between the archaeal head groups. $U_{m,crit}$ was decreased when archaeal lipids were mixed with DPPC. Similarly, Gurtovenko and Lyulina showed higher $U_{m,crit}$ in a POPE lipid bilayer with respect to POPC [74]. Higher $U_{m,crit}$ has been attributed to the primary amines in the POPE head groups capable of intra and intermolecular hydrogen bonding, in contrast to the choline moieties in the POPC head groups. POPE lipids are thus packed more densely than the POPC lipids, which hinders the penetration of water molecules in the bilayer and slows down the reorientation of the lipid head groups into the pore, as shown in Fig. 6. Mixing these two lipids in an asymmetric bilayer (POPE in one and POPC in the other leaflet) results in $U_{m,crit}$ in between the $U_{m,crit}$ of pure POPC and POPE. Besides the physical properties of the lipids, also the effect of the membrane charge was studied. When the negatively charged GUVs consisting of PC and PG lipids (1:1 ratio) were exposed to an electric pulse, a bursting effect was observed, as reported by Riske et al., and shown in Fig. 7 [114]. Despite the lack of understanding of this bursting effect, they were able to prevent the bursting effect by the addition of EDTA. However, the mechanism of the stabilizing effect of EDTA remains unknown.

[Here Fig. 6]

[Here Fig. 7]

Several studies have further shown that $U_{m,crit}$ in gel phase GUVs is higher than in fluid phase GUVs. Knorr et al. used a classical method to determine $U_{m,crit}$ based on the contrast loss of the GUV [115]. $U_{m,crit}$ of gel phase DPPC GUVs was found to be at 9.8 ± 1.1 V, compared to the 1 V for the liquid phase POPC GUVs, which they attributed to a higher bending rigidity and thickness of the gel phase membrane. The observed pores appeared to be arrested (irreversible) and were often visualized as cracks (see Fig. 8). Additionally, they reported the deformation dynamics of the gel phase GUVs during the pulse below $U_{m,crit}$. The GUVs show only small deformations below the electroporation threshold, and show a so-called intra-pulse relaxation of their deformation already during the pulse. Moreover, the deformations of these gel phase GUVs were expressed as wrinkling of the membrane instead of the ellipsoidal deformations occurring in fluid phase lipids [115]. A more detailed study by Mauroy et al. on $U_{m,crit}$ of different GUVs has elucidated that the phase state, and not the membrane thickness, plays the decisive role in the increased $U_{m,crit}$ of gel phase GUVs with respect

to fluid phase GUVs [68]. The increased $U_{m,crit}$ of gel phase GUVs with respect to fluid phase GUVs is also supported by Liu et al., who determined $U_{m,crit}$ by detecting the release of 5(6)-Carboxyfluorescein (5(6)-CF) [116]. Additionally, when mixing fluid and gel phase lipids, Liu et al. reported a decrease in the membrane permeability with an increasing percentage of gel phase lipids [116]. Recently, Majhi et al. also reported an increase in $U_{m,crit}$ when going from liquid to gel phase lipids, based on results from MD simulations [71]. Additionally, they observed slower pore resealing dynamics for DPPC in the gel phase than in the fluid phase, which shows a correlation with the experimental studies of Knorr et al. [115].

[Here Fig. 8]

As cholesterol is added to the system, the lipids organise in the liquid-ordered phase [117]. The cholesterol organizes itself in the hydrophobic core of the bilayer, where it can condense the lipids and it can alter the mechanical properties of the membrane, such as the thickness, the bending stiffness and the fluidity [118]. However, the addition of cholesterol does not always lead to the same results. Depending on the concentration of the cholesterol and the architecture of the lipid, cholesterol can either decrease or raise the electroporation threshold [60]. Also, mechanical studies on bilayers have shown the non-universal and lipid-specific effect of cholesterol [89, 119, 120]. Recent studies of Mauroy et al. have shown that an increasing concentration of cholesterol on POPC leads to a higher $U_{m,crit}$, whereas this increased cholesterol shows no significant influence on $U_{m,crit}$ of Egg PC [68]. Similar results for Egg PC have been shown before by Portet and Dimova [60]. In addition, they reported that increasing cholesterol could decrease $U_{m,crit}$ for DOPC vesicles. Surprisingly, the experimental results on the effect of cholesterol on $U_{m,crit}$ of different lipid bilayers have not been fully supported by MD simulations. Simulations on the effect of cholesterol on $U_{m,crit}$ of POPC show similar results as found experimentally on GUVs [121]. Nevertheless, MD simulations of Fernandez et al. on DOPC showed an increase of $U_{m,crit}$ when adding cholesterol [122], which is in disagreement with the experimental results on GUVs [60]. Overall, the influence of cholesterol on $U_{m,crit}$ of a lipid bilayer is non-universal and strongly dependent on the architecture of the lipids.

By mixing two different lipids together with cholesterol, coexisting liquid-ordered and liquid-disordered phases can occur in the membrane. Van Uitert et al. studied this effect of cholesterol on $U_{m,crit}$ in planar bilayers made from binary lipid mixtures [117]. They observed that the effect of cholesterol on $U_{m,crit}$ is dependent on the cholesterol percentage. At low percentages, $U_{m,crit}$ decreased slightly with respect to $U_{m,crit}$ of the pure binary mixture without cholesterol. However, above a certain threshold percentage, $U_{m,crit}$ increased together with the increase in cholesterol. From the experimental results it is difficult to interpret the molecular mechanisms of this biphasic influence of cholesterol percentage on $U_{m,crit}$. With MD simulations on heterogeneous membranes, Reigada showed that the probability of pore formation is highest in the middle of the liquid disordered phase [123].

2.3 Electrofusion

Fusion of biological membranes is a ubiquitous phenomenon in nature, which for example occurs in exocytosis, fertilization, muscle fibre and bone development, tissue regeneration, viral infection, and carcinogenesis [124-126]. Since spontaneous fusion is prevented by large electrostatic and hydration repulsive forces between the membranes, nature utilizes specialized membrane proteins, which

facilitate and control the fusion process [127-129]. Artificially, fusion can be induced by virus-based methods [130], by chemical methods such as the addition of polyethylene glycol (PEG) [131], by ultraviolet laser [132], or by electroporation-mediated fusion [42]. Artificial fusion between two cells of different types enables one to create a hybrid cell which expresses the properties of both parental cells. Electric-field induced fusion (i.e. electrofusion) has gained notable attention particularly for preparing monoclonal-antibody-producing hybridoma cells and cell vaccines for cancer immunotherapy (reviewed in [133]), for cloning organisms such as Dolly [134], and in the treatment of diabetes [135]. Similarly, electrofusion can be obtained between two different GUVs or between GUVs and cells. Applications of GUV-GUV electrofusion and cell-GUV electrofusion are described in Sections 3.1.2 and 3.1.5, respectively.

Membrane electrofusion can be induced provided that two conditions are met: the membranes need to be in close contact and the membranes need to be destabilized in the contact zone. In electrofusion experiments, GUVs (and/or cells) are most often brought into contact by low-intensity AC electric field, which arranges the GUVs into structures mimicking pearl chains [42]. The pearl-chain formation is a consequence of the GUV movement in the non-homogeneous field because, in a suspension of GUVs, the local field around each GUV is distorted by the presence of other GUVs [44]. Such movement is called dielectrophoresis. If the frequency and the intensity of the AC field are appropriate, the electrostatic interaction forces between individual GUVs are attractive and the GUVs align in a linear fashion with respect to the direction of the applied electric field [42]. Among other methods of establishing contact between the GUVs are the addition of agglutinating agents like PEG [136], or the mechanical manipulation by optical tweezers and microelectrodes [137].

The destabilization of the membranes, as the second condition for electrofusion, is achieved by electroporation of the membranes in the contact zone using strong DC electric pulses. The exact molecular mechanisms of how membrane electroporation facilitates fusion are not completely understood. Sugar et al. [138] have proposed a model, which considers that the electric field induces pores spanning across both of the adjacent membranes in the contact zone. Namely, the nucleation of a pore in one of the bilayers could locally increase the electric field and promote nucleation of another pore in the adjacent bilayer. If large numbers of such double-membrane pores are nucleated, these pores could coalesce into larger loop-like and tongue-like cracks. When the electric field is removed, the membrane parts surrounded by loop-like cracks could finally separate to form vesicles. Additionally, unstable membrane undulations induced under an electric field could facilitate local contacts between the adjacent bilayers followed by membrane merging [108-111].

High-speed optical imaging (time resolution of 50 μs) of the electrofusion process between two GUVs demonstrated that in the absence of salt in the aqueous solutions, several double-membrane pores (fusion necks) typically form in the contact zone during the pulse (Fig. 9b) [139, 140]. Expansion and subsequent coalescence of these fusion necks lead to the formation of small contact-zone vesicles, which remain trapped in the interior of the fused GUV. On the contrary, no vesicles are observed, if the GUVs are electrofused in the presence of 1 mM NaCl in the external solution, which suggests that a single or very few fusion necks form during the pulse (Fig. 9c). The expansion of the fusion neck is initially very fast (about 4 cm/s) and after ~1 ms slows down as the opening of the neck decreases the membrane tension. The value of the initial velocity implies that the formation of a single fusion neck can be completed in a few hundred nanoseconds after the onset of the applied electric pulse [139]. Interestingly, when fusion is induced between two GUVs functionalized with synthetic ligand

molecules that mimic the action of fusion proteins, the opening of the fusion neck exhibits similar kinetics (Fig. 9a).

Apart from the influence of ions, electrofusion is also influenced by the physicochemical properties of the membrane. Stoicheva et al. have reported that GUVs made from negatively charged lipids are more difficult to fuse than GUVs made of zwitterionic lipids, possibly because of larger repulsive forces between the charged lipids [141]. The inhibiting effect on the electrofusion between GUVs has also been observed in the presence of cadmium ions, presumably because they increase the membrane rigidity, which hinders the opening of the fusion neck [142].

[Here Fig. 9]

While high-speed optical microscopy allows imaging of the electrofusion process with a temporal resolution of tens of microseconds, it cannot provide the information on the processes occurring in the microsecond or submicrosecond time-scale after the onset of an electric pulse. Theoretical calculations are useful for revealing more details on U_m and the electroporation kinetics before fusion. Calculations of U_m induced on the membranes of a pair of GUVs in contact have shown that U_m at the contact zone depends on the GUV geometry (spherical or ellipsoidal shape) and the ratio $\chi = \lambda_i/\lambda_e$ between the conductivities of the internal and external aqueous solutions [143, 144]. Let us first consider two spherical GUVs of an equal size. When the membranes become fully charged and U_m reaches the steady state, the absolute value of U_m established at the contact zone is lower than at the poles of the GUV pair facing the electrodes (cf. lines A, B, and C in Fig. 10a). This suggests that, if the electric pulse is long enough for U_m to reach the steady state, electroporation of the contact zone is accompanied by electroporation of the poles of the GUV pair. However, immediately after the application of an electric pulse, while the membranes are still in the charging phase, U_m strongly depends on χ. If the internal conductivity is lower than the external conductivity ($\chi < 1$), the highest U_m always establishes at the poles of the GUV pair (not shown). On the contrary, if the internal conductivity is higher than the external ($\chi > 1$), the highest U_m transiently establishes at the contact zone (Fig. 10a). This indicates that if $\chi > 1$ and if the pulse duration is short enough, it is possible to achieve selective electroporation of the contact zone, which is exactly the condition required for inducing vesicle electrofusion. This is corroborated by numerical calculations of the density of pores, which form along the membrane, as predicted by a theoretical model of electroporation (Fig. 10b) [145]. Similar results can be observed if the GUVs in contact are spherical but of a different size (Fig. 10c,d) [146], or if the GUVs have ellipsoidal shapes caused by electrodeformation [147]. The theoretical results indicate that selective electroporation of the contact zone can be obtained for a range of pulse durations, but this range depends on the size and shape of the GUVs, and the ratio as well as the absolute values of the internal and external conductivities. Under low-conductivity conditions in which GUVs are typically electrofused, a pulse duration in the order of 10 µs would be appropriate (Fig. 10). The theoretical predictions of course have practical significance only if such short pulses are sufficient to induce electrofusion. Indeed, experiments on cells have demonstrated that the application of 20 pulses as short as 50 ns can induce electrofusion [146]. In addition, the formation of the fusion neck could indeed occur within hundreds of nanoseconds [139], as discussed above. Overall, the results suggest that by appropriately tuning the pulse duration, it is possible to induce electrofusion between GUVs while preventing any leakage from the vesicle interior, regardless of the GUV size and shape. This is

relevant, for example, when studying biochemical reactions by electrofusing GUVs, as discussed in Section 3.1.2.

[Here Fig. 10]

2.4 Approaching towards more realistic cell models

GUVs have provided unique opportunities to investigate the fundamental mechanisms of electroporation and electrofusion of cells, and the pulse-induced molecular transmembrane transport. However, several profound phenomena observed on GUVs show discrepancies compared to the observations seen on living cells. (i) Macropores have never been visualised in living cells [90]. (ii) The membrane of a GUV typically reseals and retains its impermeability within hundreds of milliseconds after pulse application [69], whereas cell membrane resealing often takes place for few minutes [148]. (iii) Lipids loss can be observed in GUVs [80], whereas cells can osmotically swell or shrink after pulse application [149, 150]. (iv) A profound difference is also observed in the mechanism of DNA transport across the electroporated membrane. DNA enters the GUV during the pulse via an electrophoretic mechanism [151], whereas in cells the DNA forms a complex with the cell membrane and most likely translocates the membrane via an endocytotic mechanism [152].

As shown above, the GUV is a simplified model of the cell. However, a GUV can be easily modified in its composition, implying the possibilities of extending this model closer towards a real cell, by increasing the GUV's complexity [153]. Cell membranes contain an asymmetric composition of a variety of lipids and cholesterol, coexisting in different lipid phases. The lipid bilayer serves as a matrix for membrane proteins, which constitute about half of the mass of a typical cell membrane [154, 155]. Furthermore, cell membranes are under an intrinsic tension due to cytoskeleton attachments [156]. The intracellular and extracellular milieus contain high concentrations of salt (about 150 mM), together with dissolved proteins and nucleic acids [154]. The cytoplasm is a crowded, compartmentalised environment with numerous membrane-bound organelles [155]. As the science of implementing these complex systems into the GUV improves, the mechanisms of pulse-induced effects on real cells can be elucidated further. Below we discuss the possibilities for extending the GUV as a model for the real cell.

The first method to increase the complexity of the GUV, as already discussed above, is to adjust the membrane composition and study GUVs containing lipid mixtures [116], cholesterol [60, 68], or GUVs made from natural lipid extract [114]. Additionally, methods of GUV preparation under physiological conditions (≥ 140 mM) have been developed [23, 157-161]. The techniques of GUV preparation have exceeded even further, enabling the preparation of much more complex GUV structures [3]. On the one hand, a complex membrane structure can be controlled by embedding membrane proteins [17, 18, 162, 163] and preparing controlled asymmetric membranes [164, 165]. On the other hand, biomaterials can be encapsulated by the GUVs, such as the actin cytoskeleton [166-169], enzymes [170] and gel-like materials mimicking the cytoplasm [171, 172]. Lira et al. have already shown that agarose encapsulated inside a GUV strongly affects both the electrodeformation and the pore dynamics, while maintaining the lateral diffusion of the lipids [173]. Therefore, it can be concluded that the electroporation mechanism is strongly influenced by the inner part of the GUVs. Simultaneously, this system is a great way to immobilize the GUV for a long-time study on, for example, the diffusive response of membrane proteins due to an electrical pulse [174]. From results

on living cells, it is also expected that the cytoskeleton plays an important role in both the resealing of the membrane [175, 176] and in the gene electrotransfer through the membrane [152, 177-179]. Adding the cytoskeleton motors (dynein, kinesin and myosin) could possibly also reveal the mechanisms by which the genetic material is transported from the cell membrane to the nucleus [152, 179].

3. Vesicle electroporation and electrofusion in biomedical applications

Electroporation and electrofusion offer a wide range of possibilities for vesicle manipulation. In Section 2, we primarily focused on using GUVs as simple models for studying the interaction of the cells with an electric field. Here, we address the use of electroporation and electrofusion for manipulating vesicles for biomedical applications. The utility of vesicles in biomedical applications largely depends on the vesicle size. GUVs are ideal candidates for *in vitro* investigations since they can be easily visualised by light microscopy, as well as transported and handled inside the observation chamber by optical tweezers or micropipettes. In addition, GUVs are particularly suitable for mimicking a cell-like environment due to their similar size and curvature. However, GUVs are generally too large to be used for therapeutic purposes. For *in vivo* delivery of drugs and other promising pharmaceuticals, submicron vesicles need to be used, since these vesicles are small enough to cross the biological barriers inside the body and deliver their cargo to the target tissue [180]. Accordingly, we discuss the use of electroporation and electrofusion for manipulating GUVs and submicron vesicles (SUVs and LUVs) in Sections 3.1 and 3.2, respectively.

3.1 Applications of electroporation and electrofusion of GUVs

3.1.1 Encapsulation of biomolecules into GUVs with electroporation

Most commonly, the GUVs are encapsulated with the desired compound already during the vesicle preparation procedure. Nevertheless, electroporation can be used as an alternative method to load GUVs with selected biomolecules after the formation process. In general, electroporation provides a simple means for delivering molecules into GUVs, regardless of how the GUVs are prepared and without the need of any sophisticated equipment. Portet et al. [151] have studied electroporative uptake of plasmid DNA (4.7 kbp) into GUVs made from Egg PC and have observed that the DNA enters the GUV predominantly by an electrophoretic mechanism. Electroporation of GUVs is, therefore, practical for loading charged biomolecules. The amount of loaded compounds can be tuned by adjusting the amplitude, duration, and number of the applied electric pulses. They have also developed a model for predicting the amount of transferred DNA as a function of the parameters of the applied electric pulses [151].

Electroporation can also promote the insertion of some type of membrane proteins and peptides into the bilayer membrane [181-186]. The so-called electroinsertion has received a lot of interest for "engineering" the membranes of living cells by electroinserting receptor molecules (e.g. antibodies or enzymes) and use the cells as biorecognition elements to detect superoxides [187, 188], viruses [189, 190], and toxins [191]. Raffy et al. [192-194] have demonstrated that electroinsertion of glycophorin A can be achieved in gel-phase (DPPC) and fluid-phase (Egg PC) GUVs and MLVs. However, they have observed that unlike in cell membranes, electroinsertion in vesicles is strongly controlled by the surface charge of the membrane; electroinsertion of glycophorin is completely inhibited in the presence of negatively charged phosphatidylserine (30% or more) or positively charged stearylamine (as low as 2%) [195]. For this reason, electroinsertion can perhaps be effectively employed only in

lipid vesicles with a certain lipid composition. Further investigation into electroinsertion of membrane proteins and peptides into lipid vesicles may have implications in the field of biosensing, where biochips based on vesicle arrays show great promise as platforms for high-throughput screening of membrane proteins, for the purposes of diagnostics and drug discovery [196]. Namely, membrane proteins play a key role in the treatment of diseases, since about 60% of currently available drugs are targeting membrane protein species [197].

3.1.2 Electrofusion of GUVs: microreactors and models of primitive cells

Almost two decades ago, Orwar et al. [27, 35] proposed that sequential electrofusion between giant vesicles, comprising different membrane and interior compositions, could be employed for creating hybrid vesicles with a higher complexity or to study complex reactions inside the vesicles. In the light of their ideas, electrofusion between GUVs has later been used for a variety of purposes. Dimova et al. [37, 140] have shown that electrofusion between GUVs with a different lipid composition can be used to prepare multicomponent vesicles. If the parental vesicles are made from nonmiscible lipids, electrofusion of these vesicles results in formation of microdomains in the fused vesicle, allowing one to study the stability and dynamics of raft-like domains. A significant advantage of electrofusion-based membrane mixing is that the final composition of the fused vesicle is precisely controlled, which is difficult to achieve when preparing multicomponent vesicles directly from a mixture of dissolved lipids [198]. Bezlyepkina et al. [198] have demonstrated the benefits of such a electrofusion approach for the determination of tie lines in a phase diagram for the ternary mixture of DOPC, egg sphingomyelin, and cholesterol.

Electrofusion between two GUVs encapsulating different reagents provides the means to trigger a biochemical reaction. Since GUVs can easily be directly visualised under the microscope, the kinetics of the biochemical reaction can be monitored via fluorescence-based methods. The relevance of using GUVs as microreactors is twofold. Firstly, fusion between GUVs encapsulating small reagent volumes (attoliters to picoliters) enables rapid diffusional mixing (in the order of microseconds to milliseconds) and allows one to study fast chemical reaction kinetics [27]. Moreover, fusion between GUVs allows precise amounts of reagents to be mixed, provided that negligible leakage occurs from the vesicles during fusion. Secondly, GUVs can mimic the size and surface properties of cells. Consequently, biochemical reactions, such as transcription and translation of genes [26], can be studied in a biologically relevant environment, which is particularly important when building an artificial cell through a bottom-up approach and for understanding the origins of life. Since lightning strikes are considered as a possible mechanism for promoting membrane electroporation and electrofusion during early evolution [199], electrofusion presents a particularly relevant method for studying reactions in primitive cells. Nevertheless, electrofusion is merely one of the approaches used when studying reactions in lipid vesicles. Further references on other techniques can be found in [200-202]. Below we discuss three example studies, which utilized electrofusion between GUVs.

Hsin and Yeung [203] have shown that the analysis of reaction kinetics in GUVs can go down to the single-molecule level. They measured the activity of alkaline phosphatase by electrofusing two GUVs, one containing a single alkaline phosphatase molecule labelled with TOTO-3 and the other one containing fluorescein diphosphate. The mixing of the contents of the GUVs initiated an enzymatic reaction that produced fluorescein, detected by fluorescence microscopy. Measurements revealed a broad distribution in the activities of individual alkaline phosphatase molecules, which were attributed to distinct conformational states. The advantage of this method is that the activity is

measured in the absence of an undesirable surface effect, since the protein rarely comes in contact with the lipid membrane.

Yang et al. [142] have studied nanoparticle synthesis inside GUVs, in order to explore whether synthesis of inorganic nanomaterials in microorganisms could occur in the absence of peptide- and protein-driven processes. They have considered a simple reaction, $Na_2S + CdCl_2 \leftrightarrow CdS + 2NaCl$, in which a solid CdS product forms already at weak millimolar (mM) concentrations. Indeed, electrofusion of GUVs containing either 0.3 mM Na_2S or $CdCl_2$ resulted in the formation of CdS nanoparticles with a diameter of 4–8 nm. Moreover, in a different protocol, where $CdCl_2$ was allowed to slowly diffuse into GUVs pre-loaded with Na_2S, larger nanoparticles with a diameter of about 50 nm were formed inside the GUVs, demonstrating the influence of the mixing kinetics on the final nanoparticle size. These findings further indicate the feasibility of carrying out nanoparticle synthesis in GUVs.

Terasawa et al. [204] have studied fusion between phospholipid GUVs encapsulating polymer molecules in their aqueous core. They observed that such GUVs can undergo spontaneous budding transformation after being electrofused (Fig. 11). The budding is a result of a depletion volume effect – the fused vesicle divides to maximise the translational entropy of the polymers inside the vesicle. This physical process mimics cell growth and division and could represent one of the mechanisms by which cells self-reproduced in the evolutionary pathway from protocells to modern life [202, 204]. Looking from a different perspective, such budding transformation can be exploited for aliquoting the reaction product after electrofusing GUVs containing different biochemical reagents [205].

[Here Fig. 11]

3.1.3 Electrofusion of GUVs in microfluidic devices

With the advancements in microfabrication techniques, the manipulation of cells and vesicles in lab-on-a-chip devices is becoming more and more popular. Microfluidic designs indeed have proven to be well-suited for electrofusing cells or GUVs [206]. The basic approach of electrofusing GUVs in a microfluidic device with micromachined electrodes is similar as when using conventional parallel-plate or wire electrodes, except that the length scales are smaller. The contacts between GUVs can be obtained by traditional dielectrophoretic alignment of GUVs into pearl chains followed by application of electroporative pulses to initiate electrofusion [207, 208]. Such microchips can even be designed for combined electroformation and electrofusion of GUVs [209]. Yet, this traditional approach neither allows controlling the number of GUVs involved in the fusion event nor the selectivity with respect to which types of GUVs are fused together. The greatest advantage of electrofusion in microfluidic devices is the possibility to integrate an array of traps that facilitate contact between selected pairs of GUVs (Fig. 12). Various designs have been proposed for trapping cells or water-in-oil droplets [210-212]. However, Robinson et al. [213] have reported that the trapping designs for cells and droplets are not entirely suitable for trapping GUVs due to their large deformability. Namely, the shear stress from the flow could easily squeeze the GUVs out of the traps. To overcome this challenge, Robinson et al. surrounded the traps by circular ring valves that were hydraulically actuated to isolate each trap and prevent any flow-induced movement of the GUVs [213].

[Here Fig. 12]

3.1.4 Microelectroinjection and vesicle-nanotube networks

Microelectroinjection is a technique, which is based on the combination of electroporation and pressure-driven microinjection [214]. Initially, this technique was applied for precisely controlling the amount of molecular loading into single lipid GUVs. Since the membrane of a lipid vesicle is typically very elastic, microneedles with an outer tip diameter of about 200 nm need to be used to mechanically puncture the membrane [215]. Such tips are extremely fragile and the small diameter of the tip limits the size of the objects that can be introduced into the GUV. To use larger micropipettes, Karlsson et al. [214] proposed the following approach. A GUV was positioned between the tip of a glass micropipette (diameter ~2 µm), equipped with a Pt electrode, and a 5-µm diameter carbon fibre electrode. A rectangular pulse with the duration of 1–10 ms was applied between the electrodes to induce electroporation below the micropipette tip, which allowed the tip to enter the vesicle. A small volume (typically 50–500 femtoliters into GUVs with diameter of 10-20 µm) was then injected into the vesicle lumen. T7-phage DNA molecules (radius of gyration 0.56 µm), 30-nm-diameter latex spheres, and 100-nm-diameter SUVs were easily injected into GUVs. Moreover, multiple reagents were sequentially injected into a single vesicle without noticeable leakage [214].

Subsequently, it turned out that the microelectroinjection method combined with electrofusion enables one to artificially create complex networks of vesicles connected by lipid nanotubes [216, 217]. Different variants of such vesicle networks have been explored as systems for analysing enzyme-catalysed reactions [218], single-molecule detection of DNA [219], and reactions of polymers with calcium ions to form hydrogels [220]. This topic has been thoroughly reviewed elsewhere [13, 221, 222], but let us illustrate an example. Cans et al. [223] used this technology to form a small vesicle inside a surface immobilized GUV as a model of a cell that undergoes exocytosis. The main steps to create this model are depicted in Fig. 13a-d. The micropipette is electroinserted into the GUV (Fig. 13a) and across the membrane at the opposite side of the GUV (Fig. 13b). Since the lipids adhere to the tip, withdrawal of the micropipette results in a lipid nanotube (Fig. 13c). Finally, a small vesicle is inflated at the pipette tip by inducing a flow from the micropipette (Fig. 13d,e). Inflation of the nanotube leads to a local increase in the membrane tension, which induces a flow of the lipids from the regions of lower tension (outer membrane) along the nanotube. As the vesicle grows in size, the nanotube shortens until it transforms into a toroid-shaped fusion pore (Fig. 13f-i). At this point the system mimics the later stages of the exocytotic process. Recently, it has been demonstrated that this simple model can represent two main modes of exocytosis, which are considered to occur naturally: one in which the content of the exocytotic vesicle is fully released into the extracellular space (as in Fig. 13f-i), and the second one in which only partial release takes place and may correspond to an extended kiss-and-run mechanism [224].

[Here Fig. 13]

3.1.5 Electrofusion of GUVs with cells

While cell-cell electrofusion and GUV-GUV electrofusion are rather well-explored, electrofusion between GUVs and cells is only now receiving greater attention. Cell-GUV electrofusion offers some unique possibilities, such as delivering large objects directly into the cytosol or dramatically changing the composition of the cell membrane through the addition of lipids and membrane proteins. The proof-of-concept was first reported by Strömberg et al. [137]. They prepared giant phosphatidylcholine MLVs with incorporated membrane protein γ-glutamyltransferase. Individual MLVs and cells were electrofused between two carbon-fibre microelectrodes, which resulted in the

integration of γ-glutamyltransferase into the cell membrane. Subsequently, Shirakashi et al. [225] demonstrated electrofusion between phosphatidylcholine GUVs and Jurkat cells based on the conventional combination of pearl-chain alignment and pulse application.

Saito et al. [226] followed a similar protocol as Shirakashi et al. [225] and aimed to introduce large particles into HeLa cells (Fig. 14). They prepared GUVs from a mixture of DOPC, DOPG and cholesterol with the water-in-oil emulsion centrifugation method. This GUV preparation method allowed them to encapsulate plasmid DNA, DNA origami structure, as well as fluorescent microbeads with diameters of 0.2, 0.5, 1, and 2 μm. The protocol was successful for delivering all particles into the cells except for 2 μm microbeads, which were apparently too large to pass the cytoskeleton network beneath the cell membrane. Most importantly, the protocol did not affect the cell viability, as the cells were able to proliferate normally for at least 5 days after electrofusion. The authors though reported that the GUVs were probably only transiently fused to the cells, and detached from the cells with post-pulse washing. Overall, the results showed great promise for introducing large functionally active objects such as micro-machines into living cells, and studying their effects on the cells.

[Here Fig. 14]

Another approach for cell-GUV electrofusion was described by Raz-Ben Aroush et al. [227]. The protocol was developed for fish epithelial keratocytes and human foreskin fibroblasts (as depicted in Fig. 15). The cells were grown on a glass coverslip in a cell culture medium. Ten minutes before electrofusion, the cells were incubated in a serum-free medium supplemented with a PEG solution, since the latter had been found to facilitate fusion. Afterwards, the solution with GUVs was added, and the GUVs were allowed to settle on top of the cells. Two parallel-plate electrodes were then inserted into the sample and the cells and GUVs were electrofused. Finally, the cells were washed with a culture medium to remove the unfused GUVs and PEG. The preparation of GUVs with fluorescently conjugated lipids enabled detection of the fused cell-GUV hybrids under a fluorescent microscope (Fig. 15). The fluorescence signal from the labelled lipids appeared evenly spread in the cell membrane within 1 min., suggesting that the fusion process was fast. This protocol was used to study the effect of membrane enlargement on the inherent moving ability of keratocytes [228]. Interestingly, the authors observed a negligible effect on the cell movement despite the substantial increase in the membrane area (~30%). Measurements of the cell membrane tension, which plays an essential role in cell motility, revealed that the tension remained practically unchanged after electrofusion. Fluorescence imaging of the lamellipodial actin network further demonstrated that the amount of filamentous actin increased and the actin network expanded in the fused cells as compared to the control, buffering the influence of the increase in the membrane area on the tension [228].

[Here Fig. 15]

3.2 Applications of electroporation and electrofusion of LUVs and SUVs

Lipid vesicles have been proposed as carriers of pharmaceuticals already in the 1970s [229]. As vesicles possess both hydrophilic and hydrophobic domains, they can carry practically any type of molecules. This makes them promising delivery vehicles for drugs, proteins, peptides, and nucleic acids in the treatment of cancer, infections, metabolic diseases, as well as autoimmune diseases [230-233]. The main objectives of encapsulating therapeutic compounds into vesicles are to protect

sensitive molecules during their transportation to the target tissue such as nucleic acids from endogenous nucleases in the blood plasma, reduce the side-effects of toxic drugs such as chemotherapeutics, and/or achieve a high localization and enhanced intracellular uptake of therapeutic compounds at disease sites [233, 234]. In clinical applications, vesicles are mostly administrated intravenously, although other routes of administration are also being considered [235]. The size of vesicles used in drug delivery is typically about 200 nm in diameter or less, which allows the vesicles to extravasate through leaky blood vessels in inflammatory and tumour sites [234, 236]. In the field of drug delivery, vesicles made from phospholipids are generally referred to as liposomes, and we adopt this notation throughout the present section. Unless otherwise noted, the sizes of the vesicles discussed in this section correspond to the size of LUVs and SUVs.

While several liposome formulations are already commercialised, and numerous formulations are in different stages of clinical trials, many challenges still exist which limit liposome applications [29, 30, 235, 237]. Conventional liposomes prepared from neutral phospholipids have low encapsulation efficiency, tend to leak the encapsulated substances, and have a short circulation time in the blood. The liposome stability can be increased by tuning the composition of the membrane, e.g., by addition of cholesterol, charged lipids, or by replacing fluid-phase with gel-phase lipids [238]. The short circulation time is mainly caused by rapid opsonisation – a process in which the liposomes become covered with opsonin proteins from the blood plasma – and subsequent uptake by the mononuclear phagocytic system [239]. The opsonisation can be reduced by covering the surface of the liposomes with PEG (or similar inert polymers), which decreases nonspecific interactions with the plasma proteins and additionally stabilizes the membrane. Such PEGylated liposomes are called stealth liposomes [240]. The specificity of liposome accumulation in the disease sites can be increased by conjugating liposomes with ligands, which are able to specifically bind to target cells. However, this approach has so far yielded scarce improvements in the therapeutic outcomes with respect to the increased cost of preparing ligand-targeted liposomes [29, 241]. Once the liposomes accumulated at the target site, they can increase the therapeutic potential if the release of the entrapped drug from the liposomes takes place at an optimized rate [29]. Furthermore, biomolecules such as proteins, DNA, and RNA, which cannot permeate across the cell membrane, need to be released after the liposomes enter the cell, generally by endocytotic mechanisms [242]. To control the release from liposomes, methods which rely on a stimulus to initiate disintegration of the liposome membrane have been proposed, such as change in pH, temperature variation, ultrasound, or light irradiation [243, 244]. To meet the challenges of liposomal drug delivery, alternative types of vesicles are being investigated such as vesicles made from archaeal lipids (archaeosomes [245]) or block copolymers (polymersomes [246]), which are characterized by greater stability compared to liposomes. Very recently, vesicles of natural origin called extracellular vesicles have been proposed as superior alternatives to artificial vesicles [247]. The use of nanotechnology for therapeutic purposes is continuously evolving and various other types of sophisticated nanocarriers are considered for drug delivery [248-252].

Electroporation and electrofusion of liposomes and other "-somes" with sizes corresponding to the size range of SUVs and LUVs has received less attention than electroporation and electrofusion of GUVs. The main fundamental studies have been conducted by Neumann et al. via electro-optic and conductometric measurements on suspended vesicles [253-256]. Similarly as for GUVs, electroporation of SUVs and LUVs is associated with vesicle electrodeformation and increased membrane permeability. However, electroporation of LUVs and SUVs tends to occur at lower $U_{m,crit}$,

which is associated with higher membrane curvature of smaller vesicles [257]. In terms of applications, electroporation can be exploited for loading the vesicles with a given compound or for controlling the release of the compound from the vesicles, as discussed below.

3.2.1 Loading a cargo into vesicles by electroporation

Liposomes can be encapsulated with the desired compound either during the formation process or by using other methods, which are typically based on creating a pH gradient across the liposome membrane [258]. While these methods are suitable for artificial vesicles such as liposomes, they can hardly be applied for loading extracellular vesicles (EVs). EVs are phospholipid vesicles, which are secreted by most types of cells and play a key role in long-distance intercellular communication, by facilitating the transfer of proteins, mRNAs and miRNAs between the donor and recipient cells. In the field of drug delivery, two subtypes of EVs are often utilized, exosomes and microvesicles, because a complete separation and purification of these subtypes is extremely laborious [259]. Exosomes are about 40–100 nm in diameter and are produced inside multivesicular endosomes. They are released into the extracellular space upon fusion of the multivesicular endosomes with the cell membrane. Their larger counterparts, microvesicles (diameter ~100–500 nm), are produced through budding and fission from the cell membrane [260]. Although many challenges need to be overcome before the therapeutic potential of EVs is effectively harnessed [261], these vesicles possess several advantages over synthetic liposomes: (i) EVs inherently have a long circulation time in the blood, (ii) they possess an intrinsic ability to cross biological barriers including the most difficult one to penetrate, i.e. the blood-brain barrier, (iii) they are immunologically inert if purified from a compatible cell source and they could even be derived from the patient's own cells to limit any potential immunogenicity, (iv) they naturally express membrane receptors which allow them to "recognize" recipient cells, and (v) they can spontaneously fuse with the recipient cells, avoiding endocytotic pathways, and directly deliver their cargo into the cytosol [259].

After the seminal work of Alvarez-Erviti et al. [262], electroporation has become one of the main methods for loading EVs with hydrophilic molecules. Alvarez-Evriti et al. [262] have used electroporation to encapsulate siRNA into EVs derived from dendritic cells and have shown that these EVs could deliver siRNA through the blood-brain barrier into the brain parenchyma of mice, suppressing the expression of a gene coding for Beta-secretase 1, which is an important therapeutic target in Alzheimer's disease. In a subsequent study, they have shown that siRNA-loaded EVs significantly reduced the accumulation of α-synuclein aggregates in mouse brain, which is a pathological hallmark in Parkinson's disease [263]. Other studies have further confirmed that EVs loaded with siRNA or miRNA by electroporation can induce specific gene knockdown in various cell types *in vitro* [264-266]. Electroporation has also been used to encapsulate the chemotherapeutic drug doxorubicin [267, 268], superparamagnetic iron oxide nanoparticles [269, 270], and porphyrin [271].

However, the use of electroporation for loading EVs has reached limited success. A careful investigation by Kooijmans et al. [272] has demonstrated that electroporation of EVs in electroporation cuvettes leads to extensive aggregation of siRNA, which can result in an overestimate in the amount of siRNA loaded into EVs. Their results have shown that aggregation is probably caused by the release of aluminium cations from the electrodes in the cuvettes. Strikingly, when EVs were electroporated under conditions which prevented siRNA aggregation, undetectable amount of siRNA was encapsulated into the vesicles. To the opposite, Lamichhane et al. [273] later showed that

DNA molecules larger than siRNA can in fact be encapsulated into EVs by electroporation. The contradictory reports on unsuccessful [272] and successful [273] loading of EVs by electroporation could at least partially be explained in the context of different electroporation protocols. According to the reported methodology, the electric field strength of the applied pulses has been four times higher in the experiments of Lamichhane et al. [273], which is expected to result in more extensive vesicle electroporation and greater molecular uptake [151, 255].

Apart from loading EVs, electroporation has been proposed as a method for loading polymersomes with macromolecules including proteins, siRNA and plasmid DNA [274, 275]. Specifically, electroporation has been found advantageous for encapsulating proteins such as myoglobin, which are difficult to encapsulate by the conventional approach where the pH-switch method is used for polymersome formation [274].

Polymersomes are characterized by greater stability and lower membrane permeability than lipid vesicles. They also offer the high flexibility of chemical modifications both before and after formation, for which they have some unique advantages as drug delivery and diagnostic agents [246]. One of the numerous possibilities is to functionalize them with magnetic nanoparticles (MNPs). Such magnetopolymersomes can then be used as contrast agents in magnetic resonance imaging or as smart therapeutic agents, whereby remote application of an alternating magnetic field induces heating of the magnetic nanoparticles to trigger drug release or cell death [276]. Recently, it has been shown that electroporation can assist the preparation of magnetopolymersomes. Bain et al. [277] prepared polymersomes with a high pH aqueous core (encapsulating NaOH) and suspended them in an iron solution. By electroporating the polymersomes, they have initiated the synthesis of magnetite nanoparticles inside the polymeric membrane. They have proposed a mechanism in which the simultaneous flux of NaOH and iron ions through the pores induced by electroporation results in the formation of nanoparticles inside the pores (Fig. 16). They have shown that by tuning the amplitude of the applied pulses, it is possible to control the MNP size. In a related study, Bakhshi et al. [278] have demonstrated that the synthesis of MNPs can be achieved also inside the aqueous core of liposomes. In addition, they have shown that high-throughput production of MNP-functionalized liposomes with a uniform size (58 ± 8 nm) can be achieved by combining electroporation-based MNP synthesis with an electrohydrodynamic atomization method for the liposome production.

[Here Fig. 16]

3.2.2 Spontaneous fusion of SUVs and LUVs with electroporated cells

Apart from using electroporation to load vesicles with desired compounds, electroporation could further be used for controlling the liposomal release at the target site. Teissié et al. [279-281] have demonstrated that lipid SUVs and LUVs can spontaneously fuse with electroporated cells, avoiding the endocytotic pathway and directly delivering their cargo into the cytoplasm. The contact between the cells and the vesicles was obtained via an electrostatic calcium bridge and the suspension was exposed to 10 or more pulses with 100 µs duration. The electric field strength of the pulse was 1.2 kV/cm, which was sufficiently high to electroporate the cells while preserving the cell viability, but was too low to electroporate the vesicles due to their smaller size (the LUVs were around 200 nm in diameter). Application of electric pulses resulted in fusion of the vesicles with the cell membrane. Large macromolecules (20 kD dextran) could easily be delivered into the cells by this approach [280]. In a more recent study [281], they also demonstrated that cell-vesicle fusion is affected by the lipid

composition of the vesicles. Most efficient fusion was achieved when PC lipids were mixed with PS (20%), PE (30%), and cholesterol (30%). Interestingly, exposing the cells to electric pulses in the presence of highly fusogenic empty LUVs had a protecting effect against the loss of cell viability due to electroporation [281]. This has implications for gene delivery by means of electroporation, since the loss of cell viability is one of the bottlenecks in gene electrotransfer applications [152].

The observation that lipid vesicles are able to spontaneously fuse with an electroporated membrane has been supported by theory [282]. However, the lipid vesicles apparently need to be metastable for spontaneous fusion. MLVs, which have a more tightly packed lipid assembly, have been unable to spontaneously fuse with the electroporated cells, regardless of the lipid composition of MLVs [279].

3.2.3 Controlling the release from SUVs and LUVs by nanosecond electric pulses

Another possible approach for controlling the release of the liposome content may be offered by electroporation with pulses in the nanosecond (ns) range [283-285]. Since the charging time of the cell membrane is typically on the order of 100 ns (when the cell is in a medium with physiological conductivity) [286], nanosecond pulses are too short to fully charge the cell membrane and the membrane remains in the charging phase throughout the duration of the pulse. During this charging phase, the cell membrane does not electrically shield the cell interior, and the external electric field penetrates into the cytoplasm. The electric field inside the cytoplasm induces U_m on the membrane of intracellular organelles with a magnitude comparable to U_m on the charging cell membrane [287]. If the external electric field is sufficiently high, it can lead to electroporation of both the cell membrane and the organelle membranes [288-292]. Since the organelles are much smaller than the cell, an electric field in the order of 10 kV/cm is required for their electroporation.

The possibility to electroporate intracellular membranes has prompted the idea of using nanosecond pulses for electroporating liposomes once they are taken up by the cells. As such, the release of the encapsulated liposome content into the cytosol can be controllably triggered. A theoretical study, considering a model of a cell with internalized liposomes (diameter 100–1000 nm), has suggested that electroporation of the liposomes without considerably affecting the cell viability would be feasible, provided that the applied pulses are about 10 ns long [283]. An alternative idea is to electroporate the liposomes when they are in close proximity of the target cells [285]. Since nanosecond pulses generally also result in electroporation of the cell membrane, the content released from the electroporated liposomes could be subsequently taken up by the electroporated cells. The possibility to control the release of the vesicle content with nanosecond pulses for now remains at the theoretical level, and its experimental feasibility is yet to be confirmed. A long-term projection may lie in combined use of liposomes and electric pulses in cancer treatment. Namely, pulses with a duration of 100 µs are routinely used in tumour treatment, whereby the pulses are delivered to the tissue via planar or needle electrodes [31]. Since the mechanism by which electric pulses induce cell death is in principle nonthermal, electroporation-based tumour treatment can be applied to tumours, which are unsuitable for surgery and thermal ablation, such as tumours in proximity of large blood vessels and nerves [293]. More recently, the application of nanosecond pulses has been proposed as an additional method for tumour ablation. Unlike longer microsecond pulses, nanosecond pulses are able to directly induce apoptotic cell death [294]. The use of nanosecond pulses to trigger cell death and simultaneously control the release of a chemotherapeutic drug from the liposomes could have a synergistic effect, comparable to observations in radio frequency ablation [295-297].

4. Future perspective

It is necessary to explore more realistic cell models in the electroporation of vesicles, which account for the complex, heterogeneous structure of the cell. Pioneering studies have been carried out to understand the basic principles of simple GUVs in electric fields, revealing the response of the membrane solely. More complex GUV systems are desired to elucidate more realistic mechanisms of electroporation of a living cell. Systematic investigation of GUVs with incorporated membrane proteins, cytoskeleton network, and dense gel-like aqueous core would reveal more insights on how these sub-cellular structures influence cell electroporation. While cell electroporation has been widely used in biomedical and technological applications, the exact mechanisms that contribute to the experimentally observed increased permeability of cell membranes are not yet fully elucidated [298]. There are many open questions, including: Why the resealing of cell membranes after electroporation generally takes orders of magnitude more time than in model membrane systems (minutes or even hours in cells versus up to hundreds of milliseconds in GUVs)? Can the increase in the cell membrane permeability after electroporation be attributed solely to lipid pores formed during exposure to electric pulses, or does lipid peroxidation present a contributing/alternative mechanism [299, 300]? How are the membrane proteins affected by the electric field and how do they participate in the increased cell membrane permeability [176, 301]? What are the molecular mechanisms of the transmembrane transport of small drugs and large macromolecules such as DNA and how is the transport influenced by the resting potential of the cell membrane [289, 302]? Why is the translocation of DNA across the cell membrane different in GUVs than in cells and what is the role of cytoskeleton in DNA translocation [151, 177, 303]? Answering these questions through controlled experiments on more complex model GUV systems would improve our understanding of cell electroporation and consequently help optimise current electroporation-based treatments (e.g. gene electrotransfer), as well as develop new ways to exploit cell electroporation for various applications in medicine, food processing, and environmental applications.

Further, studying complex GUVs in electric field could have implications in single-cell diagnostics. By increasing the complexity of a GUV, also the mechanical properties can be correlated to their intra-cellular components via electrodeformation measurements. Single-cell diagnostics have already shown that some diseases alter the mechanical properties [304], e.g. cancer cells have a lower stiffness than healthy cells [305] and even the Young's modulus of different tumour cells can be discriminated [306]. By gaining a comprehensive understanding of how different intra-cellular components contribute to the mechanical properties of living cells through a bottom-up approach, the diagnostics can be further improved. Additionally, it would open up the field to use electric fields as a contactless diagnostic tool to measure the changes in mechanical properties of cells and distinguish important biological factors associated with disease progression (such as pathological, genetic, and epigenetic factors).

To develop successful applications for the characterization and screening on the single GUV or cell level, microfluidic concepts provide unprecedented options. Furthermore, exposing GUVs or cells to an electric field in a microfluidic device offers the benefit of remote and contactless manipulation without the need of sophisticated and expensive micromanipulators. In particular, when the microfluidic design contains the posts to trap individual cells/vesicles together with integrated electrodes in close proximity to the traps, it is possible to simultaneously expose numerous cells/GUVs to the electric field, while analysing each cell/GUV separately. The possibility of trapping

individual cells and GUVs has already shown great potential in inducing controlled pairwise cell-cell electrofusion [206]. Similar concepts can be further designed to induce pairwise electrofusion between cells and GUVs. For example, by embedding selected membrane proteins into the GUV membrane and/or DNA or even micro/nanomachines inside the GUV, cell-GUV electrofusion could provide a platform for a controlled delivery of selected material into living cells and analyse its influence on cell properties and functions [137, 226].

Elucidating electroporation of GUVs in micro/nanofluidic devices would also provide important insights into fundamental electroporation mechanisms. Presence of nanostructures, such as nanochannels, nanopores, or nanowires, strongly influences the local electric field distribution and consequently, the spatial distribution of the pores formed in the GUV/cell membrane [307-309]. Fabricating nanostructures with well-defined geometries and performing electroporation of GUVs with increasing complexity next to such nanostructures would improve the theoretical knowledge of electroporation and further optimize the design of electroporation protocols. For instance, when cells are electroporated next to a nanochannel, DNA can be delivered directly into the cytoplasm [307], whereas in conventional bulk electroporation, the DNA first forms a complex with the cell membrane and then most likely translocates across the membrane via endocytotic mechanisms [152, 310].

In this review, we have focused on the following topics: electrodeformation, electroporation, and electrofusion of vesicles, highlighting both fundamental and application results. These model systems of the cell have provided unique opportunities to bridge the gap between the soft matter physics and the reality of the soft living matter. The fundamental understanding of the mechanical properties of vesicles (GUVs, LUVs, and SUVs) is an essential step towards advancing our fundamental knowledge about the complex behaviour of cell membranes in an electric field. In addition, this fundamental knowledge can inspire us to develop novel liposome approaches for practical biomedical applications.

Acknowledgements

This work was supported by the European Research Council (ERC) under the European Union's Seventh Framework Programme (FP/2007-2013)/ERC Grant, agreement no. 337820 (to P.E.B.). The authors thank Fatemeh Hashemi and Shaurya Sachdev for critical reading of the manuscript.

References

[1] Pezzulo G, Levin M. Top-down models in biology: explanation and control of complex living systems above the molecular level. Journal of The Royal Society Interface. 2016;13.
[2] Ross J, Arkin AP. Complex Systems: From chemistry to systems biology. Proceedings of the National Academy of Sciences. 2009;106:6433-4.
[3] Lagny TJ, Bassereau P. Bioinspired membrane-based systems for a physical approach of cell organization and dynamics: usefulness and limitations. Interface Focus. 2015;5.
[4] Szathmary E. Life: In search of the simplest cell. Nature. 2005;433:469-70.
[5] Liu AP, Fletcher DA. Biology under construction: in vitro reconstitution of cellular function. Nat Rev Mol Cell Biol. 2009;10:644-50.
[6] Sens P, Johannes L, Bassereau P. Biophysical approaches to protein-induced membrane deformations in trafficking. Current opinion in cell biology. 2008;20:476-82.
[7] Schwille P. Bottom-Up Synthetic Biology: Engineering in a Tinkerer's World. Science. 2011;333:1252-4.
[8] Luisi PL, Stano P. The Minimal Cell: The Biophysics of Cell Compartment and the Origin of Cell Functionality: Springer Science & Business Media; 2010.
[9] Menger FM, Keiper JS. Chemistry and physics of giant vesicles as biomembrane models. Current Opinion in Chemical Biology. 1998;2:726-32.
[10] Mozafari MR. Nanoliposomes: Preparation and Analysis. In: Weissig V, (editor). Liposomes: Humana Press; 2010. p. 29-50.
[11] Walde P, Cosentino K, Engel H, Stano P. Giant Vesicles: Preparations and Applications. Chembiochem. 2010;11:848-65.
[12] Swaay Dv, deMello A. Microfluidic methods for forming liposomes. 2013;13:752-67.
[13] Jesorka A, Orwar O. Liposomes: technologies and analytical applications. Annu Rev Anal Chem. 2008;1:801-32.
[14] Dimova R, Aranda S, Bezlyepkina N, Nikolov V, Riske KA, Lipowsky R. A practical guide to giant vesicles. Probing the membrane nanoregime via optical microscopy. Journal of Physics: Condensed Matter. 2006;18:S1151.
[15] Menger FM, Angelova MI. Giant Vesicles: Imitating the Cytological Processes of Cell Membranes. Accounts of Chemical Research. 1998;31:789-97.
[16] Bucher P, Fischer A, Luisi PL, Oberholzer T, Walde P. Giant Vesicles as Biochemical Compartments: The Use of Microinjection Techniques. Langmuir. 1998;14:2712-21.
[17] Girard P, Pécréaux J, Lenoir G, Falson P, Rigaud J-L, Bassereau P. A New Method for the Reconstitution of Membrane Proteins into Giant Unilamellar Vesicles. Biophysical Journal. 2004;87:419-29.
[18] Davidson M, Karlsson M, Sinclair J, Sott K, Orwar O. Nanotube–Vesicle Networks with Functionalized Membranes and Interiors. Journal of the American Chemical Society. 2003;125:374-8.
[19] Rigaud J-L, Pitard B, Levy D. Reconstitution of membrane proteins into liposomes: application to energy-transducing membrane proteins. Biochimica et Biophysica Acta (BBA) - Bioenergetics. 1995;1231:223-46.
[20] Sachse R, Dondapati SK, Fenz SF, Schmidt T, Kubick S. Membrane protein synthesis in cell-free systems: From bio-mimetic systems to bio-membranes. FEBS Letters. 2014;588:2774-81.
[21] Soga H, Fujii S, Yomo T, Kato Y, Watanabe H, Matsuura T. In Vitro Membrane Protein Synthesis Inside Cell-Sized Vesicles Reveals the Dependence of Membrane Protein Integration on Vesicle Volume. ACS Synthetic Biology. 2014;3:372-9.
[22] Helfrich MR, Mangeney-Slavin LK, Long MS, Djoko KY, Keating CD. Aqueous Phase Separation in Giant Vesicles. Journal of the American Chemical Society. 2002;124:13374-5.
[23] Yamashita Y, Oka M, Tanaka T, Yamazaki M. A new method for the preparation of giant liposomes in high salt concentrations and growth of protein microcrystals in them. Biochimica et Biophysica Acta (BBA) - Biomembranes. 2002;1561:129-34.

[24] Fischer A, Franco A, Oberholzer T. Giant vesicles as microreactors for enzymatic mRNA synthesis. Chembiochem. 2002;3:409-17.
[25] Michel M, Winterhalter M, Darbois L, Hemmerle J, Voegel JC, Schaaf P, et al. Giant Liposome Microreactors for Controlled Production of Calcium Phosphate Crystals. Langmuir. 2004;20:6127-33.
[26] Noireaux V, Libchaber A. A vesicle bioreactor as a step toward an artificial cell assembly. P Natl Acad Sci USA. 2004;101:17669-74.
[27] Chiu DT, Wilson CF, Ryttsén F, Strömberg A, Farre C, Karlsson A, et al. Chemical Transformations in Individual Ultrasmall Biomimetic Containers. Science. 1999;283:1892-5.
[28] Long MS, Jones CD, Helfrich MR, Mangeney-Slavin LK, Keating CD. Dynamic microcompartmentation in synthetic cells. Proceedings of the National Academy of Sciences. 2005;102:5920-5.
[29] Allen TM, Cullis PR. Liposomal drug delivery systems: From concept to clinical applications. Adv Drug Deliver Rev. 2013;65:36-48.
[30] Sercombe L, Veerati T, Moheimani F, Wu SY, Sood AK, Hua S. Advances and Challenges of Liposome Assisted Drug Delivery. Frontiers in Pharmacology. 2015;6.
[31] Yarmush ML, Golberg A, Serša G, Kotnik T, Miklavčič D. Electroporation-based technologies for medicine: Principles, applications, and challenges. Annual Review of Biomedical Engineering. 2014;16:295-320.
[32] Mahnič-Kalamiza S, Vorobiev E, Miklavčič D. Electroporation in food processing and biorefinery. J Membrain Biol. 2014;247:1279-304.
[33] Kotnik T, Frey W, Sack M, Haberl Meglič S, Peterka M, Miklavčič D. Electroporation-based applications in biotechnology. Trends in Biotechnology. 2015;33:480-8.
[34] Dimitrov DS. Electroporation and electrofusion of membranes. Handbook of Biological Physics. 1995;1:851-901.
[35] Strömberg A, Karlsson A, Ryttsén F, Davidson M, Chiu DT, Orwar O. Microfluidic Device for Combinatorial Fusion of Liposomes and Cells. Analytical Chemistry. 2001;73:126-30.
[36] Dimova R, Bezlyepkina N, Jordo MD, Knorr RL, Riske KA, Staykova M, et al. Vesicles in electric fields: Some novel aspects of membrane behavior. Soft Matter. 2009;5:3201-12.
[37] Dimova R, Riske KA, Aranda S, Bezlyepkina N, Knorr RL, Lipowsky R. Giant vesicles in electric fields. Soft Matter. 2007;3:817-27.
[38] Portet T, Mauroy C, Démery V, Houles T, Escoffre J-M, Dean DS, et al. Destabilizing Giant Vesicles with Electric Fields: An Overview of Current Applications. J Membrain Biol. 2012;245:555-64.
[39] Vlahovska PM. Voltage-morphology coupling in biomimetic membranes: dynamics of giant vesicles in applied electric fields. Soft Matter. 2015;11:7232-6.
[40] Pauly H, Schwan HP. Impendance of a suspension of ball-shaped particles with a shell; a model for the dielectric behavior of cell suspensions and protein solutions. Z Naturforsch B. 1959;14B:125-31.
[41] Schwan HP, Sher LD. Alternative-Current Field-Induced Forces and Their Biological Implications. J Electrochem Soc. 1969;116:22C-6C.
[42] Zimmermann U. Electric field-mediated fusion and related electrical phenomena. Biochimica et Biophysica Acta (BBA) - Reviews on Biomembranes. 1982;694:227-77.
[43] Chan KL, Gascoyne PRC, Becker FF, Pethig R. Electrorotation of liposomes: verification of dielectric multi-shell model for cells. Bba-Lipid Lipid Met. 1997;1349:182-96.
[44] Voldman J. Electrical forces for microscale cell manipulation. Annual Review of Biomedical Engineering. 2006;8:425-54.
[45] Kotnik T, Pucihar G. Induced transmembrane voltage – theory, modeling, and experiments. In: Pakhomov AG, Miklavčič D, Markov MS, (editors). Advanced Electroporation Techniques in Biology and Medicine: CRC Press, Boca Raton; 2010. p. 51-70.
[46] Salipante PF, Knorr RL, Dimova R, Vlahovska PM. Electrodeformation method for measuring the capacitance of bilayer membranes. Soft Matter. 2012;8:3810-6.
[47] Riske KA, Dimova R. Electro-Deformation and Poration of Giant Vesicles Viewed with High Temporal Resolution. Biophysical Journal. 2005;88:1143-55.

[48] Kotnik T, Miklavcic D. Analytical description of transmembrane voltage induced by electric fields on spheroidal cells. Biophysical Journal. 2000;79:670-9.
[49] Hibino M, Shigemori M, Itoh H, Nagayama K, Kinosita K. Membrane conductance of an electroporated cell analyzed by submicrosecond imaging of transmembrane potential. Biophysical Journal. 1991;59:209-20.
[50] Kotnik T, Miklavčič D. Second-order model of membrane electric field induced by alternating external electric fields. Ieee T Bio-Med Eng. 2000;47:1074-81.
[51] Taupin C, Dvolaitzky M, Sauterey C. Osmotic pressure-induced pores in phospholipid vesicles. Biochemistry. 1975;14:4771-5.
[52] Abidor IG, Arakelyan VB, Chernomordik LV, Chizmadzhev YA, Pastushenko VF, Tarasevich MR. Electric breakdown of bilayer lipid membranes I. The main experimental facts and their qualitative discussion. Bioelectrochemistry and Bioenergetics. 1979;6:37-52.
[53] Powell KT, Weaver JC. Transient aqueous pores in bilayer membranes: A statistical theory. Bioelectrochemistry and Bioenergetics. 1986;15:211-27.
[54] Needham D, Hochmuth RM. Electro-mechanical permeabilization of lipid vesicles. Role of membrane tension and compressibility. Biophysical Journal. 1989;55:1001-9.
[55] Lewis TJ. A model for bilayer membrane electroporation based on resultant electromechanical stress. IEEE Transactions on Dielectrics and Electrical Insulation. 2003;10:769-77.
[56] Vasilkoski Z, Esser AT, Gowrishankar TR, Weaver JC. Membrane electroporation: The absolute rate equation and nanosecond time scale pore creation. Physical Review E. 2006;74:021904.
[57] Glaser RW, Leikin SL, Chernomordik LV, Pastushenko VF, Sokirko AI. Reversible electrical breakdown of lipid bilayers: formation and evolution of pores. Biochimica et Biophysica Acta (BBA) - Biomembranes. 1988;940:275-87.
[58] Neu JC, Smith KC, Krassowska W. Electrical energy required to form large conducting pores. Bioelectrochemistry. 2003;60:107-14.
[59] Brochard-Wyart F, de Gennes PG, Sandre O. Transient pores in stretched vesicles: role of leak-out. Physica A: Statistical Mechanics and its Applications. 2000;278:32-51.
[60] Portet T, Dimova R. A New Method for Measuring Edge Tensions and Stability of Lipid Bilayers: Effect of Membrane Composition. Biophysical Journal. 2010;99:3264-73.
[61] Gurtovenko AA, Anwar J, Vattulainen I. Defect-mediated trafficking across cell membranes: Insights from in silico modeling. Chemical reviews. 2010;110:6077-103.
[62] Levine ZA, Vernier PT. Life cycle of an electropore: Field-dependent and field-independent steps in pore creation and annihilation. J Membrain Biol. 2010;236:27-36.
[63] Kandasamy SK, Larson RG. Cation and anion transport through hydrophilic pores in lipid bilayers. The Journal of Chemical Physics. 2006;125:074901.
[64] Böckmann RA, de Groot BL, Kakorin S, Neumann E, Grubmüller H. Kinetics, Statistics, and Energetics of Lipid Membrane Electroporation Studied by Molecular Dynamics Simulations. Biophysical Journal. 2008;95:1837-50.
[65] Rems L. Lipid Pores: Molecular and Continuum Models. In: Miklavcic D, (editor). Handbook of Electroporation: Springer International Publishing; 2016. p. 1-21.
[66] Tokman M, Lee JH, Levine ZA, Ho M-C, Colvin ME, Vernier PT. Electric Field-Driven Water Dipoles: Nanoscale Architecture of Electroporation. PloS one. 2013;8:e61111.
[67] Neu JC, Krassowska W. Asymptotic model of electroporation. Physical Review E. 1999;59:3471-82.
[68] Mauroy C, Rico-Lattes I, Teissie J, Rols MP. Electric Destabilization of Supramolecular Lipid Vesicles Subjected to Fast Electric Pulses. Langmuir. 2015;31:12215-22.
[69] Tekle E, Astumian RD, Friauf WA, Chock PB. Asymmetric pore distribution and loss of membrane lipid in electroporated DOPC vesicles. Biophysical Journal. 2001;81:960-8.
[70] Ziegler MJ, Vernier PT. Interface Water Dynamics and Porating Electric Fields for Phospholipid Bilayers. The Journal of Physical Chemistry B. 2008;112:13588-96.

[71] Majhi AK, Kanchi S, Venkataraman V, Ayappa KG, Maiti PK. Estimation of activation energy for electroporation and pore growth rate in liquid crystalline and gel phases of lipid bilayers using molecular dynamics simulations. Soft Matter. 2015;11:8632-40.
[72] Polak A, Tarek M, Tomšič M, Valant J, Ulrih NP, Jamnik A, et al. Electroporation of archaeal lipid membranes using MD simulations. Bioelectrochemistry. 2014;100:18-26.
[73] Polak A, Bonhenry D, Dehez F, Kramar P, Miklavčič D, Tarek M. On the Electroporation Thresholds of Lipid Bilayers: Molecular Dynamics Simulation Investigations. J Membrain Biol. 2013;246:843-50.
[74] Gurtovenko AA, Lyulina AS. Electroporation of Asymmetric Phospholipid Membranes. The Journal of Physical Chemistry B. 2014;118:9909-18.
[75] Bennett WFD, Sapay N, Tieleman DP. Atomistic Simulations of Pore Formation and Closure in Lipid Bilayers. Biophysical Journal. 2014;106:210-9.
[76] Hu Y, Sinha SK, Patel S. Investigating hydrophilic pores in model lipid bilayers using molecular simulations: Correlating bilayer properties with pore-formation thermodynamics. Langmuir. 2015;31:6615-31.
[77] Riske KA, Dimova R. Electric Pulses Induce Cylindrical Deformations on Giant Vesicles in Salt Solutions. Biophysical Journal. 2006;91:1778-86.
[78] Sadik MM, Li J, Shan JW, Shreiber DI, Lin H. Vesicle deformation and poration under strong dc electric fields. Physical Review E. 2011;83:066316.
[79] Salipante PF, Vlahovska PM. Vesicle deformation in DC electric pulses. Soft Matter. 2014;10:3386-93.
[80] Portet T, Camps i Febrer F, Escoffre J-M, Favard C, Rols M-P, Dean DS. Visualization of Membrane Loss during the Shrinkage of Giant Vesicles under Electropulsation. Biophysical Journal. 2009;96:4109-21.
[81] Helfrich W, Servuss RM. Undulations, steric interaction and cohesion of fluid membranes. Il Nuovo Cimento D. 1984;3:137-51.
[82] Evans E, Rawicz W. Entropy-driven tension and bending elasticity in condensed-fluid membranes. Phys Rev Lett. 1990;64:2094-7.
[83] Hyuga H, Kinosita Jr K, Wakabayashi N. Steady-state deformation of a vesicle in alternating electric fields. Bioelectrochemistry and Bioenergetics. 1993;32:15-25.
[84] Vlahovska PM, Gracià RS, Aranda-Espinoza S, Dimova R. Electrohydrodynamic Model of Vesicle Deformation in Alternating Electric Fields. Biophysical Journal. 2009;96:4789-803.
[85] Peterlin P. Frequency-dependent electrodeformation of giant phospholipid vesicles in AC electric field. Journal of Biological Physics. 2010;36:339-54.
[86] Nganguia H, Young YN. Equilibrium electrodeformation of a spheroidal vesicle in an ac electric field. Physical Review E. 2013;88:052718.
[87] Kummrow M, Helfrich W. Deformation of giant lipid vesicles by electric fields. Phys Rev A. 1991;44:8356-60.
[88] Aranda S, Riske KA, Lipowsky R, Dimova R. Morphological Transitions of Vesicles Induced by Alternating Electric Fields. Biophysical Journal. 2008;95:L19-L21.
[89] Gracia RS, Bezlyepkina N, Knorr RL, Lipowsky R, Dimova R. Effect of cholesterol on the rigidity of saturated and unsaturated membranes: fluctuation and electrodeformation analysis of giant vesicles. Soft Matter. 2010;6:1472-82.
[90] Kinosita K, Hibino M, Itoh H, Shigemori M, Hirano Ki, Kirino Y, et al. Events of membrane electroporation visualized on a time scale from microsecond to seconds. In: Sowers DCCMCASE, (editor). Guide to Electroporation and Electrofusion. San Diego: Academic Press; 1992. p. 29-46.
[91] Hyuga H, Kinosita K, Wakabayashi N. Deformation of vesicles under the influence of strong electric fields. Japanese Journal of Applied Physics. 1991;30:1141.
[92] Hyuga H, Kinosita K, Wakabayashi N. Deformation of vesicles under the influence of strong electric fields II. Japanese Journal of Applied Physics. 1991;30:1333.
[93] Schwalbe JT, Vlahovska PM, Miksis MJ. Vesicle electrohydrodynamics. Physical Review E. 2011;83:046309.

[94] McConnell LC, Vlahovska PM, Miksis MJ. Vesicle dynamics in uniform electric fields: squaring and breathing. Soft Matter. 2015;11:4840-6.
[95] McConnell LC, Miksis MJ, Vlahovska PM. Continuum modeling of the electric-field-induced tension in deforming lipid vesicles. The Journal of Chemical Physics. 2015;143:243132.
[96] Kolahdouz EM, Salac D. Dynamics of three-dimensional vesicles in dc electric fields. Physical Review E. 2015;92:012302.
[97] Kolahdouz E, Salac D. Electrohydrodynamics of Three-Dimensional Vesicles: A Numerical Approach. SIAM Journal on Scientific Computing. 2015;37:B473-B94.
[98] Yu M, Lira RB, Riske KA, Dimova R, Lin H. Ellipsoidal Relaxation of Deformed Vesicles. Phys Rev Lett. 2015;115:128303.
[99] Evans E, Heinrich V, Ludwig F, Rawicz W. Dynamic Tension Spectroscopy and Strength of Biomembranes. Biophysical Journal. 2003;85:2342-50.
[100] Sandre O, Moreaux L, Brochard-Wyart F. Dynamics of transient pores in stretched vesicles. Proceedings of the National Academy of Sciences. 1999;96:10591-6.
[101] Olbrich K, Rawicz W, Needham D, Evans E. Water Permeability and Mechanical Strength of Polyunsaturated Lipid Bilayers. Biophysical Journal. 2000;79:321-7.
[102] Leontiadou H, Mark AE, Marrink SJ. Molecular Dynamics Simulations of Hydrophilic Pores in Lipid Bilayers. Biophysical Journal. 2004;86:2156-64.
[103] Levadny V, Tsuboi T-a, Belaya M, Yamazaki M. Rate Constant of Tension-Induced Pore Formation in Lipid Membranes. Langmuir. 2013;29:3848-52.
[104] McConnell LC, Miksis MJ, Vlahovska PM. Vesicle electrohydrodynamics in DC electric fields. IMA Journal of Applied Mathematics. 2013;78:797-817.
[105] Mauroy C, Portet T, Winterhalder M, Bellard E, Blache MC, Teissie J, et al. Giant lipid vesicles under electric field pulses assessed by non invasive imaging. Bioelectrochemistry. 2012;87:253-9.
[106] Antonova K, Vitkova V, Meyer C. Membrane tubulation from giant lipid vesicles in alternating electric fields. Physical Review E. 2016;93.
[107] Sens P, Isambert H. Undulation instability of lipid membranes under an electric field. Phys Rev Lett. 2002;88:128102.
[108] Lacoste D, Menon GI, Bazant MZ, Joanny JF. Electrostatic and electrokinetic contributions to the elastic moduli of a driven membrane. The European Physical Journal E. 2009;28:243-64.
[109] Ziebert F, Bazant MZ, Lacoste D. Effective zero-thickness model for a conductive membrane driven by an electric field. Physical Review E. 2010;81:031912.
[110] Schwalbe JT, Vlahovska PM, Miksis MJ. Lipid membrane instability driven by capacitive charging. Phys Fluids. 2011;23:041701.
[111] Seiwert J, Miksis MJ, Vlahovska PM. Stability of biomimetic membranes in DC electric fields. Journal of Fluid Mechanics. 2012;706:58-70.
[112] Nagle JF, Tristram-Nagle S. Structure of lipid bilayers. Biochimica et Biophysica Acta (BBA) - Reviews on Biomembranes. 2000;1469:159-95.
[113] Veatch SL, Keller SL. Organization in Lipid Membranes Containing Cholesterol. Phys Rev Lett. 2002;89:268101.
[114] Riske KA, Knorr RL, Dimova R. Bursting of charged multicomponent vesicles subjected to electric pulses. Soft Matter. 2009;5:1983-6.
[115] Knorr RL, Staykova M, Gracia RS, Dimova R. Wrinkling and electroporation of giant vesicles in the gel phase. Soft Matter. 2010;6:1990-6.
[116] Liu Z-W, Zeng X-A, Sun D-W, Han Z. Effects of pulsed electric fields on the permeabilization of calcein-filled soybean lecithin vesicles. Journal of Food Engineering. 2014;131:26-32.
[117] van Uitert I, Le Gac S, van den Berg A. Determination of the electroporation onset of bilayer lipid membranes as a novel approach to establish ternary phase diagrams: example of the l-α-PC/SM/cholesterol system. Soft Matter. 2010;6:4420-9.
[118] Hung W-C, Lee M-T, Chen F-Y, Huang HW. The Condensing Effect of Cholesterol in Lipid Bilayers. Biophysical Journal. 2007;92:3960-7.

[119] Pan J, Mills TT, Tristram-Nagle S, Nagle JF. Cholesterol perturbs lipid bilayers nonuniversally. Phys Rev Lett. 2008;100:198103.
[120] Pan J, Tristram-Nagle S, Kučerka N, Nagle JF. Temperature Dependence of Structure, Bending Rigidity, and Bilayer Interactions of Dioleoylphosphatidylcholine Bilayers. Biophysical Journal.94:117-24.
[121] Casciola M, Bonhenry D, Liberti M, Apollonio F, Tarek M. A molecular dynamic study of cholesterol rich lipid membranes: comparison of electroporation protocols. Bioelectrochemistry. 2014;100:11-7.
[122] Fernández ML, Marshall G, Sagués F, Reigada R. Structural and Kinetic Molecular Dynamics Study of Electroporation in Cholesterol-Containing Bilayers. The Journal of Physical Chemistry B. 2010;114:6855-65.
[123] Reigada R. Electroporation of heterogeneous lipid membranes. Biochimica et Biophysica Acta (BBA) - Biomembranes. 2014;1838:814-21.
[124] Ogle BM, Cascalho M, Platt JL. Biological implications of cell fusion. Nature Reviews Molecular Cell Biology. 2005;6:567-75.
[125] Chen EH, Grote E, Mohler W, Vignery A. Cell–cell fusion. FEBS Letters. 2007;581:2181-93.
[126] Noubissi FK, Ogle BM. Cancer Cell Fusion: Mechanisms Slowly Unravel. International Journal of Molecular Sciences. 2016;17.
[127] Jahn R, Südhof TC. Membrane Fusion and Exocytosis. Annual Review of Biochemistry. 1999;68:863-911.
[128] Martens S, McMahon HT. Mechanisms of membrane fusion: disparate players and common principles. Nature Reviews Molecular Cell Biology. 2008;9:543-56.
[129] Chernomordik LV, Kozlov MM. Mechanics of membrane fusion. Nature Structural & Molecular Biology. 2008;15:675-83.
[130] Köhler G, Milstein C. Continuous cultures of fused cells secreting antibody of predefined specificity. Nature. 1975;256:495-7.
[131] Golestani R, Pourfathollah AA, Moazzeni SM. Cephalin as an Efficient Fusogen in Hybridoma Technology: Can It Replace Poly Ethylene Glycol? Hybridoma. 2007;26:296-301.
[132] Kulin S, Kishore R, Helmerson K, Locascio L. Optical Manipulation and Fusion of Liposomes as Microreactors. Langmuir. 2003;19:8206-10.
[133] Kandušer M, Ušaj M. Cell electrofusion: past and future perspectives for antibody production and cancer cell vaccines. Expert Opin Drug Del. 2014;11:1885-98.
[134] Campbell KHS, McWhir J, Ritchie WA, Wilmut I. Sheep cloned by nuclear transfer from a cultured cell line. Nature. 1996;380:64-6.
[135] Yanai G, Hayashi T, Zhi Q, Yang K-C, Shirouzu Y, Shimabukuro T, et al. Electrofusion of Mesenchymal Stem Cells and Islet Cells for Diabetes Therapy: A Rat Model. PloS one. 2013;8:e64499.
[136] Teissié J, Rols MP, Blangero C. Electrofusion of Mammalian Cells and Giant Unilamellar Vesicles. In: Neumann E, Sowers AE, Jordan CA, (editors). Electroporation and Electrofusion in Cell Biology. Boston, MA: Springer US; 1989. p. 203-14.
[137] Strömberg A, Ryttsén F, Chiu DT, Davidson M, Eriksson PS, Wilson CF, et al. Manipulating the genetic identity and biochemical surface properties of individual cells with electric-field-induced fusion. Proceedings of the National Academy of Sciences. 2000;97:7-11.
[138] Sugar IP, Förster W, Neumann E. Model of cell electrofusion: Membrane electroporation, pore coalescence and percolation. Biophysical Chemistry. 1987;26:321-35.
[139] Haluska CK, Riske KA, Marchi-Artzner V, Lehn J-M, Lipowsky R, Dimova R. Time scales of membrane fusion revealed by direct imaging of vesicle fusion with high temporal resolution. Proceedings of the National Academy of Sciences. 2006;103:15841-6.
[140] Riske KA, Bezlyepkina N, Lipowsky R, Dimova R. Electrofusion of model lipid membranes viewed with high-temporal resolution. Biophysical Reviews and Letters. 2006;01:387-400.
[141] Stoicheva NG, Hui SW. Electrofusion of cell-size liposomes. Biochimica et Biophysica Acta (BBA) - Biomembranes. 1994;1195:31-8.

[142] Yang P, Lipowsky R, Dimova R. Nanoparticle Formation in Giant Vesicles: Synthesis in Biomimetic Compartments. Small. 2009;5:2033-7.
[143] Washizu M, Techaumnat B. Cell membrane voltage during electrical cell fusion calculated by re-expansion method. Journal of Electrostatics. 2007;65:555-61.
[144] Techaumnat B. Numerical analysis of DC-field-induced transmembrane potential of spheroidal cells in axisymmetric orientations. IEEE Transactions on Dielectrics and Electrical Insulation. 2013;20:1567-76.
[145] DeBruin KA, Krassowska W. Modeling Electroporation in a Single Cell. I. Effects of Field Strength and Rest Potential. Biophysical Journal. 1999;77:1213-24.
[146] Rems L, Ušaj M, Kandušer M, Reberšek M, Miklavčič D, Pucihar G. Cell electrofusion using nanosecond electric pulses. Scientific reports. 2013;3:3382.
[147] Liu L, Mao Z, Zhang J, Liu N, Liu QH. The Influence of Vesicle Shape and Medium Conductivity on Possible Electrofusion under a Pulsed Electric Field. PloS one. 2016;11:e0158739.
[148] Rols MP, Teissié J. Electropermeabilization of mammalian cells. Quantitative analysis of the phenomenon. Biophysical Journal. 1990;58:1089-98.
[149] Kinosita K, Tsong TY. Formation and resealing of pores of controlled sizes in human erythrocyte membrane. Nature. 1977;268:438-41.
[150] Nesin OM, Pakhomova ON, Xiao S, Pakhomov AG. Manipulation of cell volume and membrane pore comparison following single cell permeabilization with 60- and 600-ns electric pulses. Biochimica et Biophysica Acta (BBA) - Biomembranes. 2011;1808:792-801.
[151] Portet T, Favard C, Teissie J, Dean DS, Rols M-P. Insights into the mechanisms of electromediated gene delivery and application to the loading of giant vesicles with negatively charged macromolecules. Soft Matter. 2011;7:3872-81.
[152] Rosazza C, Meglic SH, Zumbusch A, Rols M-P, Miklavcic D. Gene Electrotransfer: A Mechanistic Perspective. Current Gene Therapy. 2016;16:98-129.
[153] Fenz SF, Sengupta K. Giant vesicles as cell models. Integrative Biology. 2012;4:982-95.
[154] Alberts B, Johnson A, Lewis J, Raff M, Roberts K, Walter P. Molecular biology of the cell. 5th ed. New York: Garland Science, Taylor & Francis Group; 2008.
[155] Lodish H, Berk A, Zipursky SL, Matsudaira P, Baltimore D, Darnell J. Molecular cell biology. 4th ed. New York: W. H. Freeman and Company; 2001.
[156] Diz-Muñoz A, Fletcher DA, Weiner OD. Use the force: membrane tension as an organizer of cell shape and motility. Trends Cell Biol. 2013;23:47-53.
[157] Estes DJ, Mayer M. Giant liposomes in physiological buffer using electroformation in a flow chamber. Biochimica et Biophysica Acta (BBA) - Biomembranes. 2005;1712:152-60.
[158] Pavlič JI, Genova J, Popkirov G, Kralj-Iglič V, Iglič A, Mitov MD. Mechanoformation of neutral giant phospholipid vesicles in high ionic strength solution. Chemistry and physics of lipids. 2011;164:727-31.
[159] Montes LR, Alonso A, Goñi FM, Bagatolli LA. Giant Unilamellar Vesicles Electroformed from Native Membranes and Organic Lipid Mixtures under Physiological Conditions. Biophysical Journal. 2007;93:3548-54.
[160] Akashi K, Miyata H, Itoh H, Kinosita K. Preparation of giant liposomes in physiological conditions and their characterization under an optical microscope. Biophysical Journal. 1996;71:3242-50.
[161] Pott T, Bouvrais H, Méléard P. Giant unilamellar vesicle formation under physiologically relevant conditions. Chemistry and physics of lipids. 2008;154:115-9.
[162] Deshpande S, Caspi Y, Meijering AEC, Dekker C. Octanol-assisted liposome assembly on chip. Nature Communications. 2016;7:10447.
[163] Varnier A, Kermarrec F, Blesneac I, Moreau C, Liguori L, Lenormand JL, et al. A Simple Method for the Reconstitution of Membrane Proteins into Giant Unilamellar Vesicles. J Membrane Biol. 2010;233:85-92.
[164] Pautot S, Frisken BJ, Weitz DA. Engineering asymmetric vesicles. Proceedings of the National Academy of Sciences. 2003;100:10718-21.

[165] Chiantia S, Schwille P, Klymchenko AS, London E. Asymmetric GUVs Prepared by MβCD-Mediated Lipid Exchange: An FCS Study. Biophysical Journal. 2011;100:L1-L3.
[166] Limozin L, Sackmann E. Polymorphism of Cross-Linked Actin Networks in Giant Vesicles. Phys Rev Lett. 2002;89:168103.
[167] Pontani L-L, van der Gucht J, Salbreux G, Heuvingh J, Joanny J-F, Sykes C. Reconstitution of an Actin Cortex Inside a Liposome. Biophysical Journal. 2009;96:192-8.
[168] Limozin L, Roth A, Sackmann E. Microviscoelastic Moduli of Biomimetic Cell Envelopes. Phys Rev Lett. 2005;95:178101.
[169] Häckl W, Bärmann M, Sackmann E. Shape Changes of Self-Assembled Actin Bilayer Composite Membranes. Phys Rev Lett. 1998;80:1786-9.
[170] Walde P. Enzymatic reactions in liposomes. Curr Opin Colloid In. 1996;1:638-44.
[171] Viallat A, Dalous J, Abkarian M. Giant Lipid Vesicles Filled with a Gel: Shape Instability Induced by Osmotic Shrinkage. Biophysical Journal. 2004;86:2179-87.
[172] Osinkina L, Markström M, Orwar O, Jesorka A. A Method for Heat-Stimulated Compression of Poly(N-isopropyl acrylamide) Hydrogels Inside Single Giant Unilamellar Vesicles. Langmuir. 2010;26:1-4.
[173] Lira Rafael B, Dimova R, Riske Karin A. Giant Unilamellar Vesicles Formed by Hybrid Films of Agarose and Lipids Display Altered Mechanical Properties. Biophysical Journal. 2014;107:1609-19.
[174] Lira RB, Steinkühler J, Knorr RL, Dimova R, Riske KA. Posing for a picture: vesicle immobilization in agarose gel. Scientific reports. 2016;6:25254.
[175] Rols M-P, Teissié J. Experimental evidence for the involvement of the cytoskeleton in mammalian cell electropermeabilization. Biochimica et Biophysica Acta (BBA) - Biomembranes. 1992;1111:45-50.
[176] Teissie J, Rols M-P. Manipulation of Cell Cytoskeleton Affects the Lifetime of Cell Membrane Electropermeabilization. Annals of the New York Academy of Sciences. 1994;720:98-110.
[177] Rosazza C, Escoffre J-M, Zumbusch A, Rols M-P. The actin cytoskeleton has an active role in the electrotransfer of plasmid DNA in mammalian cells. Molecular therapy : the journal of the American Society of Gene Therapy. 2011;19:913-21.
[178] Rosazza C, Buntz A, Rieß T, Wöll D, Zumbusch A, Rols M-P. Intracellular Tracking of Single-plasmid DNA Particles After Delivery by Electroporation. Mol Ther. 2013;21:2217-26.
[179] Vaughan EE, Dean DA. Intracellular Trafficking of Plasmids during Transfection Is Mediated by Microtubules. Mol Ther. 2006;13:422-8.
[180] M. Rabanel J, Aoun V, Elkin I, Mokhtar M, Hildgen P. Drug-Loaded Nanocarriers: Passive Targeting and Crossing of Biological Barriers. Curr Med Chem. 2012;19:3070-102.
[181] Mouneimne Y, Tosi P-F, Gazitt Y, Nicolau C. Electro-insertion of xeno-glycophorin into the red blood cell membrane. Biochemical and Biophysical Research Communications. 1989;159:34-40.
[182] Zeira M, Tosi PF, Mouneimne Y, Lazarte J, Sneed L, Volsky DJ, et al. Full-length CD4 electroinserted in the erythrocyte membrane as a long-lived inhibitor of infection by human immunodeficiency virus. Proceedings of the National Academy of Sciences. 1991;88:4409-13.
[183] El Ouagari K, Benoist H, Sixou S, Teissié J. Electropermeabilization mediates a stable insertion of glycophorin A with Chinese hamster ovary cell membranes. European Journal of Biochemistry. 1994;219:1031-9.
[184] Raffy S, Lazdunski C, Teissié J. Electroinsertion and activation of the C-terminal domain of Colicin A, a voltage gated bacterial toxin, into mammalian cell membranes. Molecular membrane biology. 2004;21:237-46.
[185] Cranfield CG, Cornell BA, Grage SL, Duckworth P, Carne S, Ulrich AS, et al. Transient Potential Gradients and Impedance Measures of Tethered Bilayer Lipid Membranes: Pore-Forming Peptide Insertion and the Effect of Electroporation. Biophysical Journal. 2014;106:182-9.
[186] Kokla A, Blouchos P, Livaniou E, Zikos C, Kakabakos SE, Petrou PS, et al. Visualization of the membrane engineering concept: evidence for the specific orientation of electroinserted antibodies and selective binding of target analytes. Journal of Molecular Recognition. 2013;26:627-32.

[187] Moschopoulou G, Kintzios S. Application of “membrane-engineering” to bioelectric recognition cell sensors for the ultra-sensitive detection of superoxide radical: A novel biosensor principle. Anal Chim Acta. 2006;573–574:90-6.
[188] Moschopoulou G, Valero T, Kintzios S. Superoxide determination using membrane-engineered cells: An example of a novel concept for the construction of cell sensors with customized target recognition properties. Sensors and Actuators B: Chemical. 2012;175:78-84.
[189] Perdikaris A, Alexandropoulos N, Kintzios S. Development of a Novel, Ultra-rapid Biosensor for the Qualitative Detection of Hepatitis B Virus-associated Antigens and Anti-HBV, Based on “Membrane-engineered” Fibroblast Cells with Virus-Specific Antibodies and Antigens. Sensors. 2009;9:2176-86.
[190] Moschopoulou G, Vitsa K, Bem F, Vassilakos N, Perdikaris A, Blouhos P, et al. Engineering of the membrane of fibroblast cells with virus-specific antibodies: A novel biosensor tool for virus detection. Biosensors and Bioelectronics. 2008;24:1027-30.
[191] Larou E, Yiakoumettis I, Kaltsas G, Petropoulos A, Skandamis P, Kintzios S. High throughput cellular biosensor for the ultra-sensitive, ultra-rapid detection of aflatoxin M1. Food Control. 2013;29:208-12.
[192] Raffy S, Teissié J. Insertion of Glycophorin A, A Transmembraneous Protein, in Lipid Bilayers can be Mediated by Electropermeabilization. European Journal of Biochemistry. 1995;230:722-32.
[193] Raffy S, Teissié J. Electroinsertion of Glycophorin A in Interdigitation-Fusion Giant Unilamellar Lipid Vesicles. J Biol Chem. 1997;272:25524-30.
[194] Raffy S, Teissié J. Control of lipid membrane stability by cholesterol content. Biophysical Journal. 1999;76:2072-80.
[195] Raffy S, Teissié J. Surface Charge Control of Electropermeabilization and Glycophorin Electroinsertion with 1,2-Diacyl-sn-Glycero-3-Phosphocholine (lecithin) Liposomes. European Journal of Biochemistry. 1997;250:315-9.
[196] Bally M, Bailey K, Sugihara K, Grieshaber D, Vörös J, Städler B. Liposome and Lipid Bilayer Arrays Towards Biosensing Applications. Small. 2010;6:2481-97.
[197] Yıldırım MA, Goh K-I, Cusick ME, Barabási A-L, Vidal M. Drug—target network. Nat Biotechnol. 2007;25:1119-26.
[198] Bezlyepkina N, Gracià RS, Shchelokovskyy P, Lipowsky R, Dimova R. Phase Diagram and Tie-Line Determination for the Ternary Mixture DOPC/eSM/Cholesterol. Biophysical Journal. 2013;104:1456-64.
[199] Kotnik T. Lightning-triggered electroporation and electrofusion as possible contributors to natural horizontal gene transfer. Phys Life Rev. 2013;10:351-70.
[200] Christensen SM, Stamou D. Surface-based lipidvesicle reactor systems: fabrication and applications. 2007;3:828-36.
[201] Giustini M, Giuliani AM, Gennaro G. Natural or synthetic nucleic acids encapsulated in a closed cavity of amphiphiles. 2013;3:8618-32.
[202] Blain JC, Szostak JW. Progress Toward Synthetic Cells. Annual Review of Biochemistry. 2014;83:615-40.
[203] Hsin T-M, Yeung ES. Single-Molecule Reactions in Liposomes. Angewandte Chemie International Edition. 2007;46:8032-5.
[204] Terasawa H, Nishimura K, Suzuki H, Matsuura T, Yomo T. Coupling of the fusion and budding of giant phospholipid vesicles containing macromolecules. Proceedings of the National Academy of Sciences. 2012;109:5942-7.
[205] Shiomi H, Tsuda S, Suzuki H, Yomo T. Liposome-Based Liquid Handling Platform Featuring Addition, Mixing, and Aliquoting of Femtoliter Volumes. PloS one. 2014;9:e101820.
[206] Hu N, Yang J, Joo SW, Banerjee AN, Qian S. Cell electrofusion in microfluidic devices: A review. Sensors and Actuators B: Chemical. 2013;178:63-85.
[207] Tresset G, Takeuchi S. A Microfluidic Device for Electrofusion of Biological Vesicles. Biomed Microdevices. 2004;6:213-8.

[208] Tresset G, Takeuchi S. Utilization of Cell-Sized Lipid Containers for Nanostructure and Macromolecule Handling in Microfabricated Devices. Analytical Chemistry. 2005;77:2795-801.
[209] Wang Z, Hu N, Yeh L-H, Zheng X, Yang J, Joo SW, et al. Electroformation and electrofusion of giant vesicles in a microfluidic device. Colloids and Surfaces B: Biointerfaces. 2013;110:81-7.
[210] Skelley AM, Kirak O, Suh H, Jaenisch R, Voldman J. Microfluidic control of cell pairing and fusion. Nat Methods. 2009;6:147-52.
[211] Bai Y, He X, Liu D, Patil SN, Bratton D, Huebner A, et al. A double droplet trap system for studying mass transport across a droplet-droplet interface. 2010;10:1281-5.
[212] Huebner AM, Abell C, Huck WTS, Baroud CN, Hollfelder F. Monitoring a Reaction at Submillisecond Resolution in Picoliter Volumes. Analytical Chemistry. 2011;83:1462-8.
[213] Robinson T, Verboket PE, Eyer K, Dittrich PS. Controllable electrofusion of lipid vesicles: initiation and analysis of reactions within biomimetic containers. Lab on a Chip. 2014;14:2852-9.
[214] Karlsson M, Nolkrantz K, Davidson MJ, Strömberg A, Ryttsén F, Åkerman B, et al. Electroinjection of Colloid Particles and Biopolymers into Single Unilamellar Liposomes and Cells for Bioanalytical Applications. Analytical Chemistry. 2000;72:5857-62.
[215] Wick R, Angelova MI, Walde P, Luisi PL. Microinjection into giant vesicles and light microscopy investigation of enzyme-mediated vesicle transformations. Chemistry & Biology. 1996;3:105-11.
[216] Karlsson M, Sott K, Davidson M, Cans A-S, Linderholm P, Chiu D, et al. Formation of geometrically complex lipid nanotube-vesicle networks of higher-order topologies. Proceedings of the National Academy of Sciences. 2002;99:11573-8.
[217] Jesorka A, Stepanyants N, Zhang H, Ortmen B, Hakonen B, Orwar O. Generation of phospholipid vesicle-nanotube networks and transport of molecules therein. Nat Protocols. 2011;6:791-805.
[218] Sott K, Lobovkina T, Lizana L, Tokarz M, Bauer B, Konkoli Z, et al. Controlling Enzymatic Reactions by Geometry in a Biomimetic Nanoscale Network. Nano Letters. 2006;6:209-14.
[219] Tokarz M, Åkerman B, Olofsson J, Joanny J-F, Dommersnes P, Orwar O. Single-file electrophoretic transport and counting of individual DNA molecules in surfactant nanotubes. P Natl Acad Sci USA. 2005;102:9127-32.
[220] Jesorka A, Markström M, Orwar O. Controlling the Internal Structure of Giant Unilamellar Vesicles by Means of Reversible Temperature Dependent Sol−Gel Transition of Internalized Poly(N-isopropyl acrylamide). Langmuir. 2005;21:1230-7.
[221] Karlsson M, Davidson M, Karlsson R, Karlsson A, Bergenholtz J, Konkoli Z, et al. Biomimetic nanoscale reactors and networks. Annu Rev Phys Chem. 2004;55:613-49.
[222] Lizana L, Konkoli Z, Bauer B, Jesorka A, Orwar O. Controlling chemistry by geometry in nanoscale systems. Annual review of physical chemistry. 2009;60:449-68.
[223] Cans A-S, Wittenberg N, Karlsson R, Sombers L, Karlsson M, Orwar O, et al. Artificial cells: Unique insights into exocytosis using liposomes and lipid nanotubes. P Natl Acad Sci USA. 2003;100:400-4.
[224] Mellander LJ, Kurczy ME, Najafinobar N, Dunevall J, Ewing AG, Cans A-S. Two modes of exocytosis in an artificial cell. Scientific reports. 2014;4.
[225] Shirakashi R, Sukhorukov VL, Reuss R, Schulz A, Zimmermann U. Effects of a Pulse Electric Field on Electrofusion of Giant Unilamellar Vesicle (GUV)-Jurkat Cell. Journal of Thermal Science and Technology. 2012;7:589-602.
[226] Saito AC, Ogura T, Fujiwara K, Murata S, Nomura S-iM. Introducing Micrometer-Sized Artificial Objects into Live Cells: A Method for Cell–Giant Unilamellar Vesicle Electrofusion. PloS one. 2014;9:e106853.
[227] Raz-Ben Aroush D, Yehudai-Resheff S, Keren K. Electrofusion of giant unilamellar vesicles to cells. In: Paluch EK, (editor). Method Cell Biol. Vol. 125: Academic Press; 2015. p. 409-22.
[228] Lieber Arnon D, Yehudai-Resheff S, Barnhart Erin L, Theriot Julie A, Keren K. Membrane Tension in Rapidly Moving Cells Is Determined by Cytoskeletal Forces. Curr Biol. 2013;23:1409-17.
[229] Gregoriadis G, Ryman BE. Liposomes as carriers of enzymes or drugs: a new approach to the treatment of storage diseases. Biochem J. 1971;124:58P.

[230] Couvreur P, Vauthier C. Nanotechnology: Intelligent Design to Treat Complex Disease. Pharmaceutical Research. 2006;23:1417-50.
[231] Wang Y, Miao L, Satterlee A, Huang L. Delivery of oligonucleotides with lipid nanoparticles. Adv Drug Deliver Rev. 2015;87:68-80.
[232] Hallaj-Nezhadi S, Hassan M. Nanoliposome-based antibacterial drug delivery. Drug Delivery. 2015;22:581-9.
[233] Yingchoncharoen P, Kalinowski DS, Richardson DR. Lipid-Based Drug Delivery Systems in Cancer Therapy: What Is Available and What Is Yet to Come. Pharmacol Rev. 2016;68:701-87.
[234] Huang L, Liu Y. In Vivo Delivery of RNAi with Lipid-Based Nanoparticles. Annual Review of Biomedical Engineering. 2011;13:507-30.
[235] Chang H-I, Yeh M-K. Clinical development of liposome-based drugs: formulation, characterization, and therapeutic efficacy. Int J Nanomed. 2012;7:49-60.
[236] Wacker M. Nanocarriers for intravenous injection—The long hard road to the market. Int J Pharm. 2013;457:50-62.
[237] ElBayoumi T, Torchilin V. Current Trends in Liposome Research. In: Weissig V, (editor). Liposomes: Humana Press; 2010. p. 1-27.
[238] Lombardo D, Calandra P, Barreca D, Magazù S, Kiselev MA. Soft Interaction in Liposome Nanocarriers for Therapeutic Drug Delivery. Nanomaterials. 2016;6:125.
[239] Owens Iii DE, Peppas NA. Opsonization, biodistribution, and pharmacokinetics of polymeric nanoparticles. Int J Pharm. 2006;307:93-102.
[240] Immordino ML, Dosio F, Cattel L. Stealth liposomes: review of the basic science, rationale, and clinical applications, existing and potential. Int J Nanomed. 2006;1:297-315.
[241] Sawant RR, Torchilin VP. Challenges in Development of Targeted Liposomal Therapeutics. AAPS J. 2012;14:303-15.
[242] Hillaireau H, Couvreur P. Nanocarriers' entry into the cell: relevance to drug delivery. Cell Mol Life Sci. 2009;66:2873-96.
[243] Bibi S, Lattmann E, Mohammed AR, Perrie Y. Trigger release liposome systems: local and remote controlled delivery? Journal of Microencapsulation. 2012;29:262-76.
[244] Mura S, Nicolas J, Couvreur P. Stimuli-responsive nanocarriers for drug delivery. Nature materials. 2013;12:991-1003.
[245] Benvegnu T, Lemiegre L, Cammas-Marion S. New Generation of Liposomes Called Archaeosomes Based on Natural or Synthetic Archaeal Lipids as Innovative Formulations for Drug Delivery. Recent Patents on Drug Delivery & Formulation. 2009;3:206-20.
[246] Discher DE, Ahmed F. Polymersomes. Annual Review of Biomedical Engineering. 2006;8:323-41.
[247] Lakhal S, Wood MJA. Exosome nanotechnology: An emerging paradigm shift in drug delivery. Bioessays. 2011;33:737-41.
[248] Singh R, Lillard JW. Nanoparticle-based targeted drug delivery. Experimental and molecular pathology. 2009;86:215-23.
[249] Krishnamachari Y, Geary SM, Lemke CD, Salem AK. Nanoparticle Delivery Systems in Cancer Vaccines. Pharmaceutical Research. 2011;28:215-36.
[250] Du AW, Stenzel MH. Drug Carriers for the Delivery of Therapeutic Peptides. Biomacromolecules. 2014;15:1097-114.
[251] Zylberberg C, Matosevic S. Pharmaceutical liposomal drug delivery: a review of new delivery systems and a look at the regulatory landscape. Drug Delivery. 2016;23:3319-29.
[252] Niu Z, Conejos-Sánchez I, Griffin BT, O'Driscoll CM, Alonso MJ. Lipid-based nanocarriers for oral peptide delivery. Adv Drug Deliver Rev. 2016;106, Part B:337-54.
[253] Kakorin S, Neumann E. Electrooptical relaxation spectrometry of membrane electroporation in lipid vesicles. Colloids and Surfaces A: Physicochemical and Engineering Aspects. 2002;209:147-65.
[254] Neumann E, Kakorin S. Electrooptics of membrane electroporation and vesicle shape deformation. Curr Opin Colloid In. 1996;1:790-9.
[255] Kakorin S, Redeker E, Neumann E. Electroporative deformation of salt filled lipid vesicles. Eur Biophys J Biophy. 1998;27:43-53.

[256] Dimitrov V, Kakorin S, Neumann E. Transient oscillation of shape and membrane conductivity changes by field pulse-induced electroporation in nano-sized phospholipid vesicles. Phys Chem Chem Phys. 2013;15:6303-22.
[257] Kakorin S, Liese T, Neumann E. Membrane curvature and high-field electroporation of lipid bilayer vesicles. J Phys Chem B. 2003;107:10243-51.
[258] Gubernator J. Active methods of drug loading into liposomes: recent strategies for stable drug entrapment and increased in vivo activity. Expert Opin Drug Del. 2011;8:565-80.
[259] Batrakova EV, Kim MS. Using exosomes, naturally-equipped nanocarriers, for drug delivery. Journal of Controlled Release. 2015;219:396-405.
[260] Pol Evd, Böing AN, Harrison P, Sturk A, Nieuwland R. Classification, Functions, and Clinical Relevance of Extracellular Vesicles. Pharmacol Rev. 2012;64:676-705.
[261] Schiffelers R, Kooijmans S, Vader, van D, Van S. Exosome mimetics: a novel class of drug delivery systems. Int J Nanomed. 2012:1525.
[262] Alvarez-Erviti L, Seow Y, Yin H, Betts C, Lakhal S, Wood MJA. Delivery of siRNA to the mouse brain by systemic injection of targeted exosomes. Nat Biotechnol. 2011;29:341-5.
[263] Cooper JM, Wiklander PBO, Nordin JZ, Al-Shawi R, Wood MJ, Vithlani M, et al. Systemic exosomal siRNA delivery reduced alpha-synuclein aggregates in brains of transgenic mice. Movement Disorders. 2014;29:1476-85.
[264] Wahlgren J, Karlson TDL, Brisslert M, Vaziri Sani F, Telemo E, Sunnerhagen P, et al. Plasma exosomes can deliver exogenous short interfering RNA to monocytes and lymphocytes. Nucleic Acids Res. 2012;40:e130-e.
[265] Banizs AB, Huang T, Dryden K, Berr SS, Stone JR, Nakamoto RK, et al. In vitro evaluation of endothelial exosomes as carriers for small interfering ribonucleic acid delivery. Int J Nanomed. 2014;9:4223-30.
[266] Momen-Heravi F, Bala S, Bukong T, Szabo G. Exosome-mediated delivery of functionally active miRNA-155 inhibitor to macrophages. Nanomedicine: Nanotechnology, Biology and Medicine. 2014;10:1517-27.
[267] Tian Y, Li S, Song J, Ji T, Zhu M, Anderson GJ, et al. A doxorubicin delivery platform using engineered natural membrane vesicle exosomes for targeted tumor therapy. Biomaterials. 2014;35:2383-90.
[268] Toffoli G, Hadla M, Corona G, Caligiuri I, Palazzolo S, Semeraro S, et al. Exosomal doxorubicin reduces the cardiac toxicity of doxorubicin. Nanomedicine-Uk. 2015;10:2963-71.
[269] Hood JL, Scott MJ, Wickline SA. Maximizing exosome colloidal stability following electroporation. Anal Biochem. 2014;448:41-9.
[270] Hu L, Wickline SA, Hood JL. Magnetic resonance imaging of melanoma exosomes in lymph nodes. Magn Reson Med. 2015;74:266-71.
[271] Fuhrmann G, Serio A, Mazo M, Nair R, Stevens MM. Active loading into extracellular vesicles significantly improves the cellular uptake and photodynamic effect of porphyrins. Journal of Controlled Release. 2015;205:35-44.
[272] Kooijmans SAA, Stremersch S, Braeckmans K, de Smedt SC, Hendrix A, Wood MJA, et al. Electroporation-induced siRNA precipitation obscures the efficiency of siRNA loading into extracellular vesicles. Journal of Controlled Release. 2013;172:229-38.
[273] Lamichhane TN, Raiker RS, Jay SM. Exogenous DNA Loading into Extracellular Vesicles via Electroporation is Size-Dependent and Enables Limited Gene Delivery. Mol Pharmaceut. 2015;12:3650-7.
[274] Wang L, Chierico L, Little D, Patikarnmonthon N, Yang Z, Azzouz M, et al. Encapsulation of Biomacromolecules within Polymersomes by Electroporation. Angewandte Chemie. 2012;124:11284-7.
[275] Tian X, Nyberg S, Sharp PS, Madsen J, Daneshpour N, Armes SP, et al. LRP-1-mediated intracellular antibody delivery to the Central Nervous System. Scientific reports. 2015;5:11990.

[276] Sanson C, Diou O, Thévenot J, Ibarboure E, Soum A, Brûlet A, et al. Doxorubicin Loaded Magnetic Polymersomes: Theranostic Nanocarriers for MR Imaging and Magneto-Chemotherapy. Acs Nano. 2011;5:1122-40.
[277] Bain J, Ruiz-Pérez L, Kennerley AJ, Muench SP, Thompson R, Battaglia G, et al. In situ formation of magnetopolymersomes via electroporation for MRI. Scientific reports. 2015;5:14311.
[278] Bakhshi PK, Bain J, Gul MO, Stride E, Edirisinghe M, Staniland SS. Manufacturing Man-Made Magnetosomes: High-Throughput In Situ Synthesis of Biomimetic Magnetite Loaded Nanovesicles. Macromol Biosci. 2016;16:1555-61.
[279] Ramos C, Bonato D, Winterhalter M, Stegmann T, Teissié J. Spontaneous lipid vesicle fusion with electropermeabilized cells. FEBS Letters. 2002;518:135-8.
[280] Demange P, Réat V, Weinandy S, Ospital R, Chopinet-Mayeux L, Henri P, et al. Targeted Macromolecules Delivery by Large Lipidic Nanovesicles Electrofusion with Mammalian Cells. Journal of Biomaterials and Nanobiotechnology. 2011;02:527.
[281] Henri P, Ospital R, Teissié J. Content Delivery of Lipidic Nanovesicles in Electropermeabilized Cells. J Membrain Biol. 2015;248:849-55.
[282] Rosenheck K. Evaluation of the Electrostatic Field Strength at the Site of Exocytosis in Adrenal Chromaffin Cells. Biophysical Journal. 1998;75:1237-43.
[283] Retelj L, Pucihar G, Miklavčič D. Electroporation of intracellular liposomes using nanosecond electric pulses-A theoretical study. Ieee T Bio-Med Eng. 2013;60:2624-35.
[284] Rems L, Miklavčič D. Theoretical considerations for the potential of controlled drug release from lipid vesicles by means of electroporation or electrofusion. In: Lacković I, Vasić D, (editors). 6th European Conference of the International Federation for Medical and Biological Engineering, MBEC 2014, 7-11 September 2014, Dubrovnik, Croatia: Springer International Publishing; 2015. p. 797-800.
[285] Denzi A, Valle Ed, Apollonio F, Breton M, Mir LM, Liberti M. Exploring the Applicability of Nano-Poration for Remote Control in Smart Drug Delivery Systems. J Membrain Biol. 2016:1-10.
[286] Kotnik T, Bobanović F, Miklavčič D. Sensitivity of transmembrane voltage induced by applied electric fields—A theoretical analysis. Bioelectrochemistry and Bioenergetics. 1997;43:285-91.
[287] Kotnik T, Miklavčič D. Theoretical evaluation of voltage inducement on internal membranes of biological cells exposed to electric fields. Biophysical Journal. 2006;90:480-91.
[288] Schoenbach KH, Beebe SJ, Buescher ES. Intracellular effect of ultrashort electrical pulses. Bioelectromagnetics. 2001;22:440-8.
[289] Tekle E, Oubrahim H, Dzekunov SM, Kolb JF, Schoenbach KH, Chock PB. Selective Field Effects on Intracellular Vacuoles and Vesicle Membranes with Nanosecond Electric Pulses. Biophysical Journal. 2005;89:274-84.
[290] Scarlett SS, White JA, Blackmore PF, Schoenbach KH, Kolb JF. Regulation of intracellular calcium concentration by nanosecond pulsed electric fields. Biochimica et Biophysica Acta (BBA) - Biomembranes. 2009;1788:1168-75.
[291] Batista Napotnik T, Reberšek M, Kotnik T, Lebrasseur E, Cabodevila G, Miklavčič D. Electropermeabilization of endocytotic vesicles in B16 F1 mouse melanoma cells. Med Biol Eng Comput. 2010;48:407-13.
[292] Batista Napotnik T, Reberšek M, Vernier PT, Mali B, Miklavčič D. Effects of high voltage nanosecond electric pulses on eukaryotic cells (in vitro): A systematic review. Bioelectrochemistry. 2016;110:1-12.
[293] Scheffer HJ, Nielsen K, de Jong MC, van Tilborg AAJM, Vieveen JM, Bouwman ARA, et al. Irreversible electroporation for nonthermal tumor ablation in the clinical setting: a systematic review of safety and efficacy. Journal of vascular and interventional radiology: JVIR. 2014;25:997-1011.
[294] Nuccitelli R, Wood R, Kreis M, Athos B, Huynh J, Lui K, et al. First-in-human trial of nanoelectroablation therapy for basal cell carcinoma: proof of method. Exp Dermatol. 2014;23:135-7.
[295] Yang W, Ahmed M, Elian M, Hady E-SA, Levchenko TS, Sawant RR, et al. Do Liposomal Apoptotic Enhancers Increase Tumor Coagulation and End-Point Survival in Percutaneous Radiofrequency Ablation of Tumors in a Rat Tumor Model? Radiology. 2010;257:685-96.

[296] Goldberg SN, Girnan GD, Lukyanov AN, Ahmed M, Monsky WL, Gazelle GS, et al. Percutaneous Tumor Ablation: Increased Necrosis with Combined Radio-frequency Ablation and Intravenous Liposomal Doxorubicin in a Rat Breast Tumor Model. Radiology. 2002;222:797-804.
[297] Monsky WL, Kruskal JB, Lukyanov AN, Girnun GD, Ahmed M, Gazelle GS, et al. Radio-frequency ablation increases intratumoral liposomal doxorubicin accumulation in a rat breast tumor model. Radiology. 2002;224:823-9.
[298] Rems L, Miklavčič D. Tutorial: Electroporation of cells in complex materials and tissue. Journal of Applied Physics. 2016;119:201101.
[299] Maccarrone M, Bladergroen MR, Rosato N, Agro AF. Role of lipid peroxidation in electroporation-induced cell permeability. Biochemical and Biophysical Research Communications. 1995;209:417-25.
[300] Leguèbe M, Silve A, Mir LM, Poignard C. Conducting and permeable states of cell membrane submitted to high voltage pulses: Mathematical and numerical studies validated by the experiments. Journal of Theoretical Biology. 2014;360:83-94.
[301] Teissié J, Tsong TY. Evidence of voltage-induced channel opening in Na/K ATPase of human erythrocyte membrane. J Membrain Biol. 1980;55:133-40.
[302] Gabriel B, Teissié J. Direct observation in the millisecond time range of fluorescent molecule asymmetrical interaction with the electropermeabilized cell membrane. Biophysical Journal. 1997;73:2630-7.
[303] Golzio M, Teissié J, Rols M-P. Direct visualization at the single-cell level of electrically mediated gene delivery. Proceedings of the National Academy of Sciences. 2002;99:1292-7.
[304] Nematbakhsh Y, Lim CT. Cell biomechanics and its applications in human disease diagnosis. Acta Mechanica Sinica. 2015;31:268-73.
[305] Dahl JB, Lin J-MG, Muller SJ, Kumar S. Microfluidic strategies for understanding the mechanics of cells and cell-mimetic systems. Annual review of chemical and biomolecular engineering. 2015;6:293-317.
[306] Chivukula VK, Krog BL, Nauseef JT, Henry MD, Vigmostad SC. Alterations in cancer cell mechanical properties after fluid shear stress exposure: A micropipette aspiration study. Cell Health and Cytoskeleton. 2015;7:25-35.
[307] Boukany PE, Morss A, Liao W-c, Henslee B, Jung H, Zhang X, et al. Nanochannel electroporation delivers precise amounts of biomolecules into living cells. Nat Nanotechnol. 2011;6:747-54.
[308] Liu C, Xie X, Zhao W, Liu N, Maraccini PA, Sassoubre LM, et al. Conducting nanosponge electroporation for affordable and high-efficiency disinfection of bacteria and viruses in water. Nano Letters. 2013;13:4288-93.
[309] Xie X, Xu AM, Leal-Ortiz S, Cao Y, Garner CC, Melosh NA. Nanostraw–Electroporation System for Highly Efficient Intracellular Delivery and Transfection. Acs Nano. 2013;7:4351-8.
[310] Rosazza C, Deschout H, Buntz A, Braeckmans K, Rols M-P, Zumbusch A. Endocytosis and Endosomal Trafficking of DNA After Gene Electrotransfer In Vitro. Molecular therapy Nucleic acids. 2016;5:e286.

Figure captions

Fig. 1. Schematic of a vesicle exposed to an electric pulse.

Fig. 2. Time sequence of phase contrast images showing deformation and macroporation of GUVs exposed to a DC electric pulse under two different conductivity conditions. (A) shows the tube-like deformation of a GUV, exposed to 200 µs, 2 kV/cm pulse, at conductivity condition χ = 1.38, λ_i = 16.5 µS/cm, λ_e = 12 µS/cm. (B) Shows two disk-like deformation of two GUVs exposed to 300 µs, 3 kV/cm pulse under conductivity condition χ = 0.05, λ_i = 6 µS/cm, λ_e = 120 µS/cm. Time 0 s corresponds to the onset of the pulse. In both cases the pulse duration is comparable to the charging time of the membrane. White arrows indicate locations of macropores. Reprinted with permission from [77]. Copyright 2006 Elsevier. (C) A schematic representation of the semiaxes for determining the aspect ratio a/b of deformed GUVs.

Fig. 3. Sketch of the electric field and induced charge distribution around a GUV immersed in an electrolyte solution, following the imposition of a uniform DC field: (a,b) during the membrane charging phase under condition (a) $\chi > 1$and (b) $\chi < 1$, and (c) after the membrane becomes fully charged. The dashed lines indicate the vesicle deformation. Reprinted with permission from [79]. Copyright 2014 The Royal Society of Chemistry.

Fig. 4. Numerical calculations of the membrane tension for a GUV exposed to a DC pulse under conductivity condition χ = 0.1. Membrane tension is plotted as a function of arclength measured from the vesicle equator (0 and 0.5 correspond to the equator, 0.25 and 0.75 to the poles of the GUV). The images on the right-hand side show the associated vesicle profile at dimensionless time (a) t/t_m = 0, (b) 0.1, (c) 0.17, (d) 0.22 and (e) 0.6, where $t_m = RC_m/\lambda_e$ is a measure for the membrane charging time. The electric field is directed from top to bottom. The numerical results were reported in dimensionless form. For experimental parameters similar to those in Fig. 2A, the electric field strength in dimensional form is ~4 kV/cm and the pulse duration is ~150 µs. Note that the GUV is initially shaped as prolate spheroid since the numerical model assumes conservation of the membrane area and vesicle volume, and thus cannot predict electrodeformations for idealized spheres without any access area. Reprinted with permission from [94]. Copyright 2015 The Royal Society of Chemistry.

Fig. 5. (a) Image sequence of a fluorescently labelled GUV showing formation of macropores on the cathodic side of the membrane. The GUV was exposed to multiple 5 ms, 300 V/cm pulses. Image D1 is acquired after 15 pulses, D2 after 16 pulses, D3 after 17 pulses, etc. (b) Images of three GUVs, denoted as A, B, and C, showing the different mechanisms of lipid ejection: vesicle and tubule formation. The parameters of applied pulses were similar as in (a). Images with index 1, 2, and 3, were captured after application of 0, 12, and 24 pulses, respectively. Reprinted with permission from [80]. Copyright 2009 Elsevier.

Fig. 6. Snapshots from MD showing the creation of a pore in an asymmetric bilayer composed of POPE (green) and POPC (yellow) induced by an electric field. Reprinted with permission from [74]. Copyright 2014 American Chemical Society.

Fig. 7. (a) Confocal fluorescence microscopy (left) and phase-contrast (right) images of the bursting effect of charged GUVs (1:1 PG:PC) in salt solution. Pulse parameters: 1.4 kV/cm, t_{pulse} = 200 µs. (b)

Fast camera image sequence of a bursting GUV, made from lipid extract of human red blood cell membranes. Pulse parameters: 2 kV/cm, t_{pulse} = 300 µs. The scale bar corresponds to 15 µm. Reprinted with permission from [114]. Copyright 2009 The Royal Society of Chemistry.

Fig. 8. Images of a gel phase DPPC GUV with R = 25 µm, before and after the pulse (E = 6 kV/cm, t_{pulse} = 300 µs) in (a,d) DIC, (b,e) confocal, and (c,f) a 3D projection of the upper half of the GUV. Reprinted with permission from [115]. Copyright 2010 The Royal Society of Chemistry.

Fig. 9. Several series of snapshots for the fusion of two vesicles. (a) Fusion of two functionalized GUVs held by micropipettes (only the right pipette tip is visible on the snapshots). A third pipette (bottom right corner) is used to inject a small volume (few tens of nanoliters) of 50 µM solution of $EuCl_3$. The first image corresponding to the starting time t = 0 represents the last snapshot before the adhesion zone of the vesicles undergoes detectable changes. (b) The behaviour of a single GUV (first image) and a GUV couple (remaining images) when exposed to a 150 µs, 1.8 kV/cm pulse in the absence of salt. (c) Behaviour of a single GUV (first image) and a GUV couple (remaining images) in the presence of 1 mM NaCl in the exterior solution. In this case, the GUV couple was exposed to a 150 µs, 3 kV/cm pulse. The polarity of the electrodes is indicated with a plus (+) or a minus (−) sign. The arrows in the first images indicate porated parts of the membrane, which lead to the leakage of enclosed liquid. For both b and c, the starting time t = 0 corresponds to the onset of the pulse. In the last two snapshots of the sequence (b), the fused vesicles contain an array of internal vesicles (bright spots) as indicated by the arrows. Reprinted with permission from [139]. Copyright 2006 National Academy of Sciences.

Fig. 10. Theoretical predictions of selective electroporation of the contact zone in a pair of GUVs. (a) Time course of transmembrane voltage U_m (absolute value) induced in a pair of GUVs with radius of 20 µm, after the onset of a pulse with amplitude of 1 kV/cm. U_m is shown at three points (A, B, and C) indicated on the sketch inside the graph. Note that U_m at the contact zone (C) surpasses U_m on the poles of the GUV pair (A, B) for times up to ~150 µs. (b) Calculations of the electroporated area for pulses with three different durations (10 µs, 150 µs, and 3000 µs). The amplitude of each pulse was adjusted such that the predicted pore density at the contact zone exceeds 10 pores per µm^2. The pore density above 10 pores per µm^2 is indicated by thick red lines. (c,d) Same calculations as in (a,b), but for two GUVs with different size (radius 10 µm and 30 µm). The results were obtained in the same way as in [146], except that the model parameters were adapted to experimental conditions for GUVs. The membrane capacitance was set to 0.67 µF/cm^2, membrane conductivity to 10^{-9} S/m [43], and the radius of the contact zone to 5 µm. The external and internal conductivities are given in the graphs and correspond to pure sugar solution on the outside and sugar solution containing 1 mM NaCl on the inside of the GUVs.

Fig. 11. Repetitive cycles of fusion-to-budding transformation. After the first fusion (t = 12 s), the fused vesicle separates into two daughter vesicles (t = 43 s). The aqueous compartments of the daughter vesicles are separated, but the membranes remain associated, possibly in hemifusion. Therefore, subsequent application of an AC signal after each budding event (t = 94 and 132 s) is already sufficient to induce fusion without the need of applying an elecroporative DC pulse. The vesicles contain 3 mM PEG 6000 (5% wt⁄wt). White arrows indicate the vesicles to be fused. Gray arrows show the neck formation. Scale bar: 10 µm. Reprinted with permission from [204].

Fig. 12. Scheme of the trapping sequence and electrofusion in a microfluidic device. (a) A vesicle fusion trap with integrated electrodes in a sealable microchamber. (b) Without vesicles, fluid flow is allowed through the gaps of the PDMS posts. The fluid flow lines are indicated with blue arrows. (c) The first vesicle trapped occupies the rear of the trap and blocks the central passage from flow. (d) Shows the situation when a second vesicle of equal size enters and the flow is diverted in front of the trap. When a second smaller vesicle is trapped as shown in (e) other vesicles are allowed to enter. (f) Electrofusion is then performed. Note that the vesicles are trapped such that the contact zone between the vesicles is oriented perpendicular to the electric field established between the electrodes. This is crucial for inducing electroporation of the contact zone and consequently electrofusion. Reprinted with permission from [213]. Copyright 2014 The Royal Society of Chemistry.

Fig. 13. Formation and release of an exocytotic vesicle in an artificial cell model. (a–d) Schematics of the microelectroinjection pipette inserted first into the interior of a GUV and then through the opposing wall of the GUV. Afterwards, the micropipette is pulled back in to the interior, followed by spontaneous formation of a lipid nanotube and formation of a vesicle from flow out of the tip of the micropipette. (e) A DIC image of a GUV, with a MLV attached as a reservoir of lipid, microelectroinjection pipette (i), opposite electrode for electric pulse delivery (ii), and 30-µm diameter amperometric electrode bevelled to a 45° angle (iii). A small red line depicts the location of the lipid nanotube. (f–i) Fluid injection at a constant flow rate results in growth of the newly formed vesicle with a simultaneous shortening of the nanotube until the final stage of exocytosis takes place spontaneously and a new vesicle is formed with the attached nanotube. (j–m) Fluorescence microscopy images of fluorescein-filled vesicles showing formation and final stage of exocytosis matching the events in f–i. Scale bar represents 10 µm. Reprinted with permission from [223]. Copyright 2003 National Academy of Sciences.

Fig. 14. Introducing multiple components of microbeads and plasmids into living cells by cell–GUV electrofusion. GUVs including both the plasmid mCherry and fluorescent microbeads were prepared for electrofusion with HeLa cells. After treatment, the cells were cultured for 2 days. Confocal microscopic images show the cross section of the treated HeLa cells into which beads of 0.2 µm, 0.5 µm, and 1 µm diameter (green) had been introduced. The mCherry expression in cells is shown in red, and merged images are shown in the right column. Scale bar = 20 µm. Reprinted with permission from [226].

Fig. 15. (*Left*) Schematic representation of the protocol for electrofusion between GUVs and cells adhered on a glass coverslip. Reprinted with permission from [227]. Copyright 2015 Elsevier. (*Right*) Phase-contrast and fluorescence images of a fish keratocyte cell before and after electrofusion with a GUV. Since the GUV has been fluorescently labelled, the cell membrane becomes fluorescent upon electrofusion. Note also the increase in the membrane area after fusion. Reprinted with permission from [228]. Copyright 2013 Elsevier.

Fig. 16. Schematic of the proposed mechanism for MNP synthesis within polymersomes using electroporation (a), which opens pores within the membrane at which point influx of iron ions occurs in parallel with efflux of NaOH (encapsulated) (b). (c) shows the in situ room temperature co-precipitation that then occurs at the interface within the membrane. Reprinted with permission from [277].

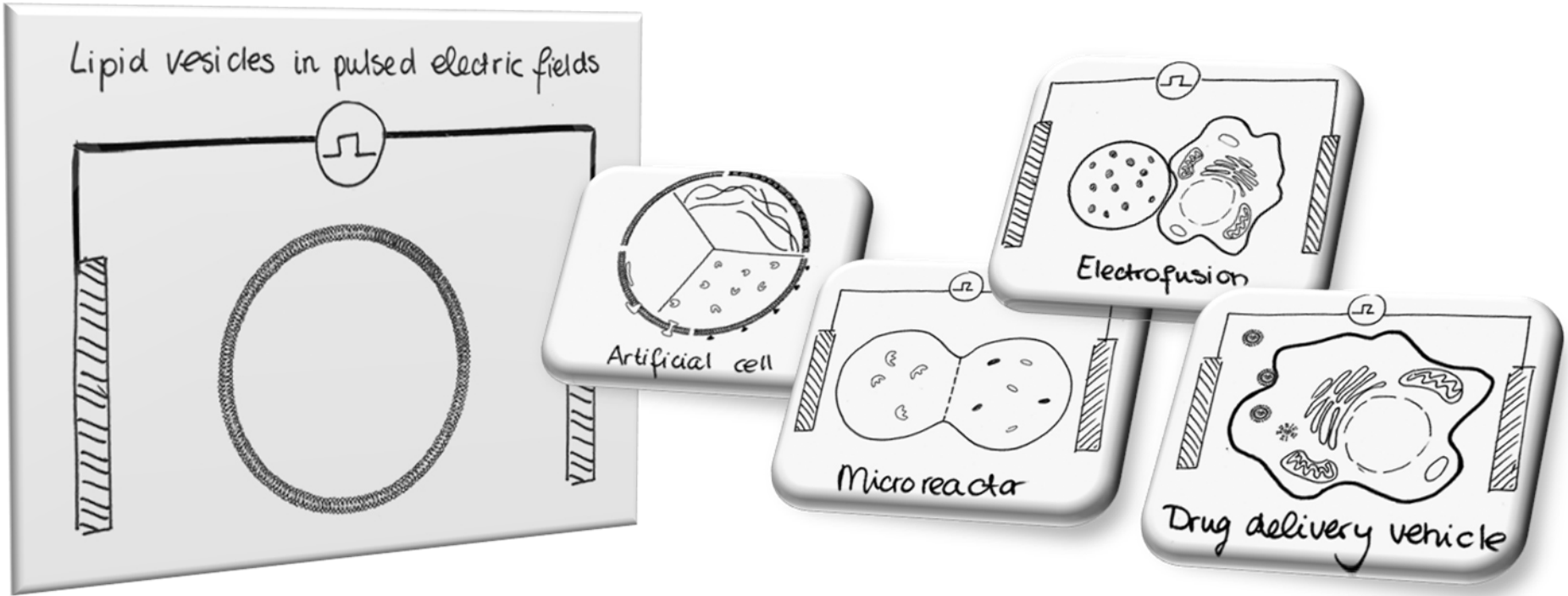
Lipid vesicles in pulsed electric fields
Artificial cell
Electrofusion
Microreactor
Drug delivery vehicle

Lipid vesicles in pulsed electric fields: fundamental principles of the membrane response and its biomedical applications

Dayinta L. Perrier, Lea Rems, and Pouyan E. Boukany*
Department of Chemical Engineering, Delft University of Technology, Delft, 2629HZ, The Netherlands

*) Author to whom correspondence should be addressed. Electronic mail: P.E.Boukany@tudelft.nl

Abstract

The present review focuses on the effects of pulsed electric fields on lipid vesicles ranging from giant unilamellar vesicles (GUVs) to small unilamellar vesicles (SUVs), from both fundamental and applicative perspectives. Lipid vesicles are the most popular model membrane systems for studying biophysical and biological processes in living cells. Furthermore, as vesicles are made from biocompatible and biodegradable materials, they provide a strategy to create safe and functionalized drug delivery systems in health-care applications. Exposure of lipid vesicles to pulsed electric fields is a common physical method to transiently increase the permeability of the lipid membrane. This method, termed electroporation, has shown many advantages for delivering exogenous molecules including drugs and genetic material into vesicles and living cells. In addition, electroporation can be applied to induce fusion between vesicles and/or cells. First, we discuss in detail how research on cell-size GUVs as model cell systems has provided novel insight into the basic mechanisms of cell electroporation and associated phenomena. Afterwards, we continue with a thorough overview how electroporation and electrofusion have been used as versatile methods to manipulate vesicles of all sizes in different biomedical applications. We conclude by summarizing the open questions in the field of electroporation and possible future directions for vesicles in the biomedical field.

Keywords

lipid vesicle, electroporation, electrofusion, artificial cell, microreactor, drug delivery vehicle

Abbreviations

AC, alternating current; CARS, Coherent Anti-Stokes Raman Scattering; DC, direct current; DIC, differential interference contrast; DOPC, dioleoyl-phosphatidylcholine; DOPG, dioleoyl-phospatidylglycerol; DPhPC, diphytanoyl-phosphatidylcholine; DPPC, dipalmitoyl-phosphatidylcholine; EDTA, ethylenediaminetetraacetic acid disodium salt dehydrate; Egg PC, L-α-phosphatidylcholine from egg yolk; EV, extracellular vesicle; GUV, giant unilamellar vesicle; LUV, large unilamellar vesicle; MD, molecular dynamics; MLV, multilamellar vesicle; MNP, magnetic nanoparticle; PDMS, polydimethylsiloxane; PEG, polyethylene glycol; PC, phosphatidylcholine; PE, phosphatidylethanolamine; PG, phospatidylglycerol; POPC, palmitoyl-oleoyl-phosphatidylcholine; POPE, palmitoyl-oleoyl-phosphatidylethanolamine; SUV, small unilamellar vesicle.

Contents

1. Introduction

Biological cells are soft microscopic entities corresponding to a class of active colloidal systems. These living systems exhibit rich mechanical responses in the presence of external forces as a result of far-from-equilibrium interactions between the cells and their surrounding environment. Many of the paramount functions of living cells are governed by the cell membrane, which encloses the cell and separates its “inside” from the “outside”. Traditionally, biologists put tremendous efforts to explain how the cell membrane contributes to the cellular shape, trafficking, motility, and communication by employing top-down approaches [1-3]. In contrast to this classical strategy, biophysicists have succeeded in developing minimal model membrane systems that decipher how cellular membranes behave and interact with intra/extracellular components ranging from nanoparticles, DNA, to proteins such as cytoskeleton [4-7]. In fact, much of our current understanding about cell biology has emerged from such simple model studies [3, 8].

Understanding of the cellular phenomena using fundamental (colloidal) laws based on soft matter physics is still far away. To overcome this issue, lipid vesicles are used as an idealized system to study fundamental biophysical and biochemical cell processes [9]. Lipid vesicles can be prepared in a variety of sizes ranging from tens of nanometres to tens of micrometres, which corresponds to the smallest membrane-enclosed intracellular organelles and to dimensions of almost any type of prokaryotic and eukaryotic cells [10-12]. Based on their size and lamellarity, the vesicles are categorized into four different groups: small unilamellar vesicles (SUVs) with diameters of ~10–100 nm, large unilamellar vesicles (LUVs) with diameters of ~100–1000 nm, giant unilamellar vesicles (GUVs) with diameters >1 μm, and multilamellar vesicles (MLVs) containing multiple bilayers [13]. Various types and mixtures of lipids can be used to prepare the vesicles [14, 15]. Moreover, several techniques are being developed for embedding proteins into the membrane, as well as for encapsulating a wide variety of materials inside the vesicle's aqueous core [16-22]. The versatile character of vesicles in terms of their size, surface functionality, and vesicle interior makes them attractive as simple cell models and ultrasmall biomimetic reactors [23-28]. Furthermore, as lipid vesicles are made from biocompatible and biodegradable materials, they provide a strategy to create safe and functionalized drug delivery systems in health-care applications [29, 30].

Cells and lipid vesicles are also characterized by heterogeneous electrical properties, for which they can be manipulated in electric field. By subjecting cells or vesicles to DC pulses, an electric potential difference (i.e. voltage) builds across the membrane, causing various phenomena. At weak pulses these membrane structures can deform under the influence of the induced electric stresses. At strong pulses, transient pores form in the lipid bilayer, which dramatically increases the membrane permeability. This phenomenon, called electroporation or electropermeabilisation, is nowadays becoming a platform technology for enhancing the transmembrane transport of drugs, genetic material, and other molecules in the areas of medicine, food processing, and in some environmental applications [31-33]. Additionally, electroporation of two cells or vesicles, which are in close proximity, can lead to fusion of the two bodies, allowing one to create hybrid cell-cell, vesicle-vesicle, or cell-vesicle fusion products [34, 35].

In this review, we discuss the responses of lipid vesicles in pulsed electric fields and their biomedical applications. In the first part of the review, we describe how vesicles respond to electric pulses based on theoretical and experimental work on GUVs, concluding with a section about the possibilities to improve the GUV as a model of cell electroporation. The first part complements the previous reviews

[36-39] and covers the recent insights. In the second part of the review, we provide a thorough overview on the use of electric pulses to manipulate GUVs, LUVs, and SUVs in applications related to fundamental biomedical research and clinical medicine.

2. Vesicles as simple models of cells in pulsed electric fields

2.1 The basic principles of membranes in electric fields

2.1.1 Induced transmembrane voltage

The amphiphilic structure of the lipid bilayer makes lipid membranes practically impermeable to ions. In addition, the hydrophobic core of the lipid bilayer is weakly polarizable in an external electric field. Thus, the lipid membrane can be viewed as a thin dielectric layer characterized by practically negligible electrical conductivity and low dielectric permittivity as compared to the surrounding aqueous solutions [40]. The theoretical models, considering the lipid membrane as a thin dielectric layer, have provided an explanation for different phenomena observed in low AC fields including electrorotation, electrodeformation, and dielectrophoretic movement of vesicles/cells [41-44]. Additionally, the models have provided insights into electroporation and electrofusion, both observed when exposing cells or vesicles to strong DC electric pulses [42].

To understand how electric pulses act on a lipid vesicle, first consider an isolated, spherical vesicle exposed to a homogeneous DC electric field (see Fig. 1). The electric field electrophoretically drives the charged particles (ions) in the internal and external solutions, for which the membrane becomes charged similarly as a capacitor. The build-up of charges along the membrane leads to an induced transmembrane voltage (U_m). After a step increase in the electric field intensity E, U_m increases with time according to the Schwan's equation [45]:

$$U_m = 1.5\, ER\cos\theta\left(1 - \mathrm{e}^{-t/\tau_{chg}}\right) \tag{1}$$

Note that U_m is proportional to the vesicle radius R and varies with the angle position θ on the membrane, as shown in Fig. 1, such that it reaches the highest absolute value at the areas facing the electrodes. The characteristic charging time τ_{chg} of the membrane depends on the vesicle radius, membrane capacitance ($C_m \approx$ 0.7 μF/cm [43, 46]), and the conductivities of the internal (λ_i) and external (λ_e) solutions:

$$\tau_{chg} = RC_m\frac{2\lambda_e + \lambda_i}{2\lambda_e\lambda_i} \tag{2}$$

[Here Fig. 1]

If the duration of the exposure to the electric field (*i.e.* the duration of the electric pulse) is longer than the charging time, $t_{pulse} \gg \tau_{chg}$, U_m reaches a steady state, $U_m = 1.5\, ER\cos\theta$. Otherwise, the membrane remains in the charging phase throughout the duration of the electric pulse. In typical experiments with GUVs, where the aqueous solutions consist of dissolved sucrose and glucose ($\lambda_i \approx \lambda_e \approx$ 5 μS/cm [47]), the charging time for a vesicle with radius of 20 μm is about 420 μs. When such GUVs are exposed to electric pulses with duration on the order of 100 μs, the membrane remains in

the charging phase. Upon addition of ions into aqueous solutions, the charging time considerably decreases.

Note that equations (1–2) are valid only for a spherical, nondeformed vesicle, and until the membrane can be considered as electrically nonconductive, i.e., before the membrane becomes electroporated [48, 49]. Furthermore, the equations are valid as long as the dielectric permittivities of the external (ε_e) and internal (ε_i) aqueous solution can be neglected, i.e., for pulse duration considerably longer than the Maxwell-Wagner polarization time $\tau_{MW} = (2\varepsilon_e + \varepsilon_i)/(2\lambda_e + \lambda_i)$ [50]. To determine U_m on deformed or electroporated vesicles, often numerical calculations need to be employed.

2.1.2 Theoretical background on electroporation

Natural pores can be nucleated spontaneously in the lipid membrane due to thermal fluctuations of the lipid molecules. But as the free energy for pore nucleation is much higher than the thermal energy kT (where k is the Boltzmann's constant and T is the absolute temperature), spontaneous occurrence of pores is a very rare event. This free energy can be reduced either by applying lateral (stretching) tension on the membrane or by exposing the membrane to an electric field [51, 52]. Since the bilayer behaves as a dielectric shell, the electric field induces electric stresses on the membrane, which act similarly to a lateral tension, as proposed in different models based on continuum theories [53-55]. If the decrease in the free energy for pore nucleation is governed by electric stresses, the rate of pore nucleation can be written as [56]

$$\nu = A\exp\left(-\frac{\delta_c}{kT} + \frac{BU_m^2}{kT}\right) \tag{3}$$

where δ_c is the nucleation free energy in the absence of U_m, A is a pre-exponential factor and B is a proportionality constant. The free energy δ_c has been estimated to be ~45 kT based on measurements on planar lipid bilayers, however it is expected to depend on the composition of the lipid bilayer [57]. After pore nucleation, the Maxwell stress expands the pores further [58]. Once the electric field is removed, the edge tension (the energy of the pore edge per unit length of the pore circumference) tends to close the pores [59, 60].

During the last decade, molecular dynamics (MD) simulations have provided an additional insight into the molecular mechanisms of pore formation [61]. When the bilayer is exposed to an electric field, the pore nucleation is initiated by formation of a water column spanning the bilayer, which (in typical zwitterionic phospholipid bilayer) is followed by migration of lipid head groups into the wall of the pore [62]. (An example of the pore nucleation sequence taken from MD simulations is shown in Fig. 6.) The average lag time before the onset of pore nucleation is a stochastic variable, but on average the nucleation rate increases exponentially with an increase in U_m [63, 64]. Although in a broader sense, the insights from MD agree with earlier theoretical predictions [65], MD suggest that the pore nucleation is predominantly mediated by the electric-field-driven reorientation of the water dipoles at the water-bilayer interface, and not by tensile electric stresses [64, 66].

Both continuum models and MD simulations indicate that U_m influences the rate of pore nucleation. Hence, it is impossible to theoretically define an absolute critical U_m above which electroporation of the lipid membrane takes place. However, as the nucleation rate increases exponentially with U_m,

electroporation experimentally appears as a threshold-like phenomenon [67]. Thus, it is possible to define a relative threshold as the critical value $U_{m,crit}$ above which electroporation can be detected in a given amount of time and under the given experimental conditions. Additionally, since electroporation is generally detected through a dramatic increase in the membrane permeability and associated molecular transport across the membrane, it is important to note that the pulse parameters influence the growth of the pores, and thus directly control the transmembrane molecular flux. As such, the determined $U_{m,crit}$ depends on the size of the molecular probe and the sensitivity of the detection system [68]. A well-known technique for detecting $U_{m,crit}$ of GUVs is through determining the contrast loss from sucrose-filled GUVs in a glucose environment. Using sucrose in the interior and glucose in the exterior of the GUV leads to a contrast difference when using phase-contrast optical microscopy. However, the presence of the pores allows the sugar molecules to exchange across the membrane, which diminishes the contrast difference after electroporation. Using of this technique $U_{m,crit}$ of fluid phase GUVs is found to be around 1 V [60]. Another method to detect $U_{m,crit}$, recently established by Mauroy et al., is based on detecting the transmembrane transport of manganese ions [68]. With this novel technique they have been able to measure a significantly lower $U_{m,crit}$ of about 6 mV for the same type of GUVs. This extremely low $U_{m,crit}$ is assigned to the small size of the manganese ions, which thus require only small defects in order to cross the bilayer. Moreover, $U_{m,crit}$ of ~650 mV is found for similar type of GUVs by tracking Ca^{2+} influx [69]. It is further worth mentioning that $U_{m,crit}$ is generally determined based on calculating the maximum absolute U_m reached at $\theta = 0$ and π from equation (1). This equation is valid only for a spherical vesicle and does not take into account the shape deformations, which are induced by electric stresses (see Section 2.2.1).

Besides these parameters, that can unintentionally change the measured $U_{m,crit}$, it has also shown that $U_{m,crit}$ can be tuned intentionally. Since both mechanical tension and electric stresses promote pore formation, $U_{m,crit}$ can be reduced by mechanically increasing the lateral tension of the membrane, e.g. by aspirating part of the GUV into a micropipette [54]. For this reason, GUVs which have some initial tension, i.e., GUVs which do not exhibit any visible thermal undulations, electroporate at lower $U_{m,crit}$ [47]. In addition, different membrane compositions influence $U_{m,crit}$. MD simulations showed that $U_{m,crit}$ is to some extent correlated with the thickness of the bilayer [70], though in general, it greatly depends on the detailed architecture of both the lipid head groups and the lipid tails, as well as the lipid phase and the temperature [71-73]. The parameter, on which $U_{m,crit}$ appears to depend predominantly, is the local pressure profile in both the head group and the tail group region, which could affect the mobility of water molecules inside the bilayer [72, 74]. Furthermore, the strong influence of the lipid architecture was also found in MD calculations of the pore nucleation free energy in the absence of the electric field (δ_c in equation (3)) [75, 76]. This shows that the ability of a bilayer to resist poration is an intrinsic property of its constituting lipids. The effect of the lipid composition on the electroporation of GUVs is discussed in greater detail in Section 2.2.3.

2.2 Responses of GUVs in pulsed electric fields

Due to the micrometre size of GUVs, their responses to electric pulses can be monitored and investigated at the microscopic level. In particular, the development of high-speed imaging has dramatically increased the knowledge on the dynamic behaviour of GUVs during and after the

exposure to electric pulses. The basic responses have been determined on GUVs made from zwitterionic phospholipids in the fluid phase such as Egg PC [47, 77, 78] and DOPC [69, 79, 80]. These experiments revealed details on the electrodeformation of the GUVs (Section 2.2.1), which is in high electric fields accompanied by the formation of macropores and lipid loss (associated with electroporation) (Section 2.2.2). Experiments on GUVs made from different lipids and lipid mixtures provided further insights into the effect of the lipid composition on electroporation and the stability of GUVs in an electric field (Section 2.2.3). These observations are outlined below. For completeness we review recent reports together with older data. More comprehensive reviews on this topic (conducted until 2012) can be found in [36-38].

2.2.1 Electrodeformation

The exposure of a GUV to an electric field induces an electrical tension on the membrane, given by the Maxwell stress tensor, which can cause deformation and stretching of the GUV. Depending on the intensity and the duration of the electric pulse, as well as the conductivity of the inner and outer solutions, the shape and the degree of GUV deformation can be significantly varied [36]. Deformation of the GUV is accompanied by an increase in the projected membrane area, which can be categorized into two regimes. For small deformations (low tension), the projected area increases as the weak electric stresses flatten the thermal undulations of the membrane. This regime is often referred to as the entropic regime and is governed by the bending rigidity of the membrane. For stronger deformations (high tension), where all membrane undulations are flattened, the electric stresses lead to elastic stretching of membrane, increasing the area-per-lipid in the bilayer [81, 82]. This regime is governed by the elastic stretching modulus of the membrane. The first studies on GUV electrodeformation were conducted in AC electric fields, which induced ellipsoidal deformations, as predicted by theory [83-88] (see Dimova et al. [36, 37] for reviews). Depending on the frequency of the applied AC field and the ratio between the conductivity of the internal and the external aqueous solutions ($\chi = \lambda_i/\lambda_e$), the GUV can deform into either a prolate or an oblate ellipsoid, with the long axis aligned either parallel or perpendicular to the direction of the electric field, respectively. By measuring electrodeformations of GUVs in AC field, it is possible to extract the information on the mechanical properties of the membrane, such as the bending rigidity [89], and the electrical properties, such as capacitance [46].

Unlike in continuous AC fields, the electrodeformation induced by DC pulses are transient and the GUVs relax back into their spherical shape rapidly after the end of the pulse; therefore, these deformations are experimentally difficult to capture with conventional cameras having a temporal resolution in the millisecond range. The first experimental observations of GUV electrodeformation induced by a 1.2 ms-long pulse were reported by Kinosita et al. [90]. They imaged fluorescently labelled GUVs using a pulsed-laser fluorescence imaging system with a temporal resolution of 100 µs. They observed that, similarly as in AC field, the shape of the deformed GUV depends on the ratio χ; if the internal conductivity is higher than the external conductivity ($\chi > 1$), the GUV deforms into a prolate shape, whereas for $\chi < 1$ the GUV deforms into an oblate shape. These observations were qualitatively corroborated by theoretical work of Hyuga et al. [91, 92]. Later, Riske and Dimova [47, 77] studied the electrodeformation of GUVs exposed to 50–300 µs pulses (where $t_{pulse} < \tau_{chg}$) with a time resolution down to 33 µs, using phase-contrast microscopy and a high-speed digital camera. They observed a similar dependence of the GUV shape on χ, but also highlighted the influence of ions in the external solution. In the absence of ions, the GUVs were deformed into prolate ellipsoids

for $\chi > 1$ [47]. Upon addition of ions, the GUVs were transiently deformed into peculiar cylindrical shapes, again depending on the ratio χ (Fig. 2) [77]. For $\chi > 1$ tube-like shapes were observed analogous to prolate ellipsoids, for $\chi \approx 1$ square-like deformations were reported, and for $\chi < 1$ disk-like deformations were observed comparable to oblate shapes. Such "squaring" of the GUV shape was also noted in the presence of gold nanoparticles [36]. Moreover, Riske and Dimova [47, 77] measured the degree of deformation by determining the aspect ratio a/b of the deformed GUVs (Fig. 2c). They demonstrated that the degree of deformation increases with the increasing electric field strength and/or the pulse duration, while it also depends on the initial tension of the GUV. Sadik et al. [78] further studied the prolate deformations by systematically varying χ (between 1.92 and 53.0). At constant χ the aspect ratio scaled quadratically with the electric field strength, confirming the dominant role of the electric stresses in driving the deformations. With increasing χ at a constant electric field strength, the aspect ratio asymptotically approached a maximum value. Note that in the experiments described above, the electrodeformations were often accompanied by macroporation of the GUV membrane (see Section 2.2.2).

[Here Fig. 2]

Analytical modelling results based on balancing the stresses acting on the GUV membrane (electric, hydrodynamic, bending, and tension) demonstrated that the shape of deformation during an electric pulse relates to the different charging kinetics on the external and internal side of the membrane (see Fig. 3) [93]. If $\chi > 1$, the charges accumulate faster on the internal side and the resulting electric stresses tend to elongate the GUV along the direction of the electric field inducing a prolate deformation (Fig. 3a). On the contrary, if $\chi < 1$, a transient oblate deformation can occur during the charging phase of the membrane, since the charges accumulate faster on the external side, and the electric stresses tend to compress the GUV in the direction of the electric field (Fig. 3b). Once the membrane is fully charged, the accumulated charges on the internal and external sides are balanced, the electric field is expelled from the interior, and the GUV is deformed into a prolate ellipsoid (Fig. 3c). Hence, under the condition $\chi > 1$, the shape deformation can only be prolate, as corroborated by experiments [47, 78]. Under the condition $\chi < 1$, an oblate-to-prolate shape transition is predicted [93]. However, the oblate-to-prolate transition is difficult to observe experimentally, as explained by Salipante and Vlahovska [79]. On one hand, the GUV can attain an oblate shape only during the charging phase of the membrane, $t < \tau_{chg}$. On the other hand, significant deformation can only occur for times longer than the characteristic time in which the electric stresses can deform the GUV during the pulse [93]

$$\tau_{el} = \frac{\mu_e\left(1 + \mu_i/\mu_e\right)}{\varepsilon_0 \varepsilon_e E^2} \tag{4}$$

where μ_e and μ_i are the viscosities of the external and internal solution, respectively. In low electric field, where $\tau_{el} > \tau_{chg}$, the deformation occurs after the membrane is fully charged and only a prolate shape can be observed. In a high electric field, where $\tau_{el} < \tau_{chg}$, the deformation occurs while the membrane is still charging. However, in typical experimental conditions, such an electric field strength leads to electroporation and the associated increase in the membrane conductivity. If the membrane becomes conductive, theory predicts that the GUV can remain oblate when $\chi < 1$ [91, 92, 94]. To demonstrate experimentally the oblate-to-prolate transition, Salipante and Vlahovska [79] used a double-pulse protocol consisting of a strong 20 µs pulse followed by a longer 50 ms pulse

with a lower intensity. The first pulse was strong enough to induce an oblate deformation but short enough to avoid electroporation, whereas the second pulse allowed full charging of the membrane leading to a prolate deformation. More complex numerical models based on electrohydrodynamic principles further corroborated the predicted oblate-to-prolate transition, and in addition revealed more complicated shapes of GUVs, including the squared shapes [94-97], resembling those observed by Riske and Dimova [77]. In summary, electrodeformation of a GUV during the pulse is dynamic and depends on the pulse duration, strength, presence of ions in the external solution, conductivity ratio χ, and membrane electroporation. As it is challenging to model the highly nonlinear dependence of pore nucleation and pore growth on U_m and associated tensile stresses, as well as the ionic and fluid exchanges across the pores, current models of GUV electrodeformation are either limited to treatment of a nonconductive membrane and are strictly valid only before the onset of electroporation [93-97], or consider a simplified case of a completely conductive membrane and are based on semi-empirical treatment of the hydrodynamic forces [78, 91, 92].

[Here Fig. 3]

After the exposure of a GUV to an electric pulse, which leads to electrodeformation, the GUV relaxes back to the spherical shape (in the absence of electric field). Provided that the GUV has not been electroporated, the characteristic relaxation time depends on the stretching regime attained by the membrane during the pulse. Relaxation of an elastically stretched GUV proceeds with a characteristic time on the order of 100 μs [47], whereas relaxation of membrane undulations strongly depends on the initial (pre-pulse) tension of the GUV. Yu et al. [98] theoretically analysed relaxation of GUVs deformed in the second (entropic) regime and showed that such analysis can be applied to measure the bending rigidity and the initial membrane tension of GUVs.

2.2.2 Electroporation: macropores and lipid loss

When applying weak electric pulses, a GUV can be electrodeformed in the absence of detectable electroporation, as discussed above. By increasing the intensity and/or duration of the electric pulse, electrodeformation becomes accompanied by electroporation of the GUV membrane. Experiments on GUVs have shown two interesting phenomena associated with electroporation, which are not observed in living cells: the creation of micrometre-sized pores (macropores) and the expel of lipids from the GUV membrane [47, 69, 77, 80, 90]. Kinosita et al. [90] reported that formation of macropores was preceded by a measurable increase in the membrane conductivity, indicating the presence of optically-undetectable nanoscale pores. Thus they postulated that macropores could arise from growth or coalescence of smaller pores, or as a consequence of electrodeformation. In the following studies, the formation of macropores was linked to the increase in the membrane tension caused by the electric field [47, 60]. As inferred from the measurements on GUVs aspirated into a micropipette, when the membrane tension exceeds a critical value called the lysis tension, the bilayer ruptures due to unlimited growth of unstable pore(s) [99]. Unlike in the aspiration experiments where the tension imposed on the membrane is controlled by the micropipette, the tension induced by an electric field relaxes as the pores grow and the fluid leaks out from the GUV [60, 100]. Therefore, large macropores can form without disintegrating the membrane. The value of the lysis tension depends on the lipid composition and varies roughly between 3 and 10 mN/m for phospholipid fluid GUVs [54, 101], although it also depends on the time and rate at which the tension is imposed [99, 102, 103]. To compare the electric tension σ_{el} induced on the membrane at given U_m with the lysis tension σ_{lys} Needham and Hochmuth proposed a simple derivation [54]

$$\sigma_{el} = \frac{1\varepsilon_m}{2h_e}\left(\frac{h}{h_e}\right) {U_m}^2 \quad (5)$$

where ε_m and h_e represent the dielectric permittivity and the thickness of the hydrohobic lipid core, respectively, whereas h represents the total thickness of the membrane. By inserting typical values for fluid phospholipids ε_m = 2·10^{-11} F/m, h_e = 2.8 nm, and h = 3.9 nm, the lysis tension of 5 mN/m is reached at $U_m \approx$ 1 V [54]. This was corroborated by the experimental observation of macropores at $U_m \approx$ 1 V when exposing GUVs to an electric pulse with a duration in the order of 100 µs [47, 54].

Under the conditions which lead to prolate deformation of a GUV, macropores are generally formed near the poles of the GUV, where the highest U_m and largest electrical tension are predicted based on theory [47, 78, 95]. Compared with non-macroporated GUVs, macroporated GUVs attain a higher aspect ratio during the pulse and relax more slowly back to spherical shape after the pulse [47]. The post-pulse relaxation of the GUV shape is governed by the closure of macropores, which takes about 10 ms to few 100 ms, depending on the size of the macropores and the residual membrane tension [47, 60]. The velocity of pore closure is determined by the interplay between the edge tension of the pore and the leak-out of the internal fluid from the GUV [47, 59, 60]. The analysis of the closure kinetics of macropores thus provides a method for measuring the edge tension in GUVs with different lipid compositions [60]. Additionally, since the leak out of the internal fluid depends on the viscosity of this fluid, the pore closure can be slowed down by increasing the viscosity, e.g. by adding glycerol to water [100].

When cylindrical deformations occurred, Riske and Dimova observed macropores at the corners of the deformed membrane (as indicated in Fig. 2 with white arrows) [77]. McConnell et al. [94, 95, 104] attempted to theoretically understand this observation by numerically calculating the time-dependent evolution of the induced membrane tension (Fig. 4). The results showed that when the GUV deforms into a cylindrical shape, the highest positive (stretching) tension is induced at the corners of the deformed GUV (Fig. 4c), which is expected to promote formation and growth of pores in these regions. If the membrane does not porate at this point of time, the highest tension shifts to the poles of the GUV (Fig. 4d-e). Indeed, Portet and Dimova [60] used similar experimental conditions as in Fig. 2b, but they exposed the GUVs to longer 5 ms pulses with lower intensity and captured macropores at the poles of the GUVs towards the end of the pulse. Note that the tension shown in Fig. 4 is not equal to the one in equation (5), but was determined numerically by a more rigorous calculation of the electric and hydrodynamic stresses acting on the membrane. More specifically, the tension in Fig. 4 corresponds to the Lagrange multiplier that enforces incompressibility of the membrane area [94].

[Here Fig. 4]

Several reports further showed an asymmetric pattern of the pore distribution [60, 69, 80, 90]. Kinosita et al. [90] reported that macropores in asolectin (soybean phospholipid) GUVs formed preferentially on the side facing the positive electrode (anode). In contrast, Tekle et al. [69] observed that macropores preferentially formed on the side facing the negative electrode (cathode) in DOPC GUVs. Macropores were rarely found on the anodic hemisphere, but the results suggested that the anodic side is permeabilized by a greater number of smaller (optically undetectable) pores [69]. Preferential macroporation of the cathodic side was also observed by Portet et al. in DOPC and Egg PC vesicles [60, 80]. Furthermore, both Tekle et al. [69] and Portet et al. [60, 80] detected

macropores in combination with a reduced size of the GUVs after the pulse. The size reduction can be attributed to the expel of lipids in the form of small vesicles and/or tubules, as reported by Portet et al. [80] based on imaging of fluorescently-labelled GUVs (Fig. 5). In some cases, multiple pulses were applied to detect visible lipid ejection, and by increasing the number of pulses, the size of the GUVs progressively decreased [80]. Mauroy et al. [105] showed similar lipid ejection by use of CARS microscopy, confirming that lipid loss is not an artefact of membrane labelling. Moreover, they demonstrated that lipid loss is controlled by the pulse duration and can be detected at a significantly lower electric field when GUVs are exposed to 5 ms pulses compared to 100 µs pulses. Portet et al. [80] assumed that the amount of ejected lipids is proportional to the permeabilized membrane area, showing good agreement with the experimental results, whereas Sadik et al. [78] reported a correlation between the post-pulse reduction in the membrane area and the aspect ratio attained by GUVs during electrodeformation. However, the mechanisms responsible for the asymmetric distribution of pores and lipid ejection are not yet completely understood. It also remains unclear whether electroporation and lipid loss are either coincident or interrelated phenomena. For instance, tubule formation can also be observed in GUVs exposed to non-electroporating AC fields [106]. Theoretical works on the instability of a lipid membrane in an electric field suggested that a bilayer can undergo undulations with an increasing amplitude [107-111], which may eventually lead to tubulation and loss of lipids. When the membrane is separating fluids with an equal conductivity and permittivity, such a membrane instability could result from ionic currents in the electric double layer next to the membrane surface [108, 109]. When the membrane is separating fluids with asymmetric electrical properties, particularly different conductivities, such an instability could also be a consequence of the transient mismatch between the ionic accumulation at the two sides of the membrane [110, 111]. These instabilities were predicted both for a nonconducting and a conducting (electroporated) membrane.

[Here Fig. 5]

2.2.3 Influence of membrane composition on electroporation

One of the main advantages of using vesicles is that the membrane composition can be controlled and thus the mechanical properties can be tuned. So far, the lipids of all systems discussed in this review have been in the fluid phase (or liquid-disordered phase), where the lipids possess high mobility and chain disorder. Lowering the temperature below the transition temperature of a lipid, brings the lipid in the so-called gel phase (or solid-ordered phase), where the lipids are tightly packed and exhibit low mobility. The transition temperature varies with different types of lipids, whereby some lipids exist in the fluid and others in the gel phase at room temperature [112]. Therefore, a simple method to change the mechanical properties of the membrane is to select a lipid with a different phase or create a two-phase system with both liquid and gel domains. The addition of cholesterol to fluid phase lipids brings the lipids in an intermediate phase, the liquid-ordered phase. Cholesterol organizes the hydrophobic core of the membrane causing ordering of the lipids while maintaining the lateral mobility [113]. Mixing cholesterol in a binary mixture of lipids induces a two-phase liquid system of liquid-ordered, containing saturated lipids and cholesterol, and liquid-disordered domains, containing unsaturated lipids and possibly a low level of cholesterol. Below, we discuss the influence of altering the lipid composition of the membrane on the critical U_m at which electroporation is detected (i.e. $U_{m,crit}$). This influence has been studied both at the molecular level by the use of MD simulations, and at the microscopic level by the use of GUVs.

Both MD simulations and experiments on GUVs demonstrated that $U_{m,crit}$ in fluid phase lipids depends on the structure of the lipid tails as well as the head groups. MD simulations indicated that for lipids with a PC head group, $U_{m,crit}$ increases with the chain length of the lipid tails [70]. In contrast with simulations, Mauroy et al., studied GUVs from different PC lipids experimentally, showing no influence of the hydrophobic chain length on $U_{m,crit}$ [68]. Apart from the influence of the chain length, MD simulations also demonstrated a considerate effect of methyl branches in the lipid tails, as well as the type of linkage between the head group and the carbonyl region [73]. Polak et al. observed that $U_{m,crit}$ increases, respectively, in linear-chained DPPC lipids, methyl-branched DPhPC with ester linkages, and DPhPC with ether linkages, all in the fluid phase. Based on their analysis, they proposed that the presence of methyl branches could reduce the mobility of water molecules in the hydrophobic core and hence increase $U_{m,crit}$. Additionally, Polak et al. also studied $U_{m,crit}$ of archaeal lipids, which have the same tail structure as DPhPC-ether lipids, whereas the archaeal head groups are formed by large sugar moieties [72]. Compared with DPhPC-ether, archaeal lipids exhibit higher $U_{m,crit}$, associated with stronger interactions between the archaeal head groups. $U_{m,crit}$ was decreased when archaeal lipids were mixed with DPPC. Similarly, Gurtovenko and Lyulina showed higher $U_{m,crit}$ in a POPE lipid bilayer with respect to POPC [74]. Higher $U_{m,crit}$ has been attributed to the primary amines in the POPE head groups capable of intra and intermolecular hydrogen bonding, in contrast to the choline moieties in the POPC head groups. POPE lipids are thus packed more densely than the POPC lipids, which hinders the penetration of water molecules in the bilayer and slows down the reorientation of the lipid head groups into the pore, as shown in Fig. 6. Mixing these two lipids in an asymmetric bilayer (POPE in one and POPC in the other leaflet) results in $U_{m,crit}$ in between the $U_{m,crit}$ of pure POPC and POPE. Besides the physical properties of the lipids, also the effect of the membrane charge was studied. When the negatively charged GUVs consisting of PC and PG lipids (1:1 ratio) were exposed to an electric pulse, a bursting effect was observed, as reported by Riske et al., and shown in Fig. 7 [114]. Despite the lack of understanding of this bursting effect, they were able to prevent the bursting effect by the addition of EDTA. However, the mechanism of the stabilizing effect of EDTA remains unknown.

[Here Fig. 6]

[Here Fig. 7]

Several studies have further shown that $U_{m,crit}$ in gel phase GUVs is higher than in fluid phase GUVs. Knorr et al. used a classical method to determine $U_{m,crit}$ based on the contrast loss of the GUV [115]. $U_{m,crit}$ of gel phase DPPC GUVs was found to be at 9.8 ± 1.1 V, compared to the 1 V for the liquid phase POPC GUVs, which they attributed to a higher bending rigidity and thickness of the gel phase membrane. The observed pores appeared to be arrested (irreversible) and were often visualized as cracks (see Fig. 8). Additionally, they reported the deformation dynamics of the gel phase GUVs during the pulse below $U_{m,crit}$. The GUVs show only small deformations below the electroporation threshold, and show a so-called intra-pulse relaxation of their deformation already during the pulse. Moreover, the deformations of these gel phase GUVs were expressed as wrinkling of the membrane instead of the ellipsoidal deformations occurring in fluid phase lipids [115]. A more detailed study by Mauroy et al. on $U_{m,crit}$ of different GUVs has elucidated that the phase state, and not the membrane thickness, plays the decisive role in the increased $U_{m,crit}$ of gel phase GUVs with respect

to fluid phase GUVs [68]. The increased $U_{m,crit}$ of gel phase GUVs with respect to fluid phase GUVs is also supported by Liu et al., who determined $U_{m,crit}$ by detecting the release of 5(6)-Carboxyfluorescein (5(6)-CF) [116]. Additionally, when mixing fluid and gel phase lipids, Liu et al. reported a decrease in the membrane permeability with an increasing percentage of gel phase lipids [116]. Recently, Majhi et al. also reported an increase in $U_{m,crit}$ when going from liquid to gel phase lipids, based on results from MD simulations [71]. Additionally, they observed slower pore resealing dynamics for DPPC in the gel phase than in the fluid phase, which shows a correlation with the experimental studies of Knorr et al. [115].

[Here Fig. 8]

As cholesterol is added to the system, the lipids organise in the liquid-ordered phase [117]. The cholesterol organizes itself in the hydrophobic core of the bilayer, where it can condense the lipids and it can alter the mechanical properties of the membrane, such as the thickness, the bending stiffness and the fluidity [118]. However, the addition of cholesterol does not always lead to the same results. Depending on the concentration of the cholesterol and the architecture of the lipid, cholesterol can either decrease or raise the electroporation threshold [60]. Also, mechanical studies on bilayers have shown the non-universal and lipid-specific effect of cholesterol [89, 119, 120]. Recent studies of Mauroy et al. have shown that an increasing concentration of cholesterol on POPC leads to a higher $U_{m,crit}$, whereas this increased cholesterol shows no significant influence on $U_{m,crit}$ of Egg PC [68]. Similar results for Egg PC have been shown before by Portet and Dimova [60]. In addition, they reported that increasing cholesterol could decrease $U_{m,crit}$ for DOPC vesicles. Surprisingly, the experimental results on the effect of cholesterol on $U_{m,crit}$ of different lipid bilayers have not been fully supported by MD simulations. Simulations on the effect of cholesterol on $U_{m,crit}$ of POPC show similar results as found experimentally on GUVs [121]. Nevertheless, MD simulations of Fernandez et al. on DOPC showed an increase of $U_{m,crit}$ when adding cholesterol [122], which is in disagreement with the experimental results on GUVs [60]. Overall, the influence of cholesterol on $U_{m,crit}$ of a lipid bilayer is non-universal and strongly dependent on the architecture of the lipids.

By mixing two different lipids together with cholesterol, coexisting liquid-ordered and liquid-disordered phases can occur in the membrane. Van Uitert et al. studied this effect of cholesterol on $U_{m,crit}$ in planar bilayers made from binary lipid mixtures [117]. They observed that the effect of cholesterol on $U_{m,crit}$ is dependent on the cholesterol percentage. At low percentages, $U_{m,crit}$ decreased slightly with respect to $U_{m,crit}$ of the pure binary mixture without cholesterol. However, above a certain threshold percentage, $U_{m,crit}$ increased together with the increase in cholesterol. From the experimental results it is difficult to interpret the molecular mechanisms of this biphasic influence of cholesterol percentage on $U_{m,crit}$. With MD simulations on heterogeneous membranes, Reigada showed that the probability of pore formation is highest in the middle of the liquid disordered phase [123].

2.3 Electrofusion

Fusion of biological membranes is a ubiquitous phenomenon in nature, which for example occurs in exocytosis, fertilization, muscle fibre and bone development, tissue regeneration, viral infection, and carcinogenesis [124-126]. Since spontaneous fusion is prevented by large electrostatic and hydration repulsive forces between the membranes, nature utilizes specialized membrane proteins, which

facilitate and control the fusion process [127-129]. Artificially, fusion can be induced by virus-based methods [130], by chemical methods such as the addition of polyethylene glycol (PEG) [131], by ultraviolet laser [132], or by electroporation-mediated fusion [42]. Artificial fusion between two cells of different types enables one to create a hybrid cell which expresses the properties of both parental cells. Electric-field induced fusion (i.e. electrofusion) has gained notable attention particularly for preparing monoclonal-antibody-producing hybridoma cells and cell vaccines for cancer immunotherapy (reviewed in [133]), for cloning organisms such as Dolly [134], and in the treatment of diabetes [135]. Similarly, electrofusion can be obtained between two different GUVs or between GUVs and cells. Applications of GUV-GUV electrofusion and cell-GUV electrofusion are described in Sections 3.1.2 and 3.1.5, respectively.

Membrane electrofusion can be induced provided that two conditions are met: the membranes need to be in close contact and the membranes need to be destabilized in the contact zone. In electrofusion experiments, GUVs (and/or cells) are most often brought into contact by low-intensity AC electric field, which arranges the GUVs into structures mimicking pearl chains [42]. The pearl-chain formation is a consequence of the GUV movement in the non-homogeneous field because, in a suspension of GUVs, the local field around each GUV is distorted by the presence of other GUVs [44]. Such movement is called dielectrophoresis. If the frequency and the intensity of the AC field are appropriate, the electrostatic interaction forces between individual GUVs are attractive and the GUVs align in a linear fashion with respect to the direction of the applied electric field [42]. Among other methods of establishing contact between the GUVs are the addition of agglutinating agents like PEG [136], or the mechanical manipulation by optical tweezers and microelectrodes [137].

The destabilization of the membranes, as the second condition for electrofusion, is achieved by electroporation of the membranes in the contact zone using strong DC electric pulses. The exact molecular mechanisms of how membrane electroporation facilitates fusion are not completely understood. Sugar et al. [138] have proposed a model, which considers that the electric field induces pores spanning across both of the adjacent membranes in the contact zone. Namely, the nucleation of a pore in one of the bilayers could locally increase the electric field and promote nucleation of another pore in the adjacent bilayer. If large numbers of such double-membrane pores are nucleated, these pores could coalesce into larger loop-like and tongue-like cracks. When the electric field is removed, the membrane parts surrounded by loop-like cracks could finally separate to form vesicles. Additionally, unstable membrane undulations induced under an electric field could facilitate local contacts between the adjacent bilayers followed by membrane merging [108-111].

High-speed optical imaging (time resolution of 50 μs) of the electrofusion process between two GUVs demonstrated that in the absence of salt in the aqueous solutions, several double-membrane pores (fusion necks) typically form in the contact zone during the pulse (Fig. 9b) [139, 140]. Expansion and subsequent coalescence of these fusion necks lead to the formation of small contact-zone vesicles, which remain trapped in the interior of the fused GUV. On the contrary, no vesicles are observed, if the GUVs are electrofused in the presence of 1 mM NaCl in the external solution, which suggests that a single or very few fusion necks form during the pulse (Fig. 9c). The expansion of the fusion neck is initially very fast (about 4 cm/s) and after ~1 ms slows down as the opening of the neck decreases the membrane tension. The value of the initial velocity implies that the formation of a single fusion neck can be completed in a few hundred nanoseconds after the onset of the applied electric pulse [139]. Interestingly, when fusion is induced between two GUVs functionalized with synthetic ligand

molecules that mimic the action of fusion proteins, the opening of the fusion neck exhibits similar kinetics (Fig. 9a).

Apart from the influence of ions, electrofusion is also influenced by the physicochemical properties of the membrane. Stoicheva et al. have reported that GUVs made from negatively charged lipids are more difficult to fuse than GUVs made of zwitterionic lipids, possibly because of larger repulsive forces between the charged lipids [141]. The inhibiting effect on the electrofusion between GUVs has also been observed in the presence of cadmium ions, presumably because they increase the membrane rigidity, which hinders the opening of the fusion neck [142].

[Here Fig. 9]

While high-speed optical microscopy allows imaging of the electrofusion process with a temporal resolution of tens of microseconds, it cannot provide the information on the processes occurring in the microsecond or submicrosecond time-scale after the onset of an electric pulse. Theoretical calculations are useful for revealing more details on U_m and the electroporation kinetics before fusion. Calculations of U_m induced on the membranes of a pair of GUVs in contact have shown that U_m at the contact zone depends on the GUV geometry (spherical or ellipsoidal shape) and the ratio $\chi = \lambda_i/\lambda_e$ between the conductivities of the internal and external aqueous solutions [143, 144]. Let us first consider two spherical GUVs of an equal size. When the membranes become fully charged and U_m reaches the steady state, the absolute value of U_m established at the contact zone is lower than at the poles of the GUV pair facing the electrodes (cf. lines A, B, and C in Fig. 10a). This suggests that, if the electric pulse is long enough for U_m to reach the steady state, electroporation of the contact zone is accompanied by electroporation of the poles of the GUV pair. However, immediately after the application of an electric pulse, while the membranes are still in the charging phase, U_m strongly depends on χ. If the internal conductivity is lower than the external conductivity ($\chi < 1$), the highest U_m always establishes at the poles of the GUV pair (not shown). On the contrary, if the internal conductivity is higher than the external ($\chi > 1$), the highest U_m transiently establishes at the contact zone (Fig. 10a). This indicates that if $\chi > 1$ and if the pulse duration is short enough, it is possible to achieve selective electroporation of the contact zone, which is exactly the condition required for inducing vesicle electrofusion. This is corroborated by numerical calculations of the density of pores, which form along the membrane, as predicted by a theoretical model of electroporation (Fig. 10b) [145]. Similar results can be observed if the GUVs in contact are spherical but of a different size (Fig. 10c,d) [146], or if the GUVs have ellipsoidal shapes caused by electrodeformation [147]. The theoretical results indicate that selective electroporation of the contact zone can be obtained for a range of pulse durations, but this range depends on the size and shape of the GUVs, and the ratio as well as the absolute values of the internal and external conductivities. Under low-conductivity conditions in which GUVs are typically electrofused, a pulse duration in the order of 10 µs would be appropriate (Fig. 10). The theoretical predictions of course have practical significance only if such short pulses are sufficient to induce electrofusion. Indeed, experiments on cells have demonstrated that the application of 20 pulses as short as 50 ns can induce electrofusion [146]. In addition, the formation of the fusion neck could indeed occur within hundreds of nanoseconds [139], as discussed above. Overall, the results suggest that by appropriately tuning the pulse duration, it is possible to induce electrofusion between GUVs while preventing any leakage from the vesicle interior, regardless of the GUV size and shape. This is

relevant, for example, when studying biochemical reactions by electrofusing GUVs, as discussed in Section 3.1.2.

[Here Fig. 10]

2.4 Approaching towards more realistic cell models

GUVs have provided unique opportunities to investigate the fundamental mechanisms of electroporation and electrofusion of cells, and the pulse-induced molecular transmembrane transport. However, several profound phenomena observed on GUVs show discrepancies compared to the observations seen on living cells. (i) Macropores have never been visualised in living cells [90]. (ii) The membrane of a GUV typically reseals and retains its impermeability within hundreds of milliseconds after pulse application [69], whereas cell membrane resealing often takes place for few minutes [148]. (iii) Lipids loss can be observed in GUVs [80], whereas cells can osmotically swell or shrink after pulse application [149, 150]. (iv) A profound difference is also observed in the mechanism of DNA transport across the electroporated membrane. DNA enters the GUV during the pulse via an electrophoretic mechanism [151], whereas in cells the DNA forms a complex with the cell membrane and most likely translocates the membrane via an endocytotic mechanism [152].

As shown above, the GUV is a simplified model of the cell. However, a GUV can be easily modified in its composition, implying the possibilities of extending this model closer towards a real cell, by increasing the GUV's complexity [153]. Cell membranes contain an asymmetric composition of a variety of lipids and cholesterol, coexisting in different lipid phases. The lipid bilayer serves as a matrix for membrane proteins, which constitute about half of the mass of a typical cell membrane [154, 155]. Furthermore, cell membranes are under an intrinsic tension due to cytoskeleton attachments [156]. The intracellular and extracellular milieus contain high concentrations of salt (about 150 mM), together with dissolved proteins and nucleic acids [154]. The cytoplasm is a crowded, compartmentalised environment with numerous membrane-bound organelles [155]. As the science of implementing these complex systems into the GUV improves, the mechanisms of pulse-induced effects on real cells can be elucidated further. Below we discuss the possibilities for extending the GUV as a model for the real cell.

The first method to increase the complexity of the GUV, as already discussed above, is to adjust the membrane composition and study GUVs containing lipid mixtures [116], cholesterol [60, 68], or GUVs made from natural lipid extract [114]. Additionally, methods of GUV preparation under physiological conditions (≥ 140 mM) have been developed [23, 157-161]. The techniques of GUV preparation have exceeded even further, enabling the preparation of much more complex GUV structures [3]. On the one hand, a complex membrane structure can be controlled by embedding membrane proteins [17, 18, 162, 163] and preparing controlled asymmetric membranes [164, 165]. On the other hand, biomaterials can be encapsulated by the GUVs, such as the actin cytoskeleton [166-169], enzymes [170] and gel-like materials mimicking the cytoplasm [171, 172]. Lira et al. have already shown that agarose encapsulated inside a GUV strongly affects both the electrodeformation and the pore dynamics, while maintaining the lateral diffusion of the lipids [173]. Therefore, it can be concluded that the electroporation mechanism is strongly influenced by the inner part of the GUVs. Simultaneously, this system is a great way to immobilize the GUV for a long-time study on, for example, the diffusive response of membrane proteins due to an electrical pulse [174]. From results

on living cells, it is also expected that the cytoskeleton plays an important role in both the resealing of the membrane [175, 176] and in the gene electrotransfer through the membrane [152, 177-179]. Adding the cytoskeleton motors (dynein, kinesin and myosin) could possibly also reveal the mechanisms by which the genetic material is transported from the cell membrane to the nucleus [152, 179].

3. Vesicle electroporation and electrofusion in biomedical applications

Electroporation and electrofusion offer a wide range of possibilities for vesicle manipulation. In Section 2, we primarily focused on using GUVs as simple models for studying the interaction of the cells with an electric field. Here, we address the use of electroporation and electrofusion for manipulating vesicles for biomedical applications. The utility of vesicles in biomedical applications largely depends on the vesicle size. GUVs are ideal candidates for *in vitro* investigations since they can be easily visualised by light microscopy, as well as transported and handled inside the observation chamber by optical tweezers or micropipettes. In addition, GUVs are particularly suitable for mimicking a cell-like environment due to their similar size and curvature. However, GUVs are generally too large to be used for therapeutic purposes. For *in vivo* delivery of drugs and other promising pharmaceuticals, submicron vesicles need to be used, since these vesicles are small enough to cross the biological barriers inside the body and deliver their cargo to the target tissue [180]. Accordingly, we discuss the use of electroporation and electrofusion for manipulating GUVs and submicron vesicles (SUVs and LUVs) in Sections 3.1 and 3.2, respectively.

3.1 Applications of electroporation and electrofusion of GUVs

3.1.1 Encapsulation of biomolecules into GUVs with electroporation

Most commonly, the GUVs are encapsulated with the desired compound already during the vesicle preparation procedure. Nevertheless, electroporation can be used as an alternative method to load GUVs with selected biomolecules after the formation process. In general, electroporation provides a simple means for delivering molecules into GUVs, regardless of how the GUVs are prepared and without the need of any sophisticated equipment. Portet et al. [151] have studied electroporative uptake of plasmid DNA (4.7 kbp) into GUVs made from Egg PC and have observed that the DNA enters the GUV predominantly by an electrophoretic mechanism. Electroporation of GUVs is, therefore, practical for loading charged biomolecules. The amount of loaded compounds can be tuned by adjusting the amplitude, duration, and number of the applied electric pulses. They have also developed a model for predicting the amount of transferred DNA as a function of the parameters of the applied electric pulses [151].

Electroporation can also promote the insertion of some type of membrane proteins and peptides into the bilayer membrane [181-186]. The so-called electroinsertion has received a lot of interest for "engineering" the membranes of living cells by electroinserting receptor molecules (e.g. antibodies or enzymes) and use the cells as biorecognition elements to detect superoxides [187, 188], viruses [189, 190], and toxins [191]. Raffy et al. [192-194] have demonstrated that electroinsertion of glycophorin A can be achieved in gel-phase (DPPC) and fluid-phase (Egg PC) GUVs and MLVs. However, they have observed that unlike in cell membranes, electroinsertion in vesicles is strongly controlled by the surface charge of the membrane; electroinsertion of glycophorin is completely inhibited in the presence of negatively charged phosphatidylserine (30% or more) or positively charged stearylamine (as low as 2%) [195]. For this reason, electroinsertion can perhaps be effectively employed only in

lipid vesicles with a certain lipid composition. Further investigation into electroinsertion of membrane proteins and peptides into lipid vesicles may have implications in the field of biosensing, where biochips based on vesicle arrays show great promise as platforms for high-throughput screening of membrane proteins, for the purposes of diagnostics and drug discovery [196]. Namely, membrane proteins play a key role in the treatment of diseases, since about 60% of currently available drugs are targeting membrane protein species [197].

3.1.2 Electrofusion of GUVs: microreactors and models of primitive cells

Almost two decades ago, Orwar et al. [27, 35] proposed that sequential electrofusion between giant vesicles, comprising different membrane and interior compositions, could be employed for creating hybrid vesicles with a higher complexity or to study complex reactions inside the vesicles. In the light of their ideas, electrofusion between GUVs has later been used for a variety of purposes. Dimova et al. [37, 140] have shown that electrofusion between GUVs with a different lipid composition can be used to prepare multicomponent vesicles. If the parental vesicles are made from nonmiscible lipids, electrofusion of these vesicles results in formation of microdomains in the fused vesicle, allowing one to study the stability and dynamics of raft-like domains. A significant advantage of electrofusion-based membrane mixing is that the final composition of the fused vesicle is precisely controlled, which is difficult to achieve when preparing multicomponent vesicles directly from a mixture of dissolved lipids [198]. Bezlyepkina et al. [198] have demonstrated the benefits of such a electrofusion approach for the determination of tie lines in a phase diagram for the ternary mixture of DOPC, egg sphingomyelin, and cholesterol.

Electrofusion between two GUVs encapsulating different reagents provides the means to trigger a biochemical reaction. Since GUVs can easily be directly visualised under the microscope, the kinetics of the biochemical reaction can be monitored via fluorescence-based methods. The relevance of using GUVs as microreactors is twofold. Firstly, fusion between GUVs encapsulating small reagent volumes (attoliters to picoliters) enables rapid diffusional mixing (in the order of microseconds to milliseconds) and allows one to study fast chemical reaction kinetics [27]. Moreover, fusion between GUVs allows precise amounts of reagents to be mixed, provided that negligible leakage occurs from the vesicles during fusion. Secondly, GUVs can mimic the size and surface properties of cells. Consequently, biochemical reactions, such as transcription and translation of genes [26], can be studied in a biologically relevant environment, which is particularly important when building an artificial cell through a bottom-up approach and for understanding the origins of life. Since lightning strikes are considered as a possible mechanism for promoting membrane electroporation and electrofusion during early evolution [199], electrofusion presents a particularly relevant method for studying reactions in primitive cells. Nevertheless, electrofusion is merely one of the approaches used when studying reactions in lipid vesicles. Further references on other techniques can be found in [200-202]. Below we discuss three example studies, which utilized electrofusion between GUVs.

Hsin and Yeung [203] have shown that the analysis of reaction kinetics in GUVs can go down to the single-molecule level. They measured the activity of alkaline phosphatase by electrofusing two GUVs, one containing a single alkaline phosphatase molecule labelled with TOTO-3 and the other one containing fluorescein diphosphate. The mixing of the contents of the GUVs initiated an enzymatic reaction that produced fluorescein, detected by fluorescence microscopy. Measurements revealed a broad distribution in the activities of individual alkaline phosphatase molecules, which were attributed to distinct conformational states. The advantage of this method is that the activity is

measured in the absence of an undesirable surface effect, since the protein rarely comes in contact with the lipid membrane.

Yang et al. [142] have studied nanoparticle synthesis inside GUVs, in order to explore whether synthesis of inorganic nanomaterials in microorganisms could occur in the absence of peptide- and protein-driven processes. They have considered a simple reaction, $Na_2S + CdCl_2 \leftrightarrow CdS + 2NaCl$, in which a solid CdS product forms already at weak millimolar (mM) concentrations. Indeed, electrofusion of GUVs containing either 0.3 mM Na_2S or $CdCl_2$ resulted in the formation of CdS nanoparticles with a diameter of 4–8 nm. Moreover, in a different protocol, where $CdCl_2$ was allowed to slowly diffuse into GUVs pre-loaded with Na_2S, larger nanoparticles with a diameter of about 50 nm were formed inside the GUVs, demonstrating the influence of the mixing kinetics on the final nanoparticle size. These findings further indicate the feasibility of carrying out nanoparticle synthesis in GUVs.

Terasawa et al. [204] have studied fusion between phospholipid GUVs encapsulating polymer molecules in their aqueous core. They observed that such GUVs can undergo spontaneous budding transformation after being electrofused (Fig. 11). The budding is a result of a depletion volume effect – the fused vesicle divides to maximise the translational entropy of the polymers inside the vesicle. This physical process mimics cell growth and division and could represent one of the mechanisms by which cells self-reproduced in the evolutionary pathway from protocells to modern life [202, 204]. Looking from a different perspective, such budding transformation can be exploited for aliquoting the reaction product after electrofusing GUVs containing different biochemical reagents [205].

[Here Fig. 11]

3.1.3 Electrofusion of GUVs in microfluidic devices

With the advancements in microfabrication techniques, the manipulation of cells and vesicles in lab-on-a-chip devices is becoming more and more popular. Microfluidic designs indeed have proven to be well-suited for electrofusing cells or GUVs [206]. The basic approach of electrofusing GUVs in a microfluidic device with micromachined electrodes is similar as when using conventional parallel-plate or wire electrodes, except that the length scales are smaller. The contacts between GUVs can be obtained by traditional dielectrophoretic alignment of GUVs into pearl chains followed by application of electroporative pulses to initiate electrofusion [207, 208]. Such microchips can even be designed for combined electroformation and electrofusion of GUVs [209]. Yet, this traditional approach neither allows controlling the number of GUVs involved in the fusion event nor the selectivity with respect to which types of GUVs are fused together. The greatest advantage of electrofusion in microfluidic devices is the possibility to integrate an array of traps that facilitate contact between selected pairs of GUVs (Fig. 12). Various designs have been proposed for trapping cells or water-in-oil droplets [210-212]. However, Robinson et al. [213] have reported that the trapping designs for cells and droplets are not entirely suitable for trapping GUVs due to their large deformability. Namely, the shear stress from the flow could easily squeeze the GUVs out of the traps. To overcome this challenge, Robinson et al. surrounded the traps by circular ring valves that were hydraulically actuated to isolate each trap and prevent any flow-induced movement of the GUVs [213].

[Here Fig. 12]

3.1.4 Microelectroinjection and vesicle-nanotube networks

Microelectroinjection is a technique, which is based on the combination of electroporation and pressure-driven microinjection [214]. Initially, this technique was applied for precisely controlling the amount of molecular loading into single lipid GUVs. Since the membrane of a lipid vesicle is typically very elastic, microneedles with an outer tip diameter of about 200 nm need to be used to mechanically puncture the membrane [215]. Such tips are extremely fragile and the small diameter of the tip limits the size of the objects that can be introduced into the GUV. To use larger micropipettes, Karlsson et al. [214] proposed the following approach. A GUV was positioned between the tip of a glass micropipette (diameter ~2 μm), equipped with a Pt electrode, and a 5-μm diameter carbon fibre electrode. A rectangular pulse with the duration of 1–10 ms was applied between the electrodes to induce electroporation below the micropipette tip, which allowed the tip to enter the vesicle. A small volume (typically 50–500 femtoliters into GUVs with diameter of 10-20 μm) was then injected into the vesicle lumen. T7-phage DNA molecules (radius of gyration 0.56 μm), 30-nm-diameter latex spheres, and 100-nm-diameter SUVs were easily injected into GUVs. Moreover, multiple reagents were sequentially injected into a single vesicle without noticeable leakage [214].

Subsequently, it turned out that the microelectroinjection method combined with electrofusion enables one to artificially create complex networks of vesicles connected by lipid nanotubes [216, 217]. Different variants of such vesicle networks have been explored as systems for analysing enzyme-catalysed reactions [218], single-molecule detection of DNA [219], and reactions of polymers with calcium ions to form hydrogels [220]. This topic has been thoroughly reviewed elsewhere [13, 221, 222], but let us illustrate an example. Cans et al. [223] used this technology to form a small vesicle inside a surface immobilized GUV as a model of a cell that undergoes exocytosis. The main steps to create this model are depicted in Fig. 13a-d. The micropipette is electroinserted into the GUV (Fig. 13a) and across the membrane at the opposite side of the GUV (Fig. 13b). Since the lipids adhere to the tip, withdrawal of the micropipette results in a lipid nanotube (Fig. 13c). Finally, a small vesicle is inflated at the pipette tip by inducing a flow from the micropipette (Fig. 13d,e). Inflation of the nanotube leads to a local increase in the membrane tension, which induces a flow of the lipids from the regions of lower tension (outer membrane) along the nanotube. As the vesicle grows in size, the nanotube shortens until it transforms into a toroid-shaped fusion pore (Fig. 13f-i). At this point the system mimics the later stages of the exocytotic process. Recently, it has been demonstrated that this simple model can represent two main modes of exocytosis, which are considered to occur naturally: one in which the content of the exocytotic vesicle is fully released into the extracellular space (as in Fig. 13f-i), and the second one in which only partial release takes place and may correspond to an extended kiss-and-run mechanism [224].

[Here Fig. 13]

3.1.5 Electrofusion of GUVs with cells

While cell-cell electrofusion and GUV-GUV electrofusion are rather well-explored, electrofusion between GUVs and cells is only now receiving greater attention. Cell-GUV electrofusion offers some unique possibilities, such as delivering large objects directly into the cytosol or dramatically changing the composition of the cell membrane through the addition of lipids and membrane proteins. The proof-of-concept was first reported by Strömberg et al. [137]. They prepared giant phosphatidylcholine MLVs with incorporated membrane protein γ-glutamyltransferase. Individual MLVs and cells were electrofused between two carbon-fibre microelectrodes, which resulted in the

integration of γ-glutamyltransferase into the cell membrane. Subsequently, Shirakashi et al. [225] demonstrated electrofusion between phosphatidylcholine GUVs and Jurkat cells based on the conventional combination of pearl-chain alignment and pulse application.

Saito et al. [226] followed a similar protocol as Shirakashi et al. [225] and aimed to introduce large particles into HeLa cells (Fig. 14). They prepared GUVs from a mixture of DOPC, DOPG and cholesterol with the water-in-oil emulsion centrifugation method. This GUV preparation method allowed them to encapsulate plasmid DNA, DNA origami structure, as well as fluorescent microbeads with diameters of 0.2, 0.5, 1, and 2 µm. The protocol was successful for delivering all particles into the cells except for 2 µm microbeads, which were apparently too large to pass the cytoskeleton network beneath the cell membrane. Most importantly, the protocol did not affect the cell viability, as the cells were able to proliferate normally for at least 5 days after electrofusion. The authors though reported that the GUVs were probably only transiently fused to the cells, and detached from the cells with post-pulse washing. Overall, the results showed great promise for introducing large functionally active objects such as micro-machines into living cells, and studying their effects on the cells.

[Here Fig. 14]

Another approach for cell-GUV electrofusion was described by Raz-Ben Aroush et al. [227]. The protocol was developed for fish epithelial keratocytes and human foreskin fibroblasts (as depicted in Fig. 15). The cells were grown on a glass coverslip in a cell culture medium. Ten minutes before electrofusion, the cells were incubated in a serum-free medium supplemented with a PEG solution, since the latter had been found to facilitate fusion. Afterwards, the solution with GUVs was added, and the GUVs were allowed to settle on top of the cells. Two parallel-plate electrodes were then inserted into the sample and the cells and GUVs were electrofused. Finally, the cells were washed with a culture medium to remove the unfused GUVs and PEG. The preparation of GUVs with fluorescently conjugated lipids enabled detection of the fused cell-GUV hybrids under a fluorescent microscope (Fig. 15). The fluorescence signal from the labelled lipids appeared evenly spread in the cell membrane within 1 min., suggesting that the fusion process was fast. This protocol was used to study the effect of membrane enlargement on the inherent moving ability of keratocytes [228]. Interestingly, the authors observed a negligible effect on the cell movement despite the substantial increase in the membrane area (~30%). Measurements of the cell membrane tension, which plays an essential role in cell motility, revealed that the tension remained practically unchanged after electrofusion. Fluorescence imaging of the lamellipodial actin network further demonstrated that the amount of filamentous actin increased and the actin network expanded in the fused cells as compared to the control, buffering the influence of the increase in the membrane area on the tension [228].

[Here Fig. 15]

3.2 Applications of electroporation and electrofusion of LUVs and SUVs

Lipid vesicles have been proposed as carriers of pharmaceuticals already in the 1970s [229]. As vesicles possess both hydrophilic and hydrophobic domains, they can carry practically any type of molecules. This makes them promising delivery vehicles for drugs, proteins, peptides, and nucleic acids in the treatment of cancer, infections, metabolic diseases, as well as autoimmune diseases [230-233]. The main objectives of encapsulating therapeutic compounds into vesicles are to protect

sensitive molecules during their transportation to the target tissue such as nucleic acids from endogenous nucleases in the blood plasma, reduce the side-effects of toxic drugs such as chemotherapeutics, and/or achieve a high localization and enhanced intracellular uptake of therapeutic compounds at disease sites [233, 234]. In clinical applications, vesicles are mostly administrated intravenously, although other routes of administration are also being considered [235]. The size of vesicles used in drug delivery is typically about 200 nm in diameter or less, which allows the vesicles to extravasate through leaky blood vessels in inflammatory and tumour sites [234, 236]. In the field of drug delivery, vesicles made from phospholipids are generally referred to as liposomes, and we adopt this notation throughout the present section. Unless otherwise noted, the sizes of the vesicles discussed in this section correspond to the size of LUVs and SUVs.

While several liposome formulations are already commercialised, and numerous formulations are in different stages of clinical trials, many challenges still exist which limit liposome applications [29, 30, 235, 237]. Conventional liposomes prepared from neutral phospholipids have low encapsulation efficiency, tend to leak the encapsulated substances, and have a short circulation time in the blood. The liposome stability can be increased by tuning the composition of the membrane, e.g., by addition of cholesterol, charged lipids, or by replacing fluid-phase with gel-phase lipids [238]. The short circulation time is mainly caused by rapid opsonisation – a process in which the liposomes become covered with opsonin proteins from the blood plasma – and subsequent uptake by the mononuclear phagocytic system [239]. The opsonisation can be reduced by covering the surface of the liposomes with PEG (or similar inert polymers), which decreases nonspecific interactions with the plasma proteins and additionally stabilizes the membrane. Such PEGylated liposomes are called stealth liposomes [240]. The specificity of liposome accumulation in the disease sites can be increased by conjugating liposomes with ligands, which are able to specifically bind to target cells. However, this approach has so far yielded scarce improvements in the therapeutic outcomes with respect to the increased cost of preparing ligand-targeted liposomes [29, 241]. Once the liposomes accumulated at the target site, they can increase the therapeutic potential if the release of the entrapped drug from the liposomes takes place at an optimized rate [29]. Furthermore, biomolecules such as proteins, DNA, and RNA, which cannot permeate across the cell membrane, need to be released after the liposomes enter the cell, generally by endocytotic mechanisms [242]. To control the release from liposomes, methods which rely on a stimulus to initiate disintegration of the liposome membrane have been proposed, such as change in pH, temperature variation, ultrasound, or light irradiation [243, 244]. To meet the challenges of liposomal drug delivery, alternative types of vesicles are being investigated such as vesicles made from archaeal lipids (archaeosomes [245]) or block copolymers (polymersomes [246]), which are characterized by greater stability compared to liposomes. Very recently, vesicles of natural origin called extracellular vesicles have been proposed as superior alternatives to artificial vesicles [247]. The use of nanotechnology for therapeutic purposes is continuously evolving and various other types of sophisticated nanocarriers are considered for drug delivery [248-252].

Electroporation and electrofusion of liposomes and other "-somes" with sizes corresponding to the size range of SUVs and LUVs has received less attention than electroporation and electrofusion of GUVs. The main fundamental studies have been conducted by Neumann et al. via electro-optic and conductometric measurements on suspended vesicles [253-256]. Similarly as for GUVs, electroporation of SUVs and LUVs is associated with vesicle electrodeformation and increased membrane permeability. However, electroporation of LUVs and SUVs tends to occur at lower $U_{m,crit}$,

which is associated with higher membrane curvature of smaller vesicles [257]. In terms of applications, electroporation can be exploited for loading the vesicles with a given compound or for controlling the release of the compound from the vesicles, as discussed below.

3.2.1 Loading a cargo into vesicles by electroporation

Liposomes can be encapsulated with the desired compound either during the formation process or by using other methods, which are typically based on creating a pH gradient across the liposome membrane [258]. While these methods are suitable for artificial vesicles such as liposomes, they can hardly be applied for loading extracellular vesicles (EVs). EVs are phospholipid vesicles, which are secreted by most types of cells and play a key role in long-distance intercellular communication, by facilitating the transfer of proteins, mRNAs and miRNAs between the donor and recipient cells. In the field of drug delivery, two subtypes of EVs are often utilized, exosomes and microvesicles, because a complete separation and purification of these subtypes is extremely laborious [259]. Exosomes are about 40–100 nm in diameter and are produced inside multivesicular endosomes. They are released into the extracellular space upon fusion of the multivesicular endosomes with the cell membrane. Their larger counterparts, microvesicles (diameter ~100–500 nm), are produced through budding and fission from the cell membrane [260]. Although many challenges need to be overcome before the therapeutic potential of EVs is effectively harnessed [261], these vesicles possess several advantages over synthetic liposomes: (i) EVs inherently have a long circulation time in the blood, (ii) they possess an intrinsic ability to cross biological barriers including the most difficult one to penetrate, i.e. the blood-brain barrier, (iii) they are immunologically inert if purified from a compatible cell source and they could even be derived from the patient's own cells to limit any potential immunogenicity, (iv) they naturally express membrane receptors which allow them to "recognize" recipient cells, and (v) they can spontaneously fuse with the recipient cells, avoiding endocytotic pathways, and directly deliver their cargo into the cytosol [259].

After the seminal work of Alvarez-Erviti et al. [262], electroporation has become one of the main methods for loading EVs with hydrophilic molecules. Alvarez-Evriti et al. [262] have used electroporation to encapsulate siRNA into EVs derived from dendritic cells and have shown that these EVs could deliver siRNA through the blood-brain barrier into the brain parenchyma of mice, suppressing the expression of a gene coding for Beta-secretase 1, which is an important therapeutic target in Alzheimer’s disease. In a subsequent study, they have shown that siRNA-loaded EVs significantly reduced the accumulation of α-synuclein aggregates in mouse brain, which is a pathological hallmark in Parkinson’s disease [263]. Other studies have further confirmed that EVs loaded with siRNA or miRNA by electroporation can induce specific gene knockdown in various cell types *in vitro* [264-266]. Electroporation has also been used to encapsulate the chemotherapeutic drug doxorubicin [267, 268], superparamagnetic iron oxide nanoparticles [269, 270], and porphyrin [271].

However, the use of electroporation for loading EVs has reached limited success. A careful investigation by Kooijmans et al. [272] has demonstrated that electroporation of EVs in electroporation cuvettes leads to extensive aggregation of siRNA, which can result in an overestimate in the amount of siRNA loaded into EVs. Their results have shown that aggregation is probably caused by the release of aluminium cations from the electrodes in the cuvettes. Strikingly, when EVs were electroporated under conditions which prevented siRNA aggregation, undetectable amount of siRNA was encapsulated into the vesicles. To the opposite, Lamichhane et al. [273] later showed that

DNA molecules larger than siRNA can in fact be encapsulated into EVs by electroporation. The contradictory reports on unsuccessful [272] and successful [273] loading of EVs by electroporation could at least partially be explained in the context of different electroporation protocols. According to the reported methodology, the electric field strength of the applied pulses has been four times higher in the experiments of Lamichhane et al. [273], which is expected to result in more extensive vesicle electroporation and greater molecular uptake [151, 255].

Apart from loading EVs, electroporation has been proposed as a method for loading polymersomes with macromolecules including proteins, siRNA and plasmid DNA [274, 275]. Specifically, electroporation has been found advantageous for encapsulating proteins such as myoglobin, which are difficult to encapsulate by the conventional approach where the pH-switch method is used for polymersome formation [274].

Polymersomes are characterized by greater stability and lower membrane permeability than lipid vesicles. They also offer the high flexibility of chemical modifications both before and after formation, for which they have some unique advantages as drug delivery and diagnostic agents [246]. One of the numerous possibilities is to functionalize them with magnetic nanoparticles (MNPs). Such magnetopolymersomes can then be used as contrast agents in magnetic resonance imaging or as smart therapeutic agents, whereby remote application of an alternating magnetic field induces heating of the magnetic nanoparticles to trigger drug release or cell death [276]. Recently, it has been shown that electroporation can assist the preparation of magnetopolymersomes. Bain et al. [277] prepared polymersomes with a high pH aqueous core (encapsulating NaOH) and suspended them in an iron solution. By electroporating the polymersomes, they have initiated the synthesis of magnetite nanoparticles inside the polymeric membrane. They have proposed a mechanism in which the simultaneous flux of NaOH and iron ions through the pores induced by electroporation results in the formation of nanoparticles inside the pores (Fig. 16). They have shown that by tuning the amplitude of the applied pulses, it is possible to control the MNP size. In a related study, Bakhshi et al. [278] have demonstrated that the synthesis of MNPs can be achieved also inside the aqueous core of liposomes. In addition, they have shown that high-throughput production of MNP-functionalized liposomes with a uniform size (58 ± 8 nm) can be achieved by combining electroporation-based MNP synthesis with an electrohydrodynamic atomization method for the liposome production.

[Here Fig. 16]

3.2.2 Spontaneous fusion of SUVs and LUVs with electroporated cells

Apart from using electroporation to load vesicles with desired compounds, electroporation could further be used for controlling the liposomal release at the target site. Teissié et al. [279-281] have demonstrated that lipid SUVs and LUVs can spontaneously fuse with electroporated cells, avoiding the endocytotic pathway and directly delivering their cargo into the cytoplasm. The contact between the cells and the vesicles was obtained via an electrostatic calcium bridge and the suspension was exposed to 10 or more pulses with 100 μs duration. The electric field strength of the pulse was 1.2 kV/cm, which was sufficiently high to electroporate the cells while preserving the cell viability, but was too low to electroporate the vesicles due to their smaller size (the LUVs were around 200 nm in diameter). Application of electric pulses resulted in fusion of the vesicles with the cell membrane. Large macromolecules (20 kD dextran) could easily be delivered into the cells by this approach [280]. In a more recent study [281], they also demonstrated that cell-vesicle fusion is affected by the lipid

composition of the vesicles. Most efficient fusion was achieved when PC lipids were mixed with PS (20%), PE (30%), and cholesterol (30%). Interestingly, exposing the cells to electric pulses in the presence of highly fusogenic empty LUVs had a protecting effect against the loss of cell viability due to electroporation [281]. This has implications for gene delivery by means of electroporation, since the loss of cell viability is one of the bottlenecks in gene electrotransfer applications [152].

The observation that lipid vesicles are able to spontaneously fuse with an electroporated membrane has been supported by theory [282]. However, the lipid vesicles apparently need to be metastable for spontaneous fusion. MLVs, which have a more tightly packed lipid assembly, have been unable to spontaneously fuse with the electroporated cells, regardless of the lipid composition of MLVs [279].

3.2.3 Controlling the release from SUVs and LUVs by nanosecond electric pulses

Another possible approach for controlling the release of the liposome content may be offered by electroporation with pulses in the nanosecond (ns) range [283-285]. Since the charging time of the cell membrane is typically on the order of 100 ns (when the cell is in a medium with physiological conductivity) [286], nanosecond pulses are too short to fully charge the cell membrane and the membrane remains in the charging phase throughout the duration of the pulse. During this charging phase, the cell membrane does not electrically shield the cell interior, and the external electric field penetrates into the cytoplasm. The electric field inside the cytoplasm induces U_m on the membrane of intracellular organelles with a magnitude comparable to U_m on the charging cell membrane [287]. If the external electric field is sufficiently high, it can lead to electroporation of both the cell membrane and the organelle membranes [288-292]. Since the organelles are much smaller than the cell, an electric field in the order of 10 kV/cm is required for their electroporation.

The possibility to electroporate intracellular membranes has prompted the idea of using nanosecond pulses for electroporating liposomes once they are taken up by the cells. As such, the release of the encapsulated liposome content into the cytosol can be controllably triggered. A theoretical study, considering a model of a cell with internalized liposomes (diameter 100–1000 nm), has suggested that electroporation of the liposomes without considerably affecting the cell viability would be feasible, provided that the applied pulses are about 10 ns long [283]. An alternative idea is to electroporate the liposomes when they are in close proximity of the target cells [285]. Since nanosecond pulses generally also result in electroporation of the cell membrane, the content released from the electroporated liposomes could be subsequently taken up by the electroporated cells. The possibility to control the release of the vesicle content with nanosecond pulses for now remains at the theoretical level, and its experimental feasibility is yet to be confirmed. A long-term projection may lie in combined use of liposomes and electric pulses in cancer treatment. Namely, pulses with a duration of 100 µs are routinely used in tumour treatment, whereby the pulses are delivered to the tissue via planar or needle electrodes [31]. Since the mechanism by which electric pulses induce cell death is in principle nonthermal, electroporation-based tumour treatment can be applied to tumours, which are unsuitable for surgery and thermal ablation, such as tumours in proximity of large blood vessels and nerves [293]. More recently, the application of nanosecond pulses has been proposed as an additional method for tumour ablation. Unlike longer microsecond pulses, nanosecond pulses are able to directly induce apoptotic cell death [294]. The use of nanosecond pulses to trigger cell death and simultaneously control the release of a chemotherapeutic drug from the liposomes could have a synergistic effect, comparable to observations in radio frequency ablation [295-297].

4. Future perspective

It is necessary to explore more realistic cell models in the electroporation of vesicles, which account for the complex, heterogeneous structure of the cell. Pioneering studies have been carried out to understand the basic principles of simple GUVs in electric fields, revealing the response of the membrane solely. More complex GUV systems are desired to elucidate more realistic mechanisms of electroporation of a living cell. Systematic investigation of GUVs with incorporated membrane proteins, cytoskeleton network, and dense gel-like aqueous core would reveal more insights on how these sub-cellular structures influence cell electroporation. While cell electroporation has been widely used in biomedical and technological applications, the exact mechanisms that contribute to the experimentally observed increased permeability of cell membranes are not yet fully elucidated [298]. There are many open questions, including: Why the resealing of cell membranes after electroporation generally takes orders of magnitude more time than in model membrane systems (minutes or even hours in cells versus up to hundreds of milliseconds in GUVs)? Can the increase in the cell membrane permeability after electroporation be attributed solely to lipid pores formed during exposure to electric pulses, or does lipid peroxidation present a contributing/alternative mechanism [299, 300]? How are the membrane proteins affected by the electric field and how do they participate in the increased cell membrane permeability [176, 301]? What are the molecular mechanisms of the transmembrane transport of small drugs and large macromolecules such as DNA and how is the transport influenced by the resting potential of the cell membrane [289, 302]? Why is the translocation of DNA across the cell membrane different in GUVs than in cells and what is the role of cytoskeleton in DNA translocation [151, 177, 303]? Answering these questions through controlled experiments on more complex model GUV systems would improve our understanding of cell electroporation and consequently help optimise current electroporation-based treatments (e.g. gene electrotransfer), as well as develop new ways to exploit cell electroporation for various applications in medicine, food processing, and environmental applications.

Further, studying complex GUVs in electric field could have implications in single-cell diagnostics. By increasing the complexity of a GUV, also the mechanical properties can be correlated to their intra-cellular components via electrodeformation measurements. Single-cell diagnostics have already shown that some diseases alter the mechanical properties [304], e.g. cancer cells have a lower stiffness than healthy cells [305] and even the Young's modulus of different tumour cells can be discriminated [306]. By gaining a comprehensive understanding of how different intra-cellular components contribute to the mechanical properties of living cells through a bottom-up approach, the diagnostics can be further improved. Additionally, it would open up the field to use electric fields as a contactless diagnostic tool to measure the changes in mechanical properties of cells and distinguish important biological factors associated with disease progression (such as pathological, genetic, and epigenetic factors).

To develop successful applications for the characterization and screening on the single GUV or cell level, microfluidic concepts provide unprecedented options. Furthermore, exposing GUVs or cells to an electric field in a microfluidic device offers the benefit of remote and contactless manipulation without the need of sophisticated and expensive micromanipulators. In particular, when the microfluidic design contains the posts to trap individual cells/vesicles together with integrated electrodes in close proximity to the traps, it is possible to simultaneously expose numerous cells/GUVs to the electric field, while analysing each cell/GUV separately. The possibility of trapping

individual cells and GUVs has already shown great potential in inducing controlled pairwise cell-cell electrofusion [206]. Similar concepts can be further designed to induce pairwise electrofusion between cells and GUVs. For example, by embedding selected membrane proteins into the GUV membrane and/or DNA or even micro/nanomachines inside the GUV, cell-GUV electrofusion could provide a platform for a controlled delivery of selected material into living cells and analyse its influence on cell properties and functions [137, 226].

Elucidating electroporation of GUVs in micro/nanofluidic devices would also provide important insights into fundamental electroporation mechanisms. Presence of nanostructures, such as nanochannels, nanopores, or nanowires, strongly influences the local electric field distribution and consequently, the spatial distribution of the pores formed in the GUV/cell membrane [307-309]. Fabricating nanostructures with well-defined geometries and performing electroporation of GUVs with increasing complexity next to such nanostructures would improve the theoretical knowledge of electroporation and further optimize the design of electroporation protocols. For instance, when cells are electroporated next to a nanochannel, DNA can be delivered directly into the cytoplasm [307], whereas in conventional bulk electroporation, the DNA first forms a complex with the cell membrane and then most likely translocates across the membrane via endocytotic mechanisms [152, 310].

In this review, we have focused on the following topics: electrodeformation, electroporation, and electrofusion of vesicles, highlighting both fundamental and application results. These model systems of the cell have provided unique opportunities to bridge the gap between the soft matter physics and the reality of the soft living matter. The fundamental understanding of the mechanical properties of vesicles (GUVs, LUVs, and SUVs) is an essential step towards advancing our fundamental knowledge about the complex behaviour of cell membranes in an electric field. In addition, this fundamental knowledge can inspire us to develop novel liposome approaches for practical biomedical applications.

Acknowledgements

This work was supported by the European Research Council (ERC) under the European Union's Seventh Framework Programme (FP/2007-2013)/ERC Grant, agreement no. 337820 (to P.E.B.). The authors thank Fatemeh Hashemi and Shaurya Sachdev for critical reading of the manuscript.

References

[1] Pezzulo G, Levin M. Top-down models in biology: explanation and control of complex living systems above the molecular level. Journal of The Royal Society Interface. 2016;13.
[2] Ross J, Arkin AP. Complex Systems: From chemistry to systems biology. Proceedings of the National Academy of Sciences. 2009;106:6433-4.
[3] Lagny TJ, Bassereau P. Bioinspired membrane-based systems for a physical approach of cell organization and dynamics: usefulness and limitations. Interface Focus. 2015;5.
[4] Szathmary E. Life: In search of the simplest cell. Nature. 2005;433:469-70.
[5] Liu AP, Fletcher DA. Biology under construction: in vitro reconstitution of cellular function. Nat Rev Mol Cell Biol. 2009;10:644-50.
[6] Sens P, Johannes L, Bassereau P. Biophysical approaches to protein-induced membrane deformations in trafficking. Current opinion in cell biology. 2008;20:476-82.
[7] Schwille P. Bottom-Up Synthetic Biology: Engineering in a Tinkerer's World. Science. 2011;333:1252-4.
[8] Luisi PL, Stano P. The Minimal Cell: The Biophysics of Cell Compartment and the Origin of Cell Functionality: Springer Science & Business Media; 2010.
[9] Menger FM, Keiper JS. Chemistry and physics of giant vesicles as biomembrane models. Current Opinion in Chemical Biology. 1998;2:726-32.
[10] Mozafari MR. Nanoliposomes: Preparation and Analysis. In: Weissig V, (editor). Liposomes: Humana Press; 2010. p. 29-50.
[11] Walde P, Cosentino K, Engel H, Stano P. Giant Vesicles: Preparations and Applications. Chembiochem. 2010;11:848-65.
[12] Swaay Dv, deMello A. Microfluidic methods for forming liposomes. 2013;13:752-67.
[13] Jesorka A, Orwar O. Liposomes: technologies and analytical applications. Annu Rev Anal Chem. 2008;1:801-32.
[14] Dimova R, Aranda S, Bezlyepkina N, Nikolov V, Riske KA, Lipowsky R. A practical guide to giant vesicles. Probing the membrane nanoregime via optical microscopy. Journal of Physics: Condensed Matter. 2006;18:S1151.
[15] Menger FM, Angelova MI. Giant Vesicles: Imitating the Cytological Processes of Cell Membranes. Accounts of Chemical Research. 1998;31:789-97.
[16] Bucher P, Fischer A, Luisi PL, Oberholzer T, Walde P. Giant Vesicles as Biochemical Compartments: The Use of Microinjection Techniques. Langmuir. 1998;14:2712-21.
[17] Girard P, Pécréaux J, Lenoir G, Falson P, Rigaud J-L, Bassereau P. A New Method for the Reconstitution of Membrane Proteins into Giant Unilamellar Vesicles. Biophysical Journal. 2004;87:419-29.
[18] Davidson M, Karlsson M, Sinclair J, Sott K, Orwar O. Nanotube–Vesicle Networks with Functionalized Membranes and Interiors. Journal of the American Chemical Society. 2003;125:374-8.
[19] Rigaud J-L, Pitard B, Levy D. Reconstitution of membrane proteins into liposomes: application to energy-transducing membrane proteins. Biochimica et Biophysica Acta (BBA) - Bioenergetics. 1995;1231:223-46.
[20] Sachse R, Dondapati SK, Fenz SF, Schmidt T, Kubick S. Membrane protein synthesis in cell-free systems: From bio-mimetic systems to bio-membranes. FEBS Letters. 2014;588:2774-81.
[21] Soga H, Fujii S, Yomo T, Kato Y, Watanabe H, Matsuura T. In Vitro Membrane Protein Synthesis Inside Cell-Sized Vesicles Reveals the Dependence of Membrane Protein Integration on Vesicle Volume. ACS Synthetic Biology. 2014;3:372-9.
[22] Helfrich MR, Mangeney-Slavin LK, Long MS, Djoko KY, Keating CD. Aqueous Phase Separation in Giant Vesicles. Journal of the American Chemical Society. 2002;124:13374-5.
[23] Yamashita Y, Oka M, Tanaka T, Yamazaki M. A new method for the preparation of giant liposomes in high salt concentrations and growth of protein microcrystals in them. Biochimica et Biophysica Acta (BBA) - Biomembranes. 2002;1561:129-34.

[24] Fischer A, Franco A, Oberholzer T. Giant vesicles as microreactors for enzymatic mRNA synthesis. Chembiochem. 2002;3:409-17.
[25] Michel M, Winterhalter M, Darbois L, Hemmerle J, Voegel JC, Schaaf P, et al. Giant Liposome Microreactors for Controlled Production of Calcium Phosphate Crystals. Langmuir. 2004;20:6127-33.
[26] Noireaux V, Libchaber A. A vesicle bioreactor as a step toward an artificial cell assembly. P Natl Acad Sci USA. 2004;101:17669-74.
[27] Chiu DT, Wilson CF, Ryttsén F, Strömberg A, Farre C, Karlsson A, et al. Chemical Transformations in Individual Ultrasmall Biomimetic Containers. Science. 1999;283:1892-5.
[28] Long MS, Jones CD, Helfrich MR, Mangeney-Slavin LK, Keating CD. Dynamic microcompartmentation in synthetic cells. Proceedings of the National Academy of Sciences. 2005;102:5920-5.
[29] Allen TM, Cullis PR. Liposomal drug delivery systems: From concept to clinical applications. Adv Drug Deliver Rev. 2013;65:36-48.
[30] Sercombe L, Veerati T, Moheimani F, Wu SY, Sood AK, Hua S. Advances and Challenges of Liposome Assisted Drug Delivery. Frontiers in Pharmacology. 2015;6.
[31] Yarmush ML, Golberg A, Serša G, Kotnik T, Miklavčič D. Electroporation-based technologies for medicine: Principles, applications, and challenges. Annual Review of Biomedical Engineering. 2014;16:295-320.
[32] Mahnič-Kalamiza S, Vorobiev E, Miklavčič D. Electroporation in food processing and biorefinery. J Membrain Biol. 2014;247:1279-304.
[33] Kotnik T, Frey W, Sack M, Haberl Meglič S, Peterka M, Miklavčič D. Electroporation-based applications in biotechnology. Trends in Biotechnology. 2015;33:480-8.
[34] Dimitrov DS. Electroporation and electrofusion of membranes. Handbook of Biological Physics. 1995;1:851-901.
[35] Strömberg A, Karlsson A, Ryttsén F, Davidson M, Chiu DT, Orwar O. Microfluidic Device for Combinatorial Fusion of Liposomes and Cells. Analytical Chemistry. 2001;73:126-30.
[36] Dimova R, Bezlyepkina N, Jordo MD, Knorr RL, Riske KA, Staykova M, et al. Vesicles in electric fields: Some novel aspects of membrane behavior. Soft Matter. 2009;5:3201-12.
[37] Dimova R, Riske KA, Aranda S, Bezlyepkina N, Knorr RL, Lipowsky R. Giant vesicles in electric fields. Soft Matter. 2007;3:817-27.
[38] Portet T, Mauroy C, Démery V, Houles T, Escoffre J-M, Dean DS, et al. Destabilizing Giant Vesicles with Electric Fields: An Overview of Current Applications. J Membrain Biol. 2012;245:555-64.
[39] Vlahovska PM. Voltage-morphology coupling in biomimetic membranes: dynamics of giant vesicles in applied electric fields. Soft Matter. 2015;11:7232-6.
[40] Pauly H, Schwan HP. Impendance of a suspension of ball-shaped particles with a shell; a model for the dielectric behavior of cell suspensions and protein solutions. Z Naturforsch B. 1959;14B:125-31.
[41] Schwan HP, Sher LD. Alternative-Current Field-Induced Forces and Their Biological Implications. J Electrochem Soc. 1969;116:22C-6C.
[42] Zimmermann U. Electric field-mediated fusion and related electrical phenomena. Biochimica et Biophysica Acta (BBA) - Reviews on Biomembranes. 1982;694:227-77.
[43] Chan KL, Gascoyne PRC, Becker FF, Pethig R. Electrorotation of liposomes: verification of dielectric multi-shell model for cells. Bba-Lipid Lipid Met. 1997;1349:182-96.
[44] Voldman J. Electrical forces for microscale cell manipulation. Annual Review of Biomedical Engineering. 2006;8:425-54.
[45] Kotnik T, Pucihar G. Induced transmembrane voltage – theory, modeling, and experiments. In: Pakhomov AG, Miklavčič D, Markov MS, (editors). Advanced Electroporation Techniques in Biology and Medicine: CRC Press, Boca Raton; 2010. p. 51-70.
[46] Salipante PF, Knorr RL, Dimova R, Vlahovska PM. Electrodeformation method for measuring the capacitance of bilayer membranes. Soft Matter. 2012;8:3810-6.
[47] Riske KA, Dimova R. Electro-Deformation and Poration of Giant Vesicles Viewed with High Temporal Resolution. Biophysical Journal. 2005;88:1143-55.

[48] Kotnik T, Miklavcic D. Analytical description of transmembrane voltage induced by electric fields on spheroidal cells. Biophysical Journal. 2000;79:670-9.
[49] Hibino M, Shigemori M, Itoh H, Nagayama K, Kinosita K. Membrane conductance of an electroporated cell analyzed by submicrosecond imaging of transmembrane potential. Biophysical Journal. 1991;59:209-20.
[50] Kotnik T, Miklavčič D. Second-order model of membrane electric field induced by alternating external electric fields. Ieee T Bio-Med Eng. 2000;47:1074-81.
[51] Taupin C, Dvolaitzky M, Sauterey C. Osmotic pressure-induced pores in phospholipid vesicles. Biochemistry. 1975;14:4771-5.
[52] Abidor IG, Arakelyan VB, Chernomordik LV, Chizmadzhev YA, Pastushenko VF, Tarasevich MR. Electric breakdown of bilayer lipid membranes I. The main experimental facts and their qualitative discussion. Bioelectrochemistry and Bioenergetics. 1979;6:37-52.
[53] Powell KT, Weaver JC. Transient aqueous pores in bilayer membranes: A statistical theory. Bioelectrochemistry and Bioenergetics. 1986;15:211-27.
[54] Needham D, Hochmuth RM. Electro-mechanical permeabilization of lipid vesicles. Role of membrane tension and compressibility. Biophysical Journal. 1989;55:1001-9.
[55] Lewis TJ. A model for bilayer membrane electroporation based on resultant electromechanical stress. IEEE Transactions on Dielectrics and Electrical Insulation. 2003;10:769-77.
[56] Vasilkoski Z, Esser AT, Gowrishankar TR, Weaver JC. Membrane electroporation: The absolute rate equation and nanosecond time scale pore creation. Physical Review E. 2006;74:021904.
[57] Glaser RW, Leikin SL, Chernomordik LV, Pastushenko VF, Sokirko AI. Reversible electrical breakdown of lipid bilayers: formation and evolution of pores. Biochimica et Biophysica Acta (BBA) - Biomembranes. 1988;940:275-87.
[58] Neu JC, Smith KC, Krassowska W. Electrical energy required to form large conducting pores. Bioelectrochemistry. 2003;60:107-14.
[59] Brochard-Wyart F, de Gennes PG, Sandre O. Transient pores in stretched vesicles: role of leak-out. Physica A: Statistical Mechanics and its Applications. 2000;278:32-51.
[60] Portet T, Dimova R. A New Method for Measuring Edge Tensions and Stability of Lipid Bilayers: Effect of Membrane Composition. Biophysical Journal. 2010;99:3264-73.
[61] Gurtovenko AA, Anwar J, Vattulainen I. Defect-mediated trafficking across cell membranes: Insights from in silico modeling. Chemical reviews. 2010;110:6077-103.
[62] Levine ZA, Vernier PT. Life cycle of an electropore: Field-dependent and field-independent steps in pore creation and annihilation. J Membrain Biol. 2010;236:27-36.
[63] Kandasamy SK, Larson RG. Cation and anion transport through hydrophilic pores in lipid bilayers. The Journal of Chemical Physics. 2006;125:074901.
[64] Böckmann RA, de Groot BL, Kakorin S, Neumann E, Grubmüller H. Kinetics, Statistics, and Energetics of Lipid Membrane Electroporation Studied by Molecular Dynamics Simulations. Biophysical Journal. 2008;95:1837-50.
[65] Rems L. Lipid Pores: Molecular and Continuum Models. In: Miklavcic D, (editor). Handbook of Electroporation: Springer International Publishing; 2016. p. 1-21.
[66] Tokman M, Lee JH, Levine ZA, Ho M-C, Colvin ME, Vernier PT. Electric Field-Driven Water Dipoles: Nanoscale Architecture of Electroporation. PloS one. 2013;8:e61111.
[67] Neu JC, Krassowska W. Asymptotic model of electroporation. Physical Review E. 1999;59:3471-82.
[68] Mauroy C, Rico-Lattes I, Teissie J, Rols MP. Electric Destabilization of Supramolecular Lipid Vesicles Subjected to Fast Electric Pulses. Langmuir. 2015;31:12215-22.
[69] Tekle E, Astumian RD, Friauf WA, Chock PB. Asymmetric pore distribution and loss of membrane lipid in electroporated DOPC vesicles. Biophysical Journal. 2001;81:960-8.
[70] Ziegler MJ, Vernier PT. Interface Water Dynamics and Porating Electric Fields for Phospholipid Bilayers. The Journal of Physical Chemistry B. 2008;112:13588-96.

[71] Majhi AK, Kanchi S, Venkataraman V, Ayappa KG, Maiti PK. Estimation of activation energy for electroporation and pore growth rate in liquid crystalline and gel phases of lipid bilayers using molecular dynamics simulations. Soft Matter. 2015;11:8632-40.
[72] Polak A, Tarek M, Tomšič M, Valant J, Ulrih NP, Jamnik A, et al. Electroporation of archaeal lipid membranes using MD simulations. Bioelectrochemistry. 2014;100:18-26.
[73] Polak A, Bonhenry D, Dehez F, Kramar P, Miklavčič D, Tarek M. On the Electroporation Thresholds of Lipid Bilayers: Molecular Dynamics Simulation Investigations. J Membrain Biol. 2013;246:843-50.
[74] Gurtovenko AA, Lyulina AS. Electroporation of Asymmetric Phospholipid Membranes. The Journal of Physical Chemistry B. 2014;118:9909-18.
[75] Bennett WFD, Sapay N, Tieleman DP. Atomistic Simulations of Pore Formation and Closure in Lipid Bilayers. Biophysical Journal. 2014;106:210-9.
[76] Hu Y, Sinha SK, Patel S. Investigating hydrophilic pores in model lipid bilayers using molecular simulations: Correlating bilayer properties with pore-formation thermodynamics. Langmuir. 2015;31:6615-31.
[77] Riske KA, Dimova R. Electric Pulses Induce Cylindrical Deformations on Giant Vesicles in Salt Solutions. Biophysical Journal. 2006;91:1778-86.
[78] Sadik MM, Li J, Shan JW, Shreiber DI, Lin H. Vesicle deformation and poration under strong dc electric fields. Physical Review E. 2011;83:066316.
[79] Salipante PF, Vlahovska PM. Vesicle deformation in DC electric pulses. Soft Matter. 2014;10:3386-93.
[80] Portet T, Camps i Febrer F, Escoffre J-M, Favard C, Rols M-P, Dean DS. Visualization of Membrane Loss during the Shrinkage of Giant Vesicles under Electropulsation. Biophysical Journal. 2009;96:4109-21.
[81] Helfrich W, Servuss RM. Undulations, steric interaction and cohesion of fluid membranes. Il Nuovo Cimento D. 1984;3:137-51.
[82] Evans E, Rawicz W. Entropy-driven tension and bending elasticity in condensed-fluid membranes. Phys Rev Lett. 1990;64:2094-7.
[83] Hyuga H, Kinosita Jr K, Wakabayashi N. Steady-state deformation of a vesicle in alternating electric fields. Bioelectrochemistry and Bioenergetics. 1993;32:15-25.
[84] Vlahovska PM, Gracià RS, Aranda-Espinoza S, Dimova R. Electrohydrodynamic Model of Vesicle Deformation in Alternating Electric Fields. Biophysical Journal. 2009;96:4789-803.
[85] Peterlin P. Frequency-dependent electrodeformation of giant phospholipid vesicles in AC electric field. Journal of Biological Physics. 2010;36:339-54.
[86] Nganguia H, Young YN. Equilibrium electrodeformation of a spheroidal vesicle in an ac electric field. Physical Review E. 2013;88:052718.
[87] Kummrow M, Helfrich W. Deformation of giant lipid vesicles by electric fields. Phys Rev A. 1991;44:8356-60.
[88] Aranda S, Riske KA, Lipowsky R, Dimova R. Morphological Transitions of Vesicles Induced by Alternating Electric Fields. Biophysical Journal. 2008;95:L19-L21.
[89] Gracia RS, Bezlyepkina N, Knorr RL, Lipowsky R, Dimova R. Effect of cholesterol on the rigidity of saturated and unsaturated membranes: fluctuation and electrodeformation analysis of giant vesicles. Soft Matter. 2010;6:1472-82.
[90] Kinosita K, Hibino M, Itoh H, Shigemori M, Hirano Ki, Kirino Y, et al. Events of membrane electroporation visualized on a time scale from microsecond to seconds. In: Sowers DCCMCASE, (editor). Guide to Electroporation and Electrofusion. San Diego: Academic Press; 1992. p. 29-46.
[91] Hyuga H, Kinosita K, Wakabayashi N. Deformation of vesicles under the influence of strong electric fields. Japanese Journal of Applied Physics. 1991;30:1141.
[92] Hyuga H, Kinosita K, Wakabayashi N. Deformation of vesicles under the influence of strong electric fields II. Japanese Journal of Applied Physics. 1991;30:1333.
[93] Schwalbe JT, Vlahovska PM, Miksis MJ. Vesicle electrohydrodynamics. Physical Review E. 2011;83:046309.

[94] McConnell LC, Vlahovska PM, Miksis MJ. Vesicle dynamics in uniform electric fields: squaring and breathing. Soft Matter. 2015;11:4840-6.
[95] McConnell LC, Miksis MJ, Vlahovska PM. Continuum modeling of the electric-field-induced tension in deforming lipid vesicles. The Journal of Chemical Physics. 2015;143:243132.
[96] Kolahdouz EM, Salac D. Dynamics of three-dimensional vesicles in dc electric fields. Physical Review E. 2015;92:012302.
[97] Kolahdouz E, Salac D. Electrohydrodynamics of Three-Dimensional Vesicles: A Numerical Approach. SIAM Journal on Scientific Computing. 2015;37:B473-B94.
[98] Yu M, Lira RB, Riske KA, Dimova R, Lin H. Ellipsoidal Relaxation of Deformed Vesicles. Phys Rev Lett. 2015;115:128303.
[99] Evans E, Heinrich V, Ludwig F, Rawicz W. Dynamic Tension Spectroscopy and Strength of Biomembranes. Biophysical Journal. 2003;85:2342-50.
[100] Sandre O, Moreaux L, Brochard-Wyart F. Dynamics of transient pores in stretched vesicles. Proceedings of the National Academy of Sciences. 1999;96:10591-6.
[101] Olbrich K, Rawicz W, Needham D, Evans E. Water Permeability and Mechanical Strength of Polyunsaturated Lipid Bilayers. Biophysical Journal. 2000;79:321-7.
[102] Leontiadou H, Mark AE, Marrink SJ. Molecular Dynamics Simulations of Hydrophilic Pores in Lipid Bilayers. Biophysical Journal. 2004;86:2156-64.
[103] Levadny V, Tsuboi T-a, Belaya M, Yamazaki M. Rate Constant of Tension-Induced Pore Formation in Lipid Membranes. Langmuir. 2013;29:3848-52.
[104] McConnell LC, Miksis MJ, Vlahovska PM. Vesicle electrohydrodynamics in DC electric fields. IMA Journal of Applied Mathematics. 2013;78:797-817.
[105] Mauroy C, Portet T, Winterhalder M, Bellard E, Blache MC, Teissie J, et al. Giant lipid vesicles under electric field pulses assessed by non invasive imaging. Bioelectrochemistry. 2012;87:253-9.
[106] Antonova K, Vitkova V, Meyer C. Membrane tubulation from giant lipid vesicles in alternating electric fields. Physical Review E. 2016;93.
[107] Sens P, Isambert H. Undulation instability of lipid membranes under an electric field. Phys Rev Lett. 2002;88:128102.
[108] Lacoste D, Menon GI, Bazant MZ, Joanny JF. Electrostatic and electrokinetic contributions to the elastic moduli of a driven membrane. The European Physical Journal E. 2009;28:243-64.
[109] Ziebert F, Bazant MZ, Lacoste D. Effective zero-thickness model for a conductive membrane driven by an electric field. Physical Review E. 2010;81:031912.
[110] Schwalbe JT, Vlahovska PM, Miksis MJ. Lipid membrane instability driven by capacitive charging. Phys Fluids. 2011;23:041701.
[111] Seiwert J, Miksis MJ, Vlahovska PM. Stability of biomimetic membranes in DC electric fields. Journal of Fluid Mechanics. 2012;706:58-70.
[112] Nagle JF, Tristram-Nagle S. Structure of lipid bilayers. Biochimica et Biophysica Acta (BBA) - Reviews on Biomembranes. 2000;1469:159-95.
[113] Veatch SL, Keller SL. Organization in Lipid Membranes Containing Cholesterol. Phys Rev Lett. 2002;89:268101.
[114] Riske KA, Knorr RL, Dimova R. Bursting of charged multicomponent vesicles subjected to electric pulses. Soft Matter. 2009;5:1983-6.
[115] Knorr RL, Staykova M, Gracia RS, Dimova R. Wrinkling and electroporation of giant vesicles in the gel phase. Soft Matter. 2010;6:1990-6.
[116] Liu Z-W, Zeng X-A, Sun D-W, Han Z. Effects of pulsed electric fields on the permeabilization of calcein-filled soybean lecithin vesicles. Journal of Food Engineering. 2014;131:26-32.
[117] van Uitert I, Le Gac S, van den Berg A. Determination of the electroporation onset of bilayer lipid membranes as a novel approach to establish ternary phase diagrams: example of the l-α-PC/SM/cholesterol system. Soft Matter. 2010;6:4420-9.
[118] Hung W-C, Lee M-T, Chen F-Y, Huang HW. The Condensing Effect of Cholesterol in Lipid Bilayers. Biophysical Journal. 2007;92:3960-7.

[119] Pan J, Mills TT, Tristram-Nagle S, Nagle JF. Cholesterol perturbs lipid bilayers nonuniversally. Phys Rev Lett. 2008;100:198103.
[120] Pan J, Tristram-Nagle S, Kučerka N, Nagle JF. Temperature Dependence of Structure, Bending Rigidity, and Bilayer Interactions of Dioleoylphosphatidylcholine Bilayers. Biophysical Journal.94:117-24.
[121] Casciola M, Bonhenry D, Liberti M, Apollonio F, Tarek M. A molecular dynamic study of cholesterol rich lipid membranes: comparison of electroporation protocols. Bioelectrochemistry. 2014;100:11-7.
[122] Fernández ML, Marshall G, Sagués F, Reigada R. Structural and Kinetic Molecular Dynamics Study of Electroporation in Cholesterol-Containing Bilayers. The Journal of Physical Chemistry B. 2010;114:6855-65.
[123] Reigada R. Electroporation of heterogeneous lipid membranes. Biochimica et Biophysica Acta (BBA) - Biomembranes. 2014;1838:814-21.
[124] Ogle BM, Cascalho M, Platt JL. Biological implications of cell fusion. Nature Reviews Molecular Cell Biology. 2005;6:567-75.
[125] Chen EH, Grote E, Mohler W, Vignery A. Cell–cell fusion. FEBS Letters. 2007;581:2181-93.
[126] Noubissi FK, Ogle BM. Cancer Cell Fusion: Mechanisms Slowly Unravel. International Journal of Molecular Sciences. 2016;17.
[127] Jahn R, Südhof TC. Membrane Fusion and Exocytosis. Annual Review of Biochemistry. 1999;68:863-911.
[128] Martens S, McMahon HT. Mechanisms of membrane fusion: disparate players and common principles. Nature Reviews Molecular Cell Biology. 2008;9:543-56.
[129] Chernomordik LV, Kozlov MM. Mechanics of membrane fusion. Nature Structural & Molecular Biology. 2008;15:675-83.
[130] Köhler G, Milstein C. Continuous cultures of fused cells secreting antibody of predefined specificity. Nature. 1975;256:495-7.
[131] Golestani R, Pourfathollah AA, Moazzeni SM. Cephalin as an Efficient Fusogen in Hybridoma Technology: Can It Replace Poly Ethylene Glycol? Hybridoma. 2007;26:296-301.
[132] Kulin S, Kishore R, Helmerson K, Locascio L. Optical Manipulation and Fusion of Liposomes as Microreactors. Langmuir. 2003;19:8206-10.
[133] Kandušer M, Ušaj M. Cell electrofusion: past and future perspectives for antibody production and cancer cell vaccines. Expert Opin Drug Del. 2014;11:1885-98.
[134] Campbell KHS, McWhir J, Ritchie WA, Wilmut I. Sheep cloned by nuclear transfer from a cultured cell line. Nature. 1996;380:64-6.
[135] Yanai G, Hayashi T, Zhi Q, Yang K-C, Shirouzu Y, Shimabukuro T, et al. Electrofusion of Mesenchymal Stem Cells and Islet Cells for Diabetes Therapy: A Rat Model. PloS one. 2013;8:e64499.
[136] Teissié J, Rols MP, Blangero C. Electrofusion of Mammalian Cells and Giant Unilamellar Vesicles. In: Neumann E, Sowers AE, Jordan CA, (editors). Electroporation and Electrofusion in Cell Biology. Boston, MA: Springer US; 1989. p. 203-14.
[137] Strömberg A, Ryttsén F, Chiu DT, Davidson M, Eriksson PS, Wilson CF, et al. Manipulating the genetic identity and biochemical surface properties of individual cells with electric-field-induced fusion. Proceedings of the National Academy of Sciences. 2000;97:7-11.
[138] Sugar IP, Förster W, Neumann E. Model of cell electrofusion: Membrane electroporation, pore coalescence and percolation. Biophysical Chemistry. 1987;26:321-35.
[139] Haluska CK, Riske KA, Marchi-Artzner V, Lehn J-M, Lipowsky R, Dimova R. Time scales of membrane fusion revealed by direct imaging of vesicle fusion with high temporal resolution. Proceedings of the National Academy of Sciences. 2006;103:15841-6.
[140] Riske KA, Bezlyepkina N, Lipowsky R, Dimova R. Electrofusion of model lipid membranes viewed with high-temporal resolution. Biophysical Reviews and Letters. 2006;01:387-400.
[141] Stoicheva NG, Hui SW. Electrofusion of cell-size liposomes. Biochimica et Biophysica Acta (BBA) - Biomembranes. 1994;1195:31-8.

[142] Yang P, Lipowsky R, Dimova R. Nanoparticle Formation in Giant Vesicles: Synthesis in Biomimetic Compartments. Small. 2009;5:2033-7.
[143] Washizu M, Techaumnat B. Cell membrane voltage during electrical cell fusion calculated by re-expansion method. Journal of Electrostatics. 2007;65:555-61.
[144] Techaumnat B. Numerical analysis of DC-field-induced transmembrane potential of spheroidal cells in axisymmetric orientations. IEEE Transactions on Dielectrics and Electrical Insulation. 2013;20:1567-76.
[145] DeBruin KA, Krassowska W. Modeling Electroporation in a Single Cell. I. Effects of Field Strength and Rest Potential. Biophysical Journal. 1999;77:1213-24.
[146] Rems L, Ušaj M, Kandušer M, Reberšek M, Miklavčič D, Pucihar G. Cell electrofusion using nanosecond electric pulses. Scientific reports. 2013;3:3382.
[147] Liu L, Mao Z, Zhang J, Liu N, Liu QH. The Influence of Vesicle Shape and Medium Conductivity on Possible Electrofusion under a Pulsed Electric Field. PloS one. 2016;11:e0158739.
[148] Rols MP, Teissié J. Electropermeabilization of mammalian cells. Quantitative analysis of the phenomenon. Biophysical Journal. 1990;58:1089-98.
[149] Kinosita K, Tsong TY. Formation and resealing of pores of controlled sizes in human erythrocyte membrane. Nature. 1977;268:438-41.
[150] Nesin OM, Pakhomova ON, Xiao S, Pakhomov AG. Manipulation of cell volume and membrane pore comparison following single cell permeabilization with 60- and 600-ns electric pulses. Biochimica et Biophysica Acta (BBA) - Biomembranes. 2011;1808:792-801.
[151] Portet T, Favard C, Teissie J, Dean DS, Rols M-P. Insights into the mechanisms of electromediated gene delivery and application to the loading of giant vesicles with negatively charged macromolecules. Soft Matter. 2011;7:3872-81.
[152] Rosazza C, Meglic SH, Zumbusch A, Rols M-P, Miklavcic D. Gene Electrotransfer: A Mechanistic Perspective. Current Gene Therapy. 2016;16:98-129.
[153] Fenz SF, Sengupta K. Giant vesicles as cell models. Integrative Biology. 2012;4:982-95.
[154] Alberts B, Johnson A, Lewis J, Raff M, Roberts K, Walter P. Molecular biology of the cell. 5th ed. New York: Garland Science, Taylor & Francis Group; 2008.
[155] Lodish H, Berk A, Zipursky SL, Matsudaira P, Baltimore D, Darnell J. Molecular cell biology. 4th ed. New York: W. H. Freeman and Company; 2001.
[156] Diz-Muñoz A, Fletcher DA, Weiner OD. Use the force: membrane tension as an organizer of cell shape and motility. Trends Cell Biol. 2013;23:47-53.
[157] Estes DJ, Mayer M. Giant liposomes in physiological buffer using electroformation in a flow chamber. Biochimica et Biophysica Acta (BBA) - Biomembranes. 2005;1712:152-60.
[158] Pavlič JI, Genova J, Popkirov G, Kralj-Iglič V, Iglič A, Mitov MD. Mechanoformation of neutral giant phospholipid vesicles in high ionic strength solution. Chemistry and physics of lipids. 2011;164:727-31.
[159] Montes LR, Alonso A, Goñi FM, Bagatolli LA. Giant Unilamellar Vesicles Electroformed from Native Membranes and Organic Lipid Mixtures under Physiological Conditions. Biophysical Journal. 2007;93:3548-54.
[160] Akashi K, Miyata H, Itoh H, Kinosita K. Preparation of giant liposomes in physiological conditions and their characterization under an optical microscope. Biophysical Journal. 1996;71:3242-50.
[161] Pott T, Bouvrais H, Méléard P. Giant unilamellar vesicle formation under physiologically relevant conditions. Chemistry and physics of lipids. 2008;154:115-9.
[162] Deshpande S, Caspi Y, Meijering AEC, Dekker C. Octanol-assisted liposome assembly on chip. Nature Communications. 2016;7:10447.
[163] Varnier A, Kermarrec F, Blesneac I, Moreau C, Liguori L, Lenormand JL, et al. A Simple Method for the Reconstitution of Membrane Proteins into Giant Unilamellar Vesicles. J Membrane Biol. 2010;233:85-92.
[164] Pautot S, Frisken BJ, Weitz DA. Engineering asymmetric vesicles. Proceedings of the National Academy of Sciences. 2003;100:10718-21.

[165] Chiantia S, Schwille P, Klymchenko AS, London E. Asymmetric GUVs Prepared by MβCD-Mediated Lipid Exchange: An FCS Study. Biophysical Journal. 2011;100:L1-L3.
[166] Limozin L, Sackmann E. Polymorphism of Cross-Linked Actin Networks in Giant Vesicles. Phys Rev Lett. 2002;89:168103.
[167] Pontani L-L, van der Gucht J, Salbreux G, Heuvingh J, Joanny J-F, Sykes C. Reconstitution of an Actin Cortex Inside a Liposome. Biophysical Journal. 2009;96:192-8.
[168] Limozin L, Roth A, Sackmann E. Microviscoelastic Moduli of Biomimetic Cell Envelopes. Phys Rev Lett. 2005;95:178101.
[169] Häckl W, Bärmann M, Sackmann E. Shape Changes of Self-Assembled Actin Bilayer Composite Membranes. Phys Rev Lett. 1998;80:1786-9.
[170] Walde P. Enzymatic reactions in liposomes. Curr Opin Colloid In. 1996;1:638-44.
[171] Viallat A, Dalous J, Abkarian M. Giant Lipid Vesicles Filled with a Gel: Shape Instability Induced by Osmotic Shrinkage. Biophysical Journal. 2004;86:2179-87.
[172] Osinkina L, Markström M, Orwar O, Jesorka A. A Method for Heat-Stimulated Compression of Poly(N-isopropyl acrylamide) Hydrogels Inside Single Giant Unilamellar Vesicles. Langmuir. 2010;26:1-4.
[173] Lira Rafael B, Dimova R, Riske Karin A. Giant Unilamellar Vesicles Formed by Hybrid Films of Agarose and Lipids Display Altered Mechanical Properties. Biophysical Journal. 2014;107:1609-19.
[174] Lira RB, Steinkühler J, Knorr RL, Dimova R, Riske KA. Posing for a picture: vesicle immobilization in agarose gel. Scientific reports. 2016;6:25254.
[175] Rols M-P, Teissié J. Experimental evidence for the involvement of the cytoskeleton in mammalian cell electropermeabilization. Biochimica et Biophysica Acta (BBA) - Biomembranes. 1992;1111:45-50.
[176] Teissie J, Rols M-P. Manipulation of Cell Cytoskeleton Affects the Lifetime of Cell Membrane Electropermeabilization. Annals of the New York Academy of Sciences. 1994;720:98-110.
[177] Rosazza C, Escoffre J-M, Zumbusch A, Rols M-P. The actin cytoskeleton has an active role in the electrotransfer of plasmid DNA in mammalian cells. Molecular therapy : the journal of the American Society of Gene Therapy. 2011;19:913-21.
[178] Rosazza C, Buntz A, Rieß T, Wöll D, Zumbusch A, Rols M-P. Intracellular Tracking of Single-plasmid DNA Particles After Delivery by Electroporation. Mol Ther. 2013;21:2217-26.
[179] Vaughan EE, Dean DA. Intracellular Trafficking of Plasmids during Transfection Is Mediated by Microtubules. Mol Ther. 2006;13:422-8.
[180] M. Rabanel J, Aoun V, Elkin I, Mokhtar M, Hildgen P. Drug-Loaded Nanocarriers: Passive Targeting and Crossing of Biological Barriers. Curr Med Chem. 2012;19:3070-102.
[181] Mouneimne Y, Tosi P-F, Gazitt Y, Nicolau C. Electro-insertion of xeno-glycophorin into the red blood cell membrane. Biochemical and Biophysical Research Communications. 1989;159:34-40.
[182] Zeira M, Tosi PF, Mouneimne Y, Lazarte J, Sneed L, Volsky DJ, et al. Full-length CD4 electroinserted in the erythrocyte membrane as a long-lived inhibitor of infection by human immunodeficiency virus. Proceedings of the National Academy of Sciences. 1991;88:4409-13.
[183] El Ouagari K, Benoist H, Sixou S, Teissié J. Electropermeabilization mediates a stable insertion of glycophorin A with Chinese hamster ovary cell membranes. European Journal of Biochemistry. 1994;219:1031-9.
[184] Raffy S, Lazdunski C, Teissié J. Electroinsertion and activation of the C-terminal domain of Colicin A, a voltage gated bacterial toxin, into mammalian cell membranes. Molecular membrane biology. 2004;21:237-46.
[185] Cranfield CG, Cornell BA, Grage SL, Duckworth P, Carne S, Ulrich AS, et al. Transient Potential Gradients and Impedance Measures of Tethered Bilayer Lipid Membranes: Pore-Forming Peptide Insertion and the Effect of Electroporation. Biophysical Journal. 2014;106:182-9.
[186] Kokla A, Blouchos P, Livaniou E, Zikos C, Kakabakos SE, Petrou PS, et al. Visualization of the membrane engineering concept: evidence for the specific orientation of electroinserted antibodies and selective binding of target analytes. Journal of Molecular Recognition. 2013;26:627-32.

[187] Moschopoulou G, Kintzios S. Application of “membrane-engineering” to bioelectric recognition cell sensors for the ultra-sensitive detection of superoxide radical: A novel biosensor principle. Anal Chim Acta. 2006;573–574:90-6.
[188] Moschopoulou G, Valero T, Kintzios S. Superoxide determination using membrane-engineered cells: An example of a novel concept for the construction of cell sensors with customized target recognition properties. Sensors and Actuators B: Chemical. 2012;175:78-84.
[189] Perdikaris A, Alexandropoulos N, Kintzios S. Development of a Novel, Ultra-rapid Biosensor for the Qualitative Detection of Hepatitis B Virus-associated Antigens and Anti-HBV, Based on “Membrane-engineered” Fibroblast Cells with Virus-Specific Antibodies and Antigens. Sensors. 2009;9:2176-86.
[190] Moschopoulou G, Vitsa K, Bem F, Vassilakos N, Perdikaris A, Blouhos P, et al. Engineering of the membrane of fibroblast cells with virus-specific antibodies: A novel biosensor tool for virus detection. Biosensors and Bioelectronics. 2008;24:1027-30.
[191] Larou E, Yiakoumettis I, Kaltsas G, Petropoulos A, Skandamis P, Kintzios S. High throughput cellular biosensor for the ultra-sensitive, ultra-rapid detection of aflatoxin M1. Food Control. 2013;29:208-12.
[192] Raffy S, Teissié J. Insertion of Glycophorin A, A Transmembraneous Protein, in Lipid Bilayers can be Mediated by Electropermeabilization. European Journal of Biochemistry. 1995;230:722-32.
[193] Raffy S, Teissié J. Electroinsertion of Glycophorin A in Interdigitation-Fusion Giant Unilamellar Lipid Vesicles. J Biol Chem. 1997;272:25524-30.
[194] Raffy S, Teissié J. Control of lipid membrane stability by cholesterol content. Biophysical Journal. 1999;76:2072-80.
[195] Raffy S, Teissié J. Surface Charge Control of Electropermeabilization and Glycophorin Electroinsertion with 1,2-Diacyl-sn-Glycero-3-Phosphocholine (lecithin) Liposomes. European Journal of Biochemistry. 1997;250:315-9.
[196] Bally M, Bailey K, Sugihara K, Grieshaber D, Vörös J, Städler B. Liposome and Lipid Bilayer Arrays Towards Biosensing Applications. Small. 2010;6:2481-97.
[197] Yıldırım MA, Goh K-I, Cusick ME, Barabási A-L, Vidal M. Drug—target network. Nat Biotechnol. 2007;25:1119-26.
[198] Bezlyepkina N, Gracià RS, Shchelokovskyy P, Lipowsky R, Dimova R. Phase Diagram and Tie-Line Determination for the Ternary Mixture DOPC/eSM/Cholesterol. Biophysical Journal. 2013;104:1456-64.
[199] Kotnik T. Lightning-triggered electroporation and electrofusion as possible contributors to natural horizontal gene transfer. Phys Life Rev. 2013;10:351-70.
[200] Christensen SM, Stamou D. Surface-based lipidvesicle reactor systems: fabrication and applications. 2007;3:828-36.
[201] Giustini M, Giuliani AM, Gennaro G. Natural or synthetic nucleic acids encapsulated in a closed cavity of amphiphiles. 2013;3:8618-32.
[202] Blain JC, Szostak JW. Progress Toward Synthetic Cells. Annual Review of Biochemistry. 2014;83:615-40.
[203] Hsin T-M, Yeung ES. Single-Molecule Reactions in Liposomes. Angewandte Chemie International Edition. 2007;46:8032-5.
[204] Terasawa H, Nishimura K, Suzuki H, Matsuura T, Yomo T. Coupling of the fusion and budding of giant phospholipid vesicles containing macromolecules. Proceedings of the National Academy of Sciences. 2012;109:5942-7.
[205] Shiomi H, Tsuda S, Suzuki H, Yomo T. Liposome-Based Liquid Handling Platform Featuring Addition, Mixing, and Aliquoting of Femtoliter Volumes. PloS one. 2014;9:e101820.
[206] Hu N, Yang J, Joo SW, Banerjee AN, Qian S. Cell electrofusion in microfluidic devices: A review. Sensors and Actuators B: Chemical. 2013;178:63-85.
[207] Tresset G, Takeuchi S. A Microfluidic Device for Electrofusion of Biological Vesicles. Biomed Microdevices. 2004;6:213-8.

[208] Tresset G, Takeuchi S. Utilization of Cell-Sized Lipid Containers for Nanostructure and Macromolecule Handling in Microfabricated Devices. Analytical Chemistry. 2005;77:2795-801.
[209] Wang Z, Hu N, Yeh L-H, Zheng X, Yang J, Joo SW, et al. Electroformation and electrofusion of giant vesicles in a microfluidic device. Colloids and Surfaces B: Biointerfaces. 2013;110:81-7.
[210] Skelley AM, Kirak O, Suh H, Jaenisch R, Voldman J. Microfluidic control of cell pairing and fusion. Nat Methods. 2009;6:147-52.
[211] Bai Y, He X, Liu D, Patil SN, Bratton D, Huebner A, et al. A double droplet trap system for studying mass transport across a droplet-droplet interface. 2010;10:1281-5.
[212] Huebner AM, Abell C, Huck WTS, Baroud CN, Hollfelder F. Monitoring a Reaction at Submillisecond Resolution in Picoliter Volumes. Analytical Chemistry. 2011;83:1462-8.
[213] Robinson T, Verboket PE, Eyer K, Dittrich PS. Controllable electrofusion of lipid vesicles: initiation and analysis of reactions within biomimetic containers. Lab on a Chip. 2014;14:2852-9.
[214] Karlsson M, Nolkrantz K, Davidson MJ, Strömberg A, Ryttsén F, Åkerman B, et al. Electroinjection of Colloid Particles and Biopolymers into Single Unilamellar Liposomes and Cells for Bioanalytical Applications. Analytical Chemistry. 2000;72:5857-62.
[215] Wick R, Angelova MI, Walde P, Luisi PL. Microinjection into giant vesicles and light microscopy investigation of enzyme-mediated vesicle transformations. Chemistry & Biology. 1996;3:105-11.
[216] Karlsson M, Sott K, Davidson M, Cans A-S, Linderholm P, Chiu D, et al. Formation of geometrically complex lipid nanotube-vesicle networks of higher-order topologies. Proceedings of the National Academy of Sciences. 2002;99:11573-8.
[217] Jesorka A, Stepanyants N, Zhang H, Ortmen B, Hakonen B, Orwar O. Generation of phospholipid vesicle-nanotube networks and transport of molecules therein. Nat Protocols. 2011;6:791-805.
[218] Sott K, Lobovkina T, Lizana L, Tokarz M, Bauer B, Konkoli Z, et al. Controlling Enzymatic Reactions by Geometry in a Biomimetic Nanoscale Network. Nano Letters. 2006;6:209-14.
[219] Tokarz M, Åkerman B, Olofsson J, Joanny J-F, Dommersnes P, Orwar O. Single-file electrophoretic transport and counting of individual DNA molecules in surfactant nanotubes. P Natl Acad Sci USA. 2005;102:9127-32.
[220] Jesorka A, Markström M, Orwar O. Controlling the Internal Structure of Giant Unilamellar Vesicles by Means of Reversible Temperature Dependent Sol−Gel Transition of Internalized Poly(N-isopropyl acrylamide). Langmuir. 2005;21:1230-7.
[221] Karlsson M, Davidson M, Karlsson R, Karlsson A, Bergenholtz J, Konkoli Z, et al. Biomimetic nanoscale reactors and networks. Annu Rev Phys Chem. 2004;55:613-49.
[222] Lizana L, Konkoli Z, Bauer B, Jesorka A, Orwar O. Controlling chemistry by geometry in nanoscale systems. Annual review of physical chemistry. 2009;60:449-68.
[223] Cans A-S, Wittenberg N, Karlsson R, Sombers L, Karlsson M, Orwar O, et al. Artificial cells: Unique insights into exocytosis using liposomes and lipid nanotubes. P Natl Acad Sci USA. 2003;100:400-4.
[224] Mellander LJ, Kurczy ME, Najafinobar N, Dunevall J, Ewing AG, Cans A-S. Two modes of exocytosis in an artificial cell. Scientific reports. 2014;4.
[225] Shirakashi R, Sukhorukov VL, Reuss R, Schulz A, Zimmermann U. Effects of a Pulse Electric Field on Electrofusion of Giant Unilamellar Vesicle (GUV)-Jurkat Cell. Journal of Thermal Science and Technology. 2012;7:589-602.
[226] Saito AC, Ogura T, Fujiwara K, Murata S, Nomura S-iM. Introducing Micrometer-Sized Artificial Objects into Live Cells: A Method for Cell–Giant Unilamellar Vesicle Electrofusion. PloS one. 2014;9:e106853.
[227] Raz-Ben Aroush D, Yehudai-Resheff S, Keren K. Electrofusion of giant unilamellar vesicles to cells. In: Paluch EK, (editor). Method Cell Biol. Vol. 125: Academic Press; 2015. p. 409-22.
[228] Lieber Arnon D, Yehudai-Resheff S, Barnhart Erin L, Theriot Julie A, Keren K. Membrane Tension in Rapidly Moving Cells Is Determined by Cytoskeletal Forces. Curr Biol. 2013;23:1409-17.
[229] Gregoriadis G, Ryman BE. Liposomes as carriers of enzymes or drugs: a new approach to the treatment of storage diseases. Biochem J. 1971;124:58P.

[230] Couvreur P, Vauthier C. Nanotechnology: Intelligent Design to Treat Complex Disease. Pharmaceutical Research. 2006;23:1417-50.
[231] Wang Y, Miao L, Satterlee A, Huang L. Delivery of oligonucleotides with lipid nanoparticles. Adv Drug Deliver Rev. 2015;87:68-80.
[232] Hallaj-Nezhadi S, Hassan M. Nanoliposome-based antibacterial drug delivery. Drug Delivery. 2015;22:581-9.
[233] Yingchoncharoen P, Kalinowski DS, Richardson DR. Lipid-Based Drug Delivery Systems in Cancer Therapy: What Is Available and What Is Yet to Come. Pharmacol Rev. 2016;68:701-87.
[234] Huang L, Liu Y. In Vivo Delivery of RNAi with Lipid-Based Nanoparticles. Annual Review of Biomedical Engineering. 2011;13:507-30.
[235] Chang H-I, Yeh M-K. Clinical development of liposome-based drugs: formulation, characterization, and therapeutic efficacy. Int J Nanomed. 2012;7:49-60.
[236] Wacker M. Nanocarriers for intravenous injection—The long hard road to the market. Int J Pharm. 2013;457:50-62.
[237] ElBayoumi T, Torchilin V. Current Trends in Liposome Research. In: Weissig V, (editor). Liposomes: Humana Press; 2010. p. 1-27.
[238] Lombardo D, Calandra P, Barreca D, Magazù S, Kiselev MA. Soft Interaction in Liposome Nanocarriers for Therapeutic Drug Delivery. Nanomaterials. 2016;6:125.
[239] Owens Iii DE, Peppas NA. Opsonization, biodistribution, and pharmacokinetics of polymeric nanoparticles. Int J Pharm. 2006;307:93-102.
[240] Immordino ML, Dosio F, Cattel L. Stealth liposomes: review of the basic science, rationale, and clinical applications, existing and potential. Int J Nanomed. 2006;1:297-315.
[241] Sawant RR, Torchilin VP. Challenges in Development of Targeted Liposomal Therapeutics. AAPS J. 2012;14:303-15.
[242] Hillaireau H, Couvreur P. Nanocarriers' entry into the cell: relevance to drug delivery. Cell Mol Life Sci. 2009;66:2873-96.
[243] Bibi S, Lattmann E, Mohammed AR, Perrie Y. Trigger release liposome systems: local and remote controlled delivery? Journal of Microencapsulation. 2012;29:262-76.
[244] Mura S, Nicolas J, Couvreur P. Stimuli-responsive nanocarriers for drug delivery. Nature materials. 2013;12:991-1003.
[245] Benvegnu T, Lemiegre L, Cammas-Marion S. New Generation of Liposomes Called Archaeosomes Based on Natural or Synthetic Archaeal Lipids as Innovative Formulations for Drug Delivery. Recent Patents on Drug Delivery & Formulation. 2009;3:206-20.
[246] Discher DE, Ahmed F. Polymersomes. Annual Review of Biomedical Engineering. 2006;8:323-41.
[247] Lakhal S, Wood MJA. Exosome nanotechnology: An emerging paradigm shift in drug delivery. Bioessays. 2011;33:737-41.
[248] Singh R, Lillard JW. Nanoparticle-based targeted drug delivery. Experimental and molecular pathology. 2009;86:215-23.
[249] Krishnamachari Y, Geary SM, Lemke CD, Salem AK. Nanoparticle Delivery Systems in Cancer Vaccines. Pharmaceutical Research. 2011;28:215-36.
[250] Du AW, Stenzel MH. Drug Carriers for the Delivery of Therapeutic Peptides. Biomacromolecules. 2014;15:1097-114.
[251] Zylberberg C, Matosevic S. Pharmaceutical liposomal drug delivery: a review of new delivery systems and a look at the regulatory landscape. Drug Delivery. 2016;23:3319-29.
[252] Niu Z, Conejos-Sánchez I, Griffin BT, O'Driscoll CM, Alonso MJ. Lipid-based nanocarriers for oral peptide delivery. Adv Drug Deliver Rev. 2016;106, Part B:337-54.
[253] Kakorin S, Neumann E. Electrooptical relaxation spectrometry of membrane electroporation in lipid vesicles. Colloids and Surfaces A: Physicochemical and Engineering Aspects. 2002;209:147-65.
[254] Neumann E, Kakorin S. Electrooptics of membrane electroporation and vesicle shape deformation. Curr Opin Colloid In. 1996;1:790-9.
[255] Kakorin S, Redeker E, Neumann E. Electroporative deformation of salt filled lipid vesicles. Eur Biophys J Biophy. 1998;27:43-53.

[256] Dimitrov V, Kakorin S, Neumann E. Transient oscillation of shape and membrane conductivity changes by field pulse-induced electroporation in nano-sized phospholipid vesicles. Phys Chem Chem Phys. 2013;15:6303-22.
[257] Kakorin S, Liese T, Neumann E. Membrane curvature and high-field electroporation of lipid bilayer vesicles. J Phys Chem B. 2003;107:10243-51.
[258] Gubernator J. Active methods of drug loading into liposomes: recent strategies for stable drug entrapment and increased in vivo activity. Expert Opin Drug Del. 2011;8:565-80.
[259] Batrakova EV, Kim MS. Using exosomes, naturally-equipped nanocarriers, for drug delivery. Journal of Controlled Release. 2015;219:396-405.
[260] Pol Evd, Böing AN, Harrison P, Sturk A, Nieuwland R. Classification, Functions, and Clinical Relevance of Extracellular Vesicles. Pharmacol Rev. 2012;64:676-705.
[261] Schiffelers R, Kooijmans S, Vader, van D, Van S. Exosome mimetics: a novel class of drug delivery systems. Int J Nanomed. 2012:1525.
[262] Alvarez-Erviti L, Seow Y, Yin H, Betts C, Lakhal S, Wood MJA. Delivery of siRNA to the mouse brain by systemic injection of targeted exosomes. Nat Biotechnol. 2011;29:341-5.
[263] Cooper JM, Wiklander PBO, Nordin JZ, Al-Shawi R, Wood MJ, Vithlani M, et al. Systemic exosomal siRNA delivery reduced alpha-synuclein aggregates in brains of transgenic mice. Movement Disorders. 2014;29:1476-85.
[264] Wahlgren J, Karlson TDL, Brisslert M, Vaziri Sani F, Telemo E, Sunnerhagen P, et al. Plasma exosomes can deliver exogenous short interfering RNA to monocytes and lymphocytes. Nucleic Acids Res. 2012;40:e130-e.
[265] Banizs AB, Huang T, Dryden K, Berr SS, Stone JR, Nakamoto RK, et al. In vitro evaluation of endothelial exosomes as carriers for small interfering ribonucleic acid delivery. Int J Nanomed. 2014;9:4223-30.
[266] Momen-Heravi F, Bala S, Bukong T, Szabo G. Exosome-mediated delivery of functionally active miRNA-155 inhibitor to macrophages. Nanomedicine: Nanotechnology, Biology and Medicine. 2014;10:1517-27.
[267] Tian Y, Li S, Song J, Ji T, Zhu M, Anderson GJ, et al. A doxorubicin delivery platform using engineered natural membrane vesicle exosomes for targeted tumor therapy. Biomaterials. 2014;35:2383-90.
[268] Toffoli G, Hadla M, Corona G, Caligiuri I, Palazzolo S, Semeraro S, et al. Exosomal doxorubicin reduces the cardiac toxicity of doxorubicin. Nanomedicine-Uk. 2015;10:2963-71.
[269] Hood JL, Scott MJ, Wickline SA. Maximizing exosome colloidal stability following electroporation. Anal Biochem. 2014;448:41-9.
[270] Hu L, Wickline SA, Hood JL. Magnetic resonance imaging of melanoma exosomes in lymph nodes. Magn Reson Med. 2015;74:266-71.
[271] Fuhrmann G, Serio A, Mazo M, Nair R, Stevens MM. Active loading into extracellular vesicles significantly improves the cellular uptake and photodynamic effect of porphyrins. Journal of Controlled Release. 2015;205:35-44.
[272] Kooijmans SAA, Stremersch S, Braeckmans K, de Smedt SC, Hendrix A, Wood MJA, et al. Electroporation-induced siRNA precipitation obscures the efficiency of siRNA loading into extracellular vesicles. Journal of Controlled Release. 2013;172:229-38.
[273] Lamichhane TN, Raiker RS, Jay SM. Exogenous DNA Loading into Extracellular Vesicles via Electroporation is Size-Dependent and Enables Limited Gene Delivery. Mol Pharmaceut. 2015;12:3650-7.
[274] Wang L, Chierico L, Little D, Patikarnmonthon N, Yang Z, Azzouz M, et al. Encapsulation of Biomacromolecules within Polymersomes by Electroporation. Angewandte Chemie. 2012;124:11284-7.
[275] Tian X, Nyberg S, Sharp PS, Madsen J, Daneshpour N, Armes SP, et al. LRP-1-mediated intracellular antibody delivery to the Central Nervous System. Scientific reports. 2015;5:11990.

[276] Sanson C, Diou O, Thévenot J, Ibarboure E, Soum A, Brûlet A, et al. Doxorubicin Loaded Magnetic Polymersomes: Theranostic Nanocarriers for MR Imaging and Magneto-Chemotherapy. Acs Nano. 2011;5:1122-40.
[277] Bain J, Ruiz-Pérez L, Kennerley AJ, Muench SP, Thompson R, Battaglia G, et al. In situ formation of magnetopolymersomes via electroporation for MRI. Scientific reports. 2015;5:14311.
[278] Bakhshi PK, Bain J, Gul MO, Stride E, Edirisinghe M, Staniland SS. Manufacturing Man-Made Magnetosomes: High-Throughput In Situ Synthesis of Biomimetic Magnetite Loaded Nanovesicles. Macromol Biosci. 2016;16:1555-61.
[279] Ramos C, Bonato D, Winterhalter M, Stegmann T, Teissié J. Spontaneous lipid vesicle fusion with electropermeabilized cells. FEBS Letters. 2002;518:135-8.
[280] Demange P, Réat V, Weinandy S, Ospital R, Chopinet-Mayeux L, Henri P, et al. Targeted Macromolecules Delivery by Large Lipidic Nanovesicles Electrofusion with Mammalian Cells. Journal of Biomaterials and Nanobiotechnology. 2011;02:527.
[281] Henri P, Ospital R, Teissié J. Content Delivery of Lipidic Nanovesicles in Electropermeabilized Cells. J Membrain Biol. 2015;248:849-55.
[282] Rosenheck K. Evaluation of the Electrostatic Field Strength at the Site of Exocytosis in Adrenal Chromaffin Cells. Biophysical Journal. 1998;75:1237-43.
[283] Retelj L, Pucihar G, Miklavčič D. Electroporation of intracellular liposomes using nanosecond electric pulses-A theoretical study. Ieee T Bio-Med Eng. 2013;60:2624-35.
[284] Rems L, Miklavčič D. Theoretical considerations for the potential of controlled drug release from lipid vesicles by means of electroporation or electrofusion. In: Lacković I, Vasić D, (editors). 6th European Conference of the International Federation for Medical and Biological Engineering, MBEC 2014, 7-11 September 2014, Dubrovnik, Croatia: Springer International Publishing; 2015. p. 797-800.
[285] Denzi A, Valle Ed, Apollonio F, Breton M, Mir LM, Liberti M. Exploring the Applicability of Nano-Poration for Remote Control in Smart Drug Delivery Systems. J Membrain Biol. 2016:1-10.
[286] Kotnik T, Bobanović F, Miklavčič D. Sensitivity of transmembrane voltage induced by applied electric fields—A theoretical analysis. Bioelectrochemistry and Bioenergetics. 1997;43:285-91.
[287] Kotnik T, Miklavčič D. Theoretical evaluation of voltage inducement on internal membranes of biological cells exposed to electric fields. Biophysical Journal. 2006;90:480-91.
[288] Schoenbach KH, Beebe SJ, Buescher ES. Intracellular effect of ultrashort electrical pulses. Bioelectromagnetics. 2001;22:440-8.
[289] Tekle E, Oubrahim H, Dzekunov SM, Kolb JF, Schoenbach KH, Chock PB. Selective Field Effects on Intracellular Vacuoles and Vesicle Membranes with Nanosecond Electric Pulses. Biophysical Journal. 2005;89:274-84.
[290] Scarlett SS, White JA, Blackmore PF, Schoenbach KH, Kolb JF. Regulation of intracellular calcium concentration by nanosecond pulsed electric fields. Biochimica et Biophysica Acta (BBA) - Biomembranes. 2009;1788:1168-75.
[291] Batista Napotnik T, Reberšek M, Kotnik T, Lebrasseur E, Cabodevila G, Miklavčič D. Electropermeabilization of endocytotic vesicles in B16 F1 mouse melanoma cells. Med Biol Eng Comput. 2010;48:407-13.
[292] Batista Napotnik T, Reberšek M, Vernier PT, Mali B, Miklavčič D. Effects of high voltage nanosecond electric pulses on eukaryotic cells (in vitro): A systematic review. Bioelectrochemistry. 2016;110:1-12.
[293] Scheffer HJ, Nielsen K, de Jong MC, van Tilborg AAJM, Vieveen JM, Bouwman ARA, et al. Irreversible electroporation for nonthermal tumor ablation in the clinical setting: a systematic review of safety and efficacy. Journal of vascular and interventional radiology: JVIR. 2014;25:997-1011.
[294] Nuccitelli R, Wood R, Kreis M, Athos B, Huynh J, Lui K, et al. First-in-human trial of nanoelectroablation therapy for basal cell carcinoma: proof of method. Exp Dermatol. 2014;23:135-7.
[295] Yang W, Ahmed M, Elian M, Hady E-SA, Levchenko TS, Sawant RR, et al. Do Liposomal Apoptotic Enhancers Increase Tumor Coagulation and End-Point Survival in Percutaneous Radiofrequency Ablation of Tumors in a Rat Tumor Model? Radiology. 2010;257:685-96.

[296] Goldberg SN, Girnan GD, Lukyanov AN, Ahmed M, Monsky WL, Gazelle GS, et al. Percutaneous Tumor Ablation: Increased Necrosis with Combined Radio-frequency Ablation and Intravenous Liposomal Doxorubicin in a Rat Breast Tumor Model. Radiology. 2002;222:797-804.
[297] Monsky WL, Kruskal JB, Lukyanov AN, Girnun GD, Ahmed M, Gazelle GS, et al. Radio-frequency ablation increases intratumoral liposomal doxorubicin accumulation in a rat breast tumor model. Radiology. 2002;224:823-9.
[298] Rems L, Miklavčič D. Tutorial: Electroporation of cells in complex materials and tissue. Journal of Applied Physics. 2016;119:201101.
[299] Maccarrone M, Bladergroen MR, Rosato N, Agro AF. Role of lipid peroxidation in electroporation-induced cell permeability. Biochemical and Biophysical Research Communications. 1995;209:417-25.
[300] Leguèbe M, Silve A, Mir LM, Poignard C. Conducting and permeable states of cell membrane submitted to high voltage pulses: Mathematical and numerical studies validated by the experiments. Journal of Theoretical Biology. 2014;360:83-94.
[301] Teissié J, Tsong TY. Evidence of voltage-induced channel opening in Na/K ATPase of human erythrocyte membrane. J Membrain Biol. 1980;55:133-40.
[302] Gabriel B, Teissié J. Direct observation in the millisecond time range of fluorescent molecule asymmetrical interaction with the electropermeabilized cell membrane. Biophysical Journal. 1997;73:2630-7.
[303] Golzio M, Teissié J, Rols M-P. Direct visualization at the single-cell level of electrically mediated gene delivery. Proceedings of the National Academy of Sciences. 2002;99:1292-7.
[304] Nematbakhsh Y, Lim CT. Cell biomechanics and its applications in human disease diagnosis. Acta Mechanica Sinica. 2015;31:268-73.
[305] Dahl JB, Lin J-MG, Muller SJ, Kumar S. Microfluidic strategies for understanding the mechanics of cells and cell-mimetic systems. Annual review of chemical and biomolecular engineering. 2015;6:293-317.
[306] Chivukula VK, Krog BL, Nauseef JT, Henry MD, Vigmostad SC. Alterations in cancer cell mechanical properties after fluid shear stress exposure: A micropipette aspiration study. Cell Health and Cytoskeleton. 2015;7:25-35.
[307] Boukany PE, Morss A, Liao W-c, Henslee B, Jung H, Zhang X, et al. Nanochannel electroporation delivers precise amounts of biomolecules into living cells. Nat Nanotechnol. 2011;6:747-54.
[308] Liu C, Xie X, Zhao W, Liu N, Maraccini PA, Sassoubre LM, et al. Conducting nanosponge electroporation for affordable and high-efficiency disinfection of bacteria and viruses in water. Nano Letters. 2013;13:4288-93.
[309] Xie X, Xu AM, Leal-Ortiz S, Cao Y, Garner CC, Melosh NA. Nanostraw–Electroporation System for Highly Efficient Intracellular Delivery and Transfection. Acs Nano. 2013;7:4351-8.
[310] Rosazza C, Deschout H, Buntz A, Braeckmans K, Rols M-P, Zumbusch A. Endocytosis and Endosomal Trafficking of DNA After Gene Electrotransfer In Vitro. Molecular therapy Nucleic acids. 2016;5:e286.

Figure captions

Fig. 1. Schematic of a vesicle exposed to an electric pulse.

Fig. 2. Time sequence of phase contrast images showing deformation and macroporation of GUVs exposed to a DC electric pulse under two different conductivity conditions. (A) shows the tube-like deformation of a GUV, exposed to 200 μs, 2 kV/cm pulse, at conductivity condition χ = 1.38, λ_i = 16.5 μS/cm, λ_e = 12 μS/cm. (B) Shows two disk-like deformation of two GUVs exposed to 300 μs, 3 kV/cm pulse under conductivity condition χ = 0.05, λ_i = 6 μS/cm, λ_e = 120 μS/cm. Time 0 s corresponds to the onset of the pulse. In both cases the pulse duration is comparable to the charging time of the membrane. White arrows indicate locations of macropores. Reprinted with permission from [77]. Copyright 2006 Elsevier. (C) A schematic representation of the semiaxes for determining the aspect ratio a/b of deformed GUVs.

Fig. 3. Sketch of the electric field and induced charge distribution around a GUV immersed in an electrolyte solution, following the imposition of a uniform DC field: (a,b) during the membrane charging phase under condition (a) $\chi > 1$and (b) $\chi < 1$, and (c) after the membrane becomes fully charged. The dashed lines indicate the vesicle deformation. Reprinted with permission from [79]. Copyright 2014 The Royal Society of Chemistry.

Fig. 4. Numerical calculations of the membrane tension for a GUV exposed to a DC pulse under conductivity condition χ = 0.1. Membrane tension is plotted as a function of arclength measured from the vesicle equator (0 and 0.5 correspond to the equator, 0.25 and 0.75 to the poles of the GUV). The images on the right-hand side show the associated vesicle profile at dimensionless time (a) t/t_m = 0, (b) 0.1, (c) 0.17, (d) 0.22 and (e) 0.6, where $t_m = RC_m/\lambda_e$ is a measure for the membrane charging time. The electric field is directed from top to bottom. The numerical results were reported in dimensionless form. For experimental parameters similar to those in Fig. 2A, the electric field strength in dimensional form is ~4 kV/cm and the pulse duration is ~150 μs. Note that the GUV is initially shaped as prolate spheroid since the numerical model assumes conservation of the membrane area and vesicle volume, and thus cannot predict electrodeformations for idealized spheres without any access area. Reprinted with permission from [94]. Copyright 2015 The Royal Society of Chemistry.

Fig. 5. (a) Image sequence of a fluorescently labelled GUV showing formation of macropores on the cathodic side of the membrane. The GUV was exposed to multiple 5 ms, 300 V/cm pulses. Image D1 is acquired after 15 pulses, D2 after 16 pulses, D3 after 17 pulses, etc. (b) Images of three GUVs, denoted as A, B, and C, showing the different mechanisms of lipid ejection: vesicle and tubule formation. The parameters of applied pulses were similar as in (a). Images with index 1, 2, and 3, were captured after application of 0, 12, and 24 pulses, respectively. Reprinted with permission from [80]. Copyright 2009 Elsevier.

Fig. 6. Snapshots from MD showing the creation of a pore in an asymmetric bilayer composed of POPE (green) and POPC (yellow) induced by an electric field. Reprinted with permission from [74]. Copyright 2014 American Chemical Society.

Fig. 7. (a) Confocal fluorescence microscopy (left) and phase-contrast (right) images of the bursting effect of charged GUVs (1:1 PG:PC) in salt solution. Pulse parameters: 1.4 kV/cm, t_{pulse} = 200 μs. (b)

Fast camera image sequence of a bursting GUV, made from lipid extract of human red blood cell membranes. Pulse parameters: 2 kV/cm, t_{pulse} = 300 µs. The scale bar corresponds to 15 µm. Reprinted with permission from [114]. Copyright 2009 The Royal Society of Chemistry.

Fig. 8. Images of a gel phase DPPC GUV with R = 25 µm, before and after the pulse (E = 6 kV/cm, t_{pulse} = 300 µs) in (a,d) DIC, (b,e) confocal, and (c,f) a 3D projection of the upper half of the GUV. Reprinted with permission from [115]. Copyright 2010 The Royal Society of Chemistry.

Fig. 9. Several series of snapshots for the fusion of two vesicles. (a) Fusion of two functionalized GUVs held by micropipettes (only the right pipette tip is visible on the snapshots). A third pipette (bottom right corner) is used to inject a small volume (few tens of nanoliters) of 50 µM solution of $EuCl_3$. The first image corresponding to the starting time t = 0 represents the last snapshot before the adhesion zone of the vesicles undergoes detectable changes. (b) The behaviour of a single GUV (first image) and a GUV couple (remaining images) when exposed to a 150 µs, 1.8 kV/cm pulse in the absence of salt. (c) Behaviour of a single GUV (first image) and a GUV couple (remaining images) in the presence of 1 mM NaCl in the exterior solution. In this case, the GUV couple was exposed to a 150 µs, 3 kV/cm pulse. The polarity of the electrodes is indicated with a plus (+) or a minus (−) sign. The arrows in the first images indicate porated parts of the membrane, which lead to the leakage of enclosed liquid. For both b and c, the starting time t = 0 corresponds to the onset of the pulse. In the last two snapshots of the sequence (b), the fused vesicles contain an array of internal vesicles (bright spots) as indicated by the arrows. Reprinted with permission from [139]. Copyright 2006 National Academy of Sciences.

Fig. 10. Theoretical predictions of selective electroporation of the contact zone in a pair of GUVs. (a) Time course of transmembrane voltage U_m (absolute value) induced in a pair of GUVs with radius of 20 µm, after the onset of a pulse with amplitude of 1 kV/cm. U_m is shown at three points (A, B, and C) indicated on the sketch inside the graph. Note that U_m at the contact zone (C) surpasses U_m on the poles of the GUV pair (A, B) for times up to ~150 µs. (b) Calculations of the electroporated area for pulses with three different durations (10 µs, 150 µs, and 3000 µs). The amplitude of each pulse was adjusted such that the predicted pore density at the contact zone exceeds 10 pores per μm^2. The pore density above 10 pores per μm^2 is indicated by thick red lines. (c,d) Same calculations as in (a,b), but for two GUVs with different size (radius 10 µm and 30 µm). The results were obtained in the same way as in [146], except that the model parameters were adapted to experimental conditions for GUVs. The membrane capacitance was set to 0.67 $\mu F/cm^2$, membrane conductivity to 10^{-9} S/m [43], and the radius of the contact zone to 5 µm. The external and internal conductivities are given in the graphs and correspond to pure sugar solution on the outside and sugar solution containing 1 mM NaCl on the inside of the GUVs.

Fig. 11. Repetitive cycles of fusion-to-budding transformation. After the first fusion (t = 12 s), the fused vesicle separates into two daughter vesicles (t = 43 s). The aqueous compartments of the daughter vesicles are separated, but the membranes remain associated, possibly in hemifusion. Therefore, subsequent application of an AC signal after each budding event (t = 94 and 132 s) is already sufficient to induce fusion without the need of applying an elecroporative DC pulse. The vesicles contain 3 mM PEG 6000 (5% wt⁄wt). White arrows indicate the vesicles to be fused. Gray arrows show the neck formation. Scale bar: 10 µm. Reprinted with permission from [204].

Fig. 12. Scheme of the trapping sequence and electrofusion in a microfluidic device. (a) A vesicle fusion trap with integrated electrodes in a sealable microchamber. (b) Without vesicles, fluid flow is allowed through the gaps of the PDMS posts. The fluid flow lines are indicated with blue arrows. (c) The first vesicle trapped occupies the rear of the trap and blocks the central passage from flow. (d) Shows the situation when a second vesicle of equal size enters and the flow is diverted in front of the trap. When a second smaller vesicle is trapped as shown in (e) other vesicles are allowed to enter. (f) Electrofusion is then performed. Note that the vesicles are trapped such that the contact zone between the vesicles is oriented perpendicular to the electric field established between the electrodes. This is crucial for inducing electroporation of the contact zone and consequently electrofusion. Reprinted with permission from [213]. Copyright 2014 The Royal Society of Chemistry.

Fig. 13. Formation and release of an exocytotic vesicle in an artificial cell model. (a–d) Schematics of the microelectroinjection pipette inserted first into the interior of a GUV and then through the opposing wall of the GUV. Afterwards, the micropipette is pulled back in to the interior, followed by spontaneous formation of a lipid nanotube and formation of a vesicle from flow out of the tip of the micropipette. (e) A DIC image of a GUV, with a MLV attached as a reservoir of lipid, microelectroinjection pipette (i), opposite electrode for electric pulse delivery (ii), and 30-µm diameter amperometric electrode bevelled to a 45° angle (iii). A small red line depicts the location of the lipid nanotube. (f–i) Fluid injection at a constant flow rate results in growth of the newly formed vesicle with a simultaneous shortening of the nanotube until the final stage of exocytosis takes place spontaneously and a new vesicle is formed with the attached nanotube. (j–m) Fluorescence microscopy images of fluorescein-filled vesicles showing formation and final stage of exocytosis matching the events in f–i. Scale bar represents 10 µm. Reprinted with permission from [223]. Copyright 2003 National Academy of Sciences.

Fig. 14. Introducing multiple components of microbeads and plasmids into living cells by cell–GUV electrofusion. GUVs including both the plasmid mCherry and fluorescent microbeads were prepared for electrofusion with HeLa cells. After treatment, the cells were cultured for 2 days. Confocal microscopic images show the cross section of the treated HeLa cells into which beads of 0.2 µm, 0.5 µm, and 1 µm diameter (green) had been introduced. The mCherry expression in cells is shown in red, and merged images are shown in the right column. Scale bar = 20 µm. Reprinted with permission from [226].

Fig. 15. (*Left*) Schematic representation of the protocol for electrofusion between GUVs and cells adhered on a glass coverslip. Reprinted with permission from [227]. Copyright 2015 Elsevier. (*Right*) Phase-contrast and fluorescence images of a fish keratocyte cell before and after electrofusion with a GUV. Since the GUV has been fluorescently labelled, the cell membrane becomes fluorescent upon electrofusion. Note also the increase in the membrane area after fusion. Reprinted with permission from [228]. Copyright 2013 Elsevier.

Fig. 16. Schematic of the proposed mechanism for MNP synthesis within polymersomes using electroporation (a), which opens pores within the membrane at which point influx of iron ions occurs in parallel with efflux of NaOH (encapsulated) (b). (c) shows the in situ room temperature co-precipitation that then occurs at the interface within the membrane. Reprinted with permission from [277].

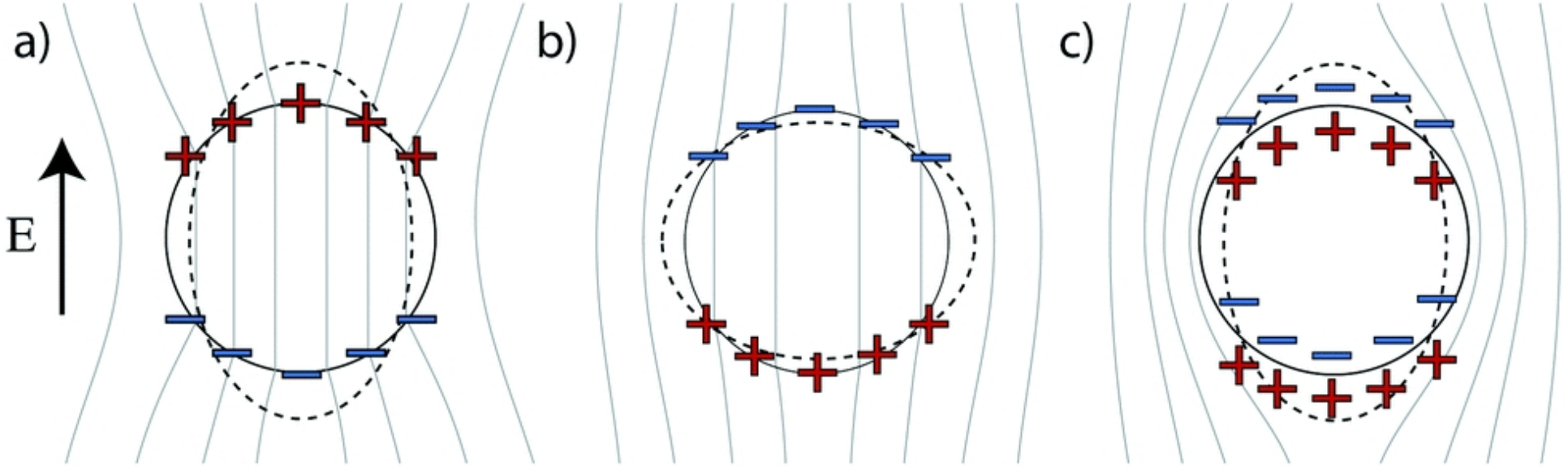
a)
E
b)
c)

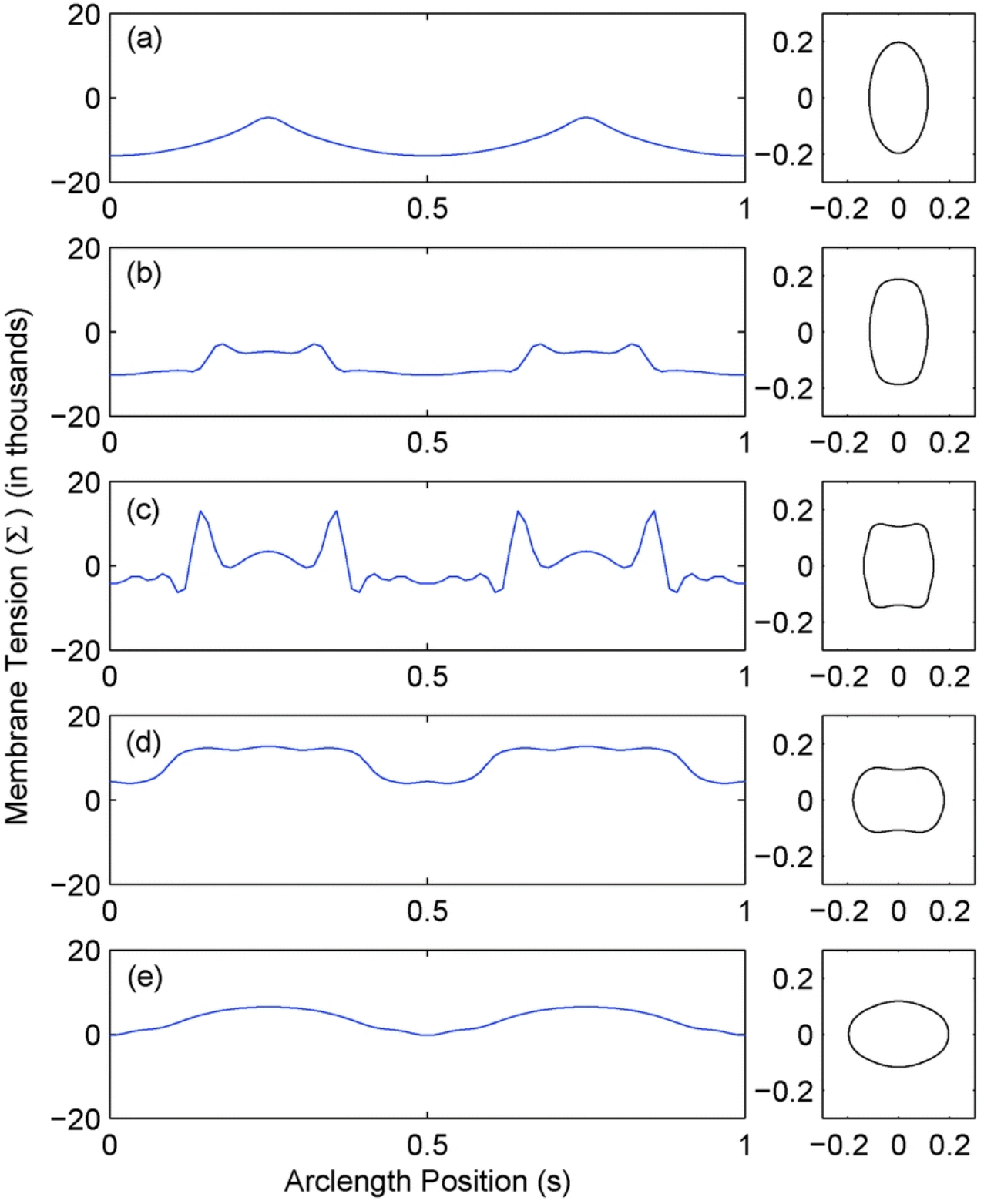
(a)
(b)
(c)
(d)
(e)
20
0
−20
0
0.5
1
0.2
0
−0.2
−0.2
0
0.2
Membrane Tension (Σ) (in thousands)
Arclength Position (s)

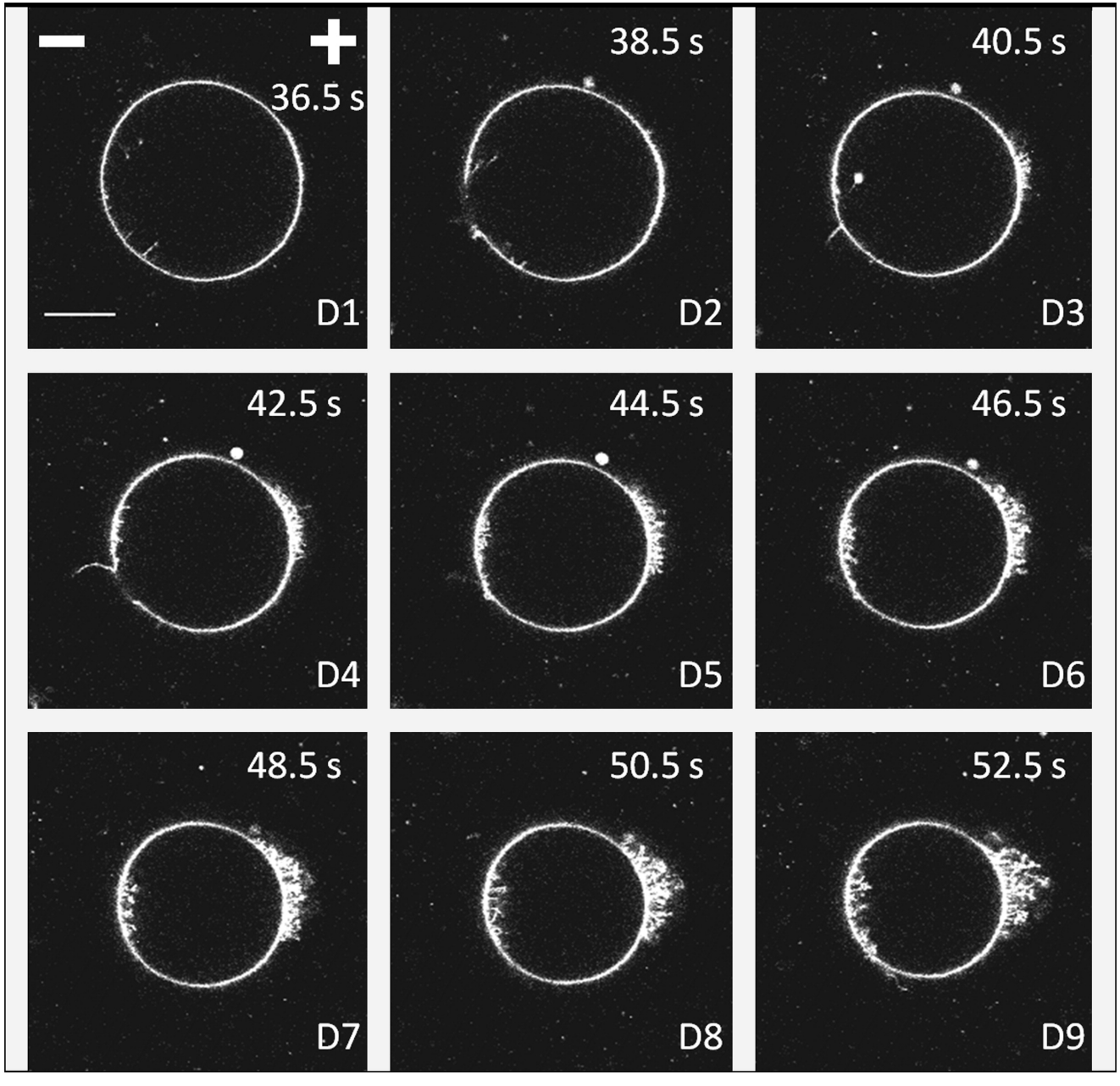
−
+
36.5 s
D1
38.5 s
D2
40.5 s
D3
42.5 s
D4
44.5 s
D5
46.5 s
D6
48.5 s
D7
50.5 s
D8
52.5 s
D9

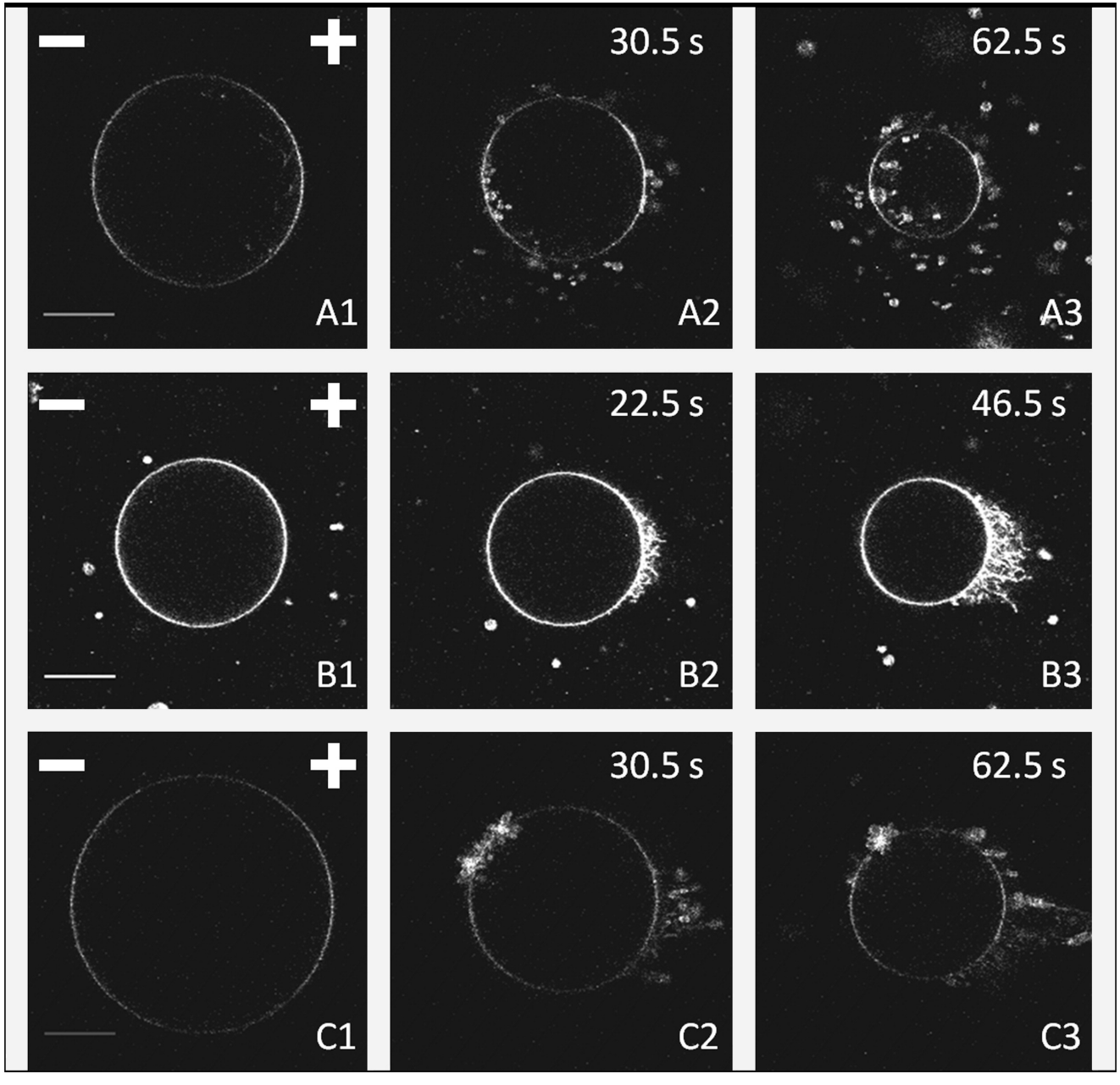
−
+
A1
30.5 s
A2
62.5 s
A3
−
+
B1
22.5 s
B2
46.5 s
B3
−
+
C1
30.5 s
C2
62.5 s
C3

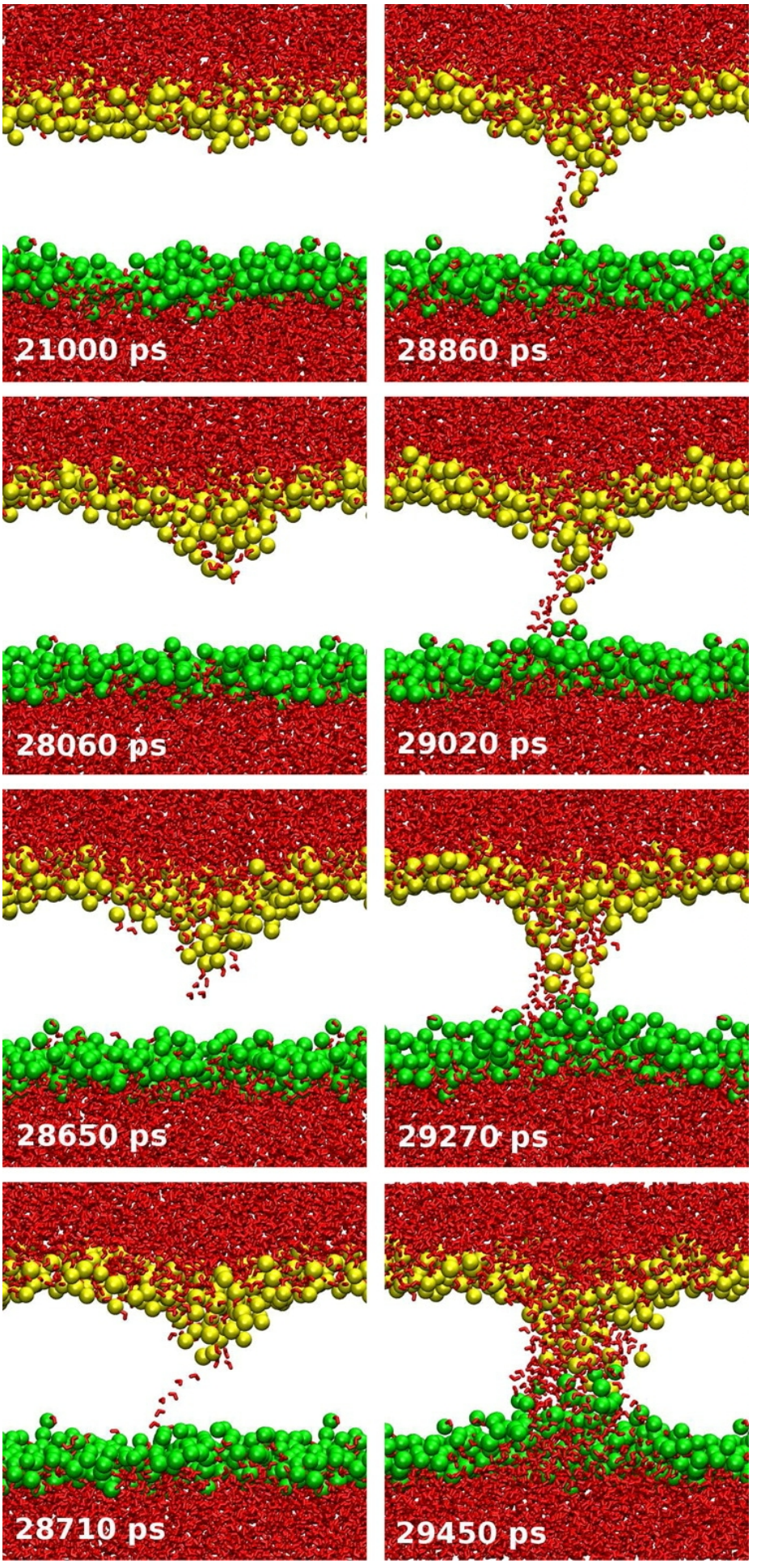
21000 ps
28860 ps
28060 ps
29020 ps
28650 ps
29270 ps
28710 ps
29450 ps

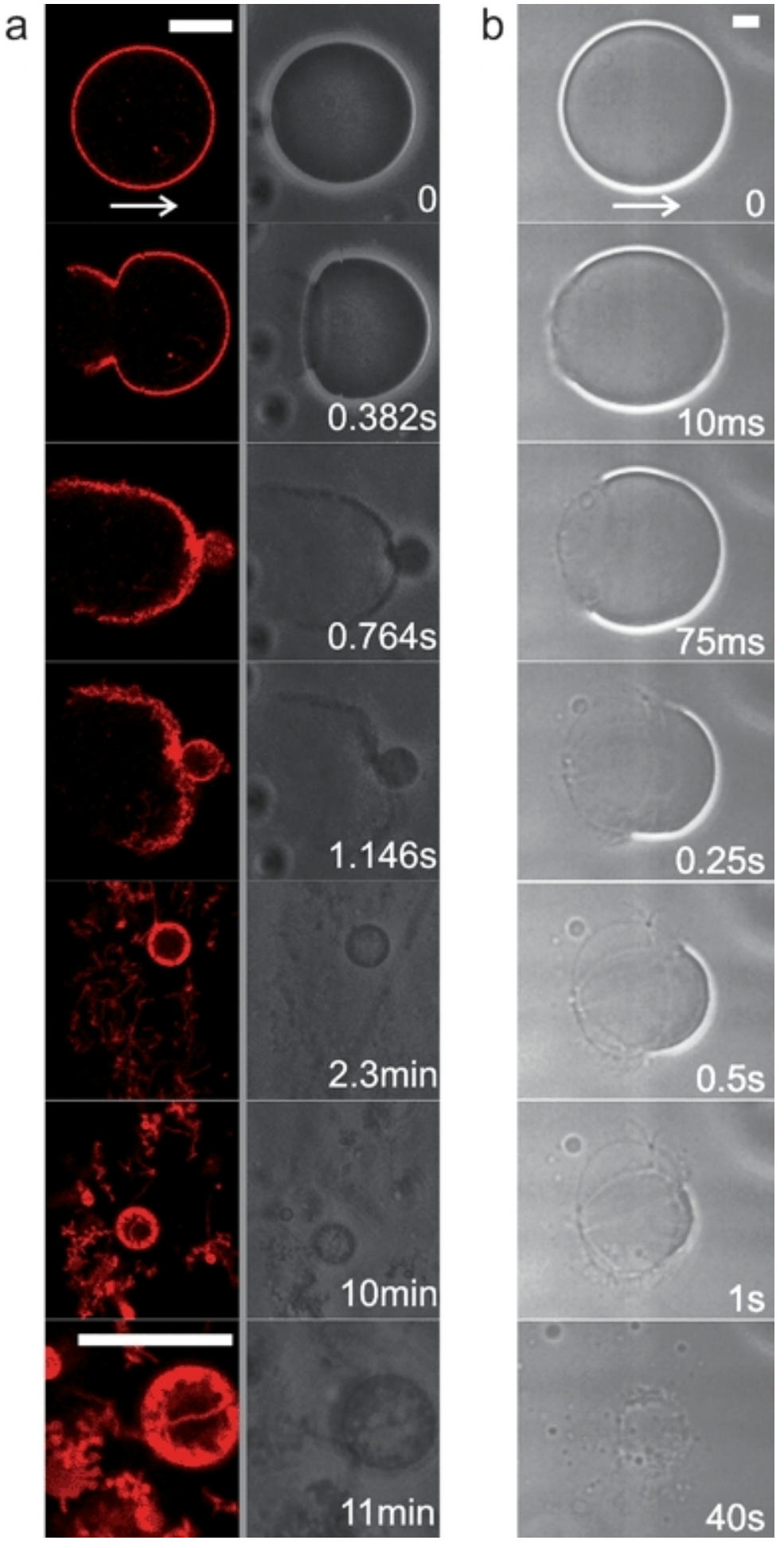
a
b
0
0.382s
0.764s
1.146s
2.3min
10min
11min
0
10ms
75ms
0.25s
0.5s
1s
40s

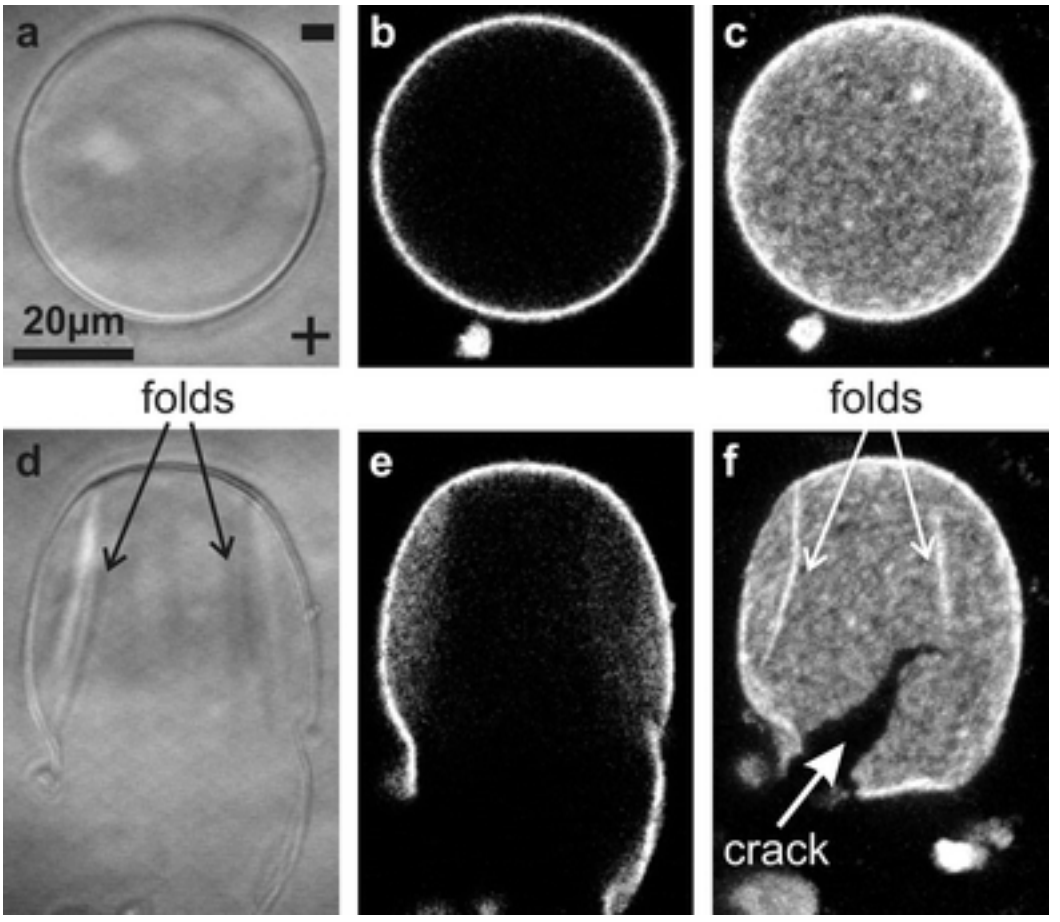
a
20μm
b
c
folds
folds
d
e
f
crack

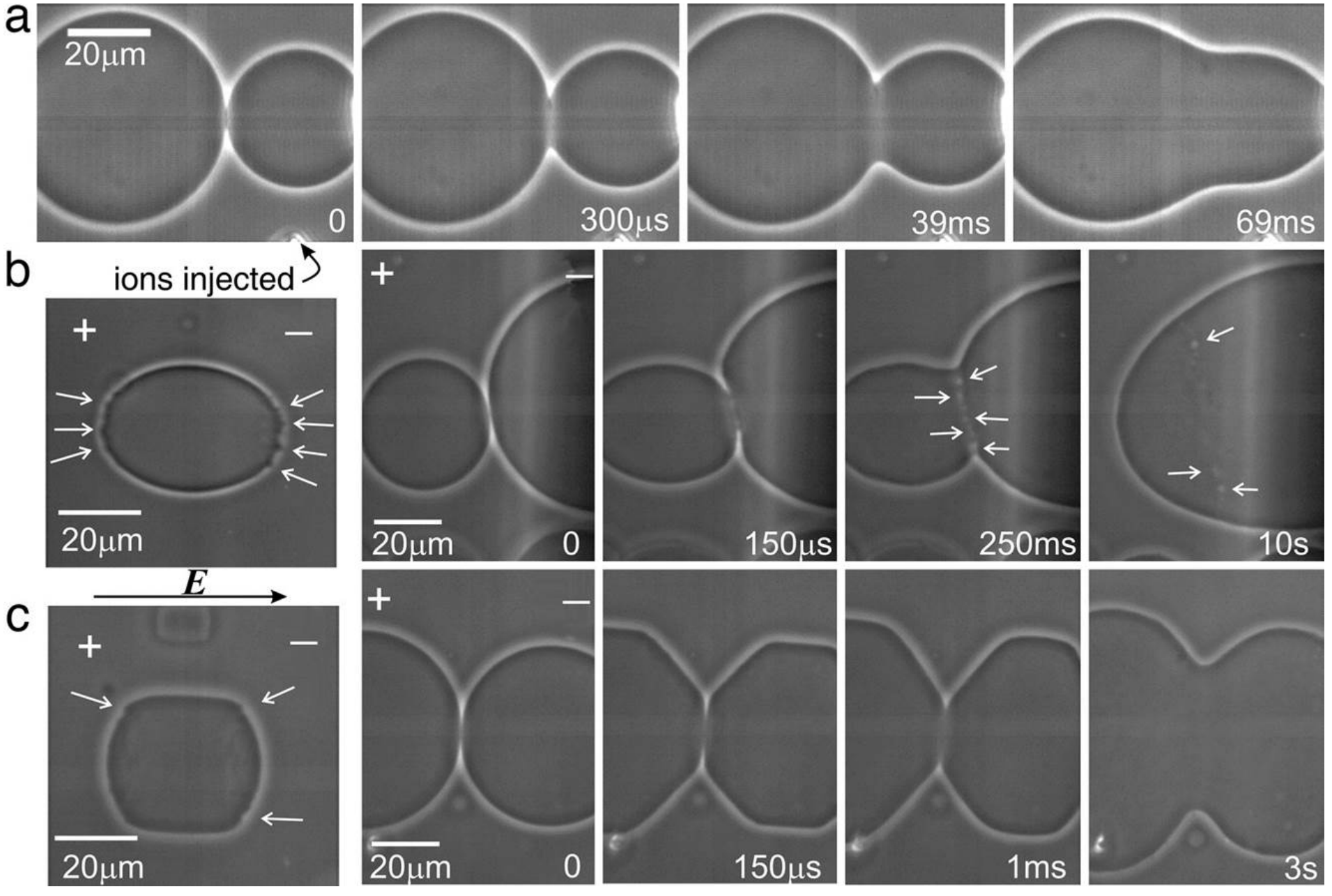
a
20μm
0
300μs
39ms
69ms
b
ions injected
+
–
20μm
0
150μs
250ms
10s
c
E
+
–
20μm
0
150μs
1ms
3s

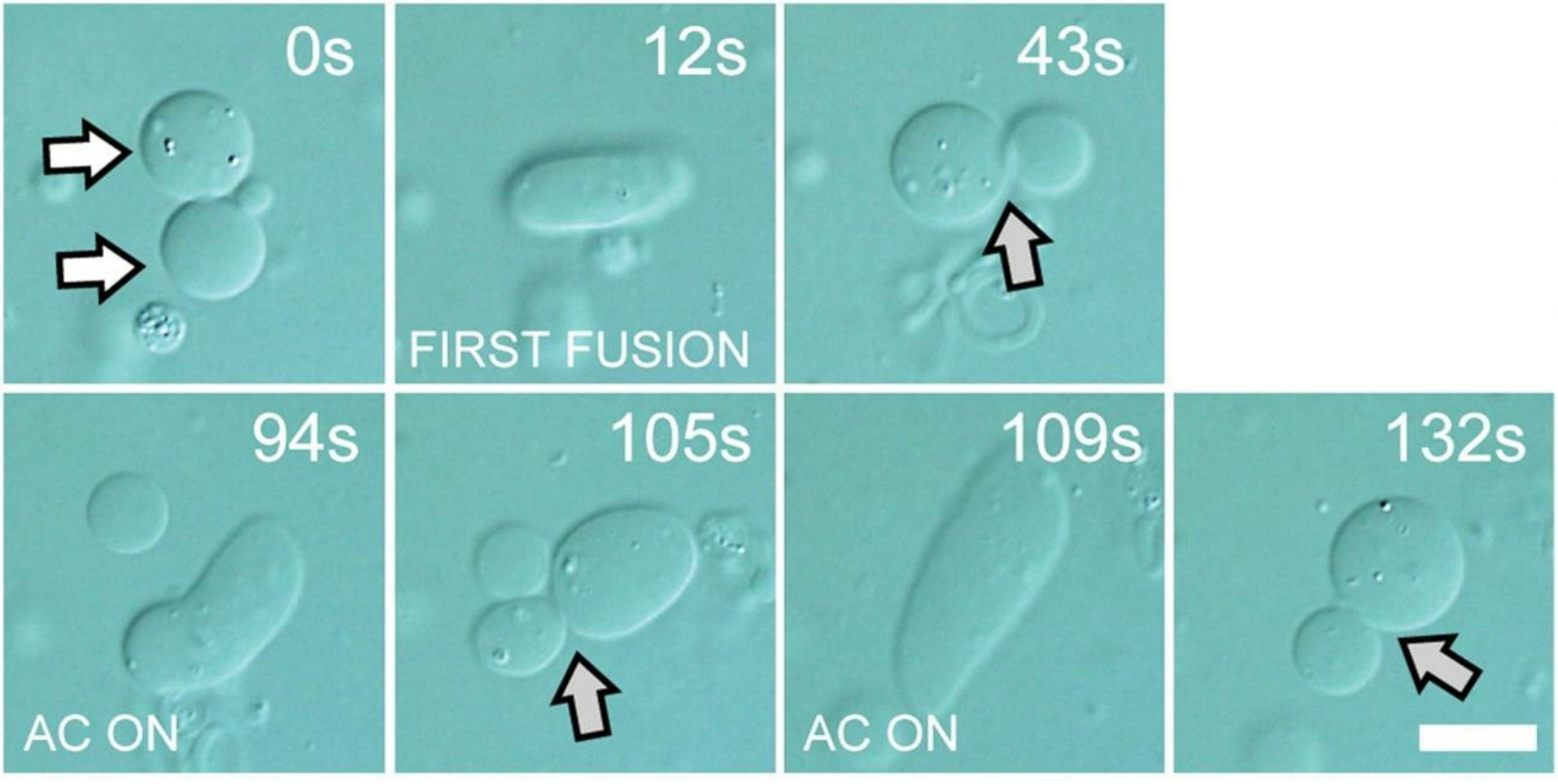
0s
12s
43s
FIRST FUSION
94s
105s
109s
132s
AC ON
AC ON

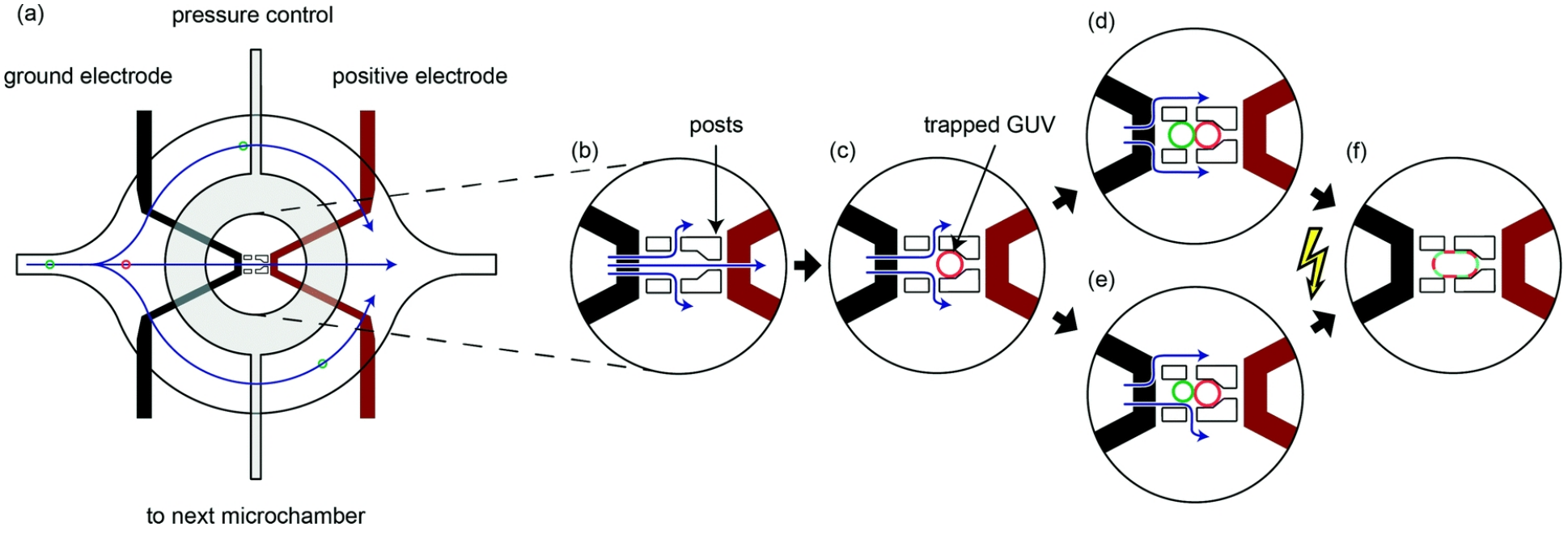
(a)
pressure control
ground electrode
positive electrode
to next microchamber
(b)
posts
(c)
trapped GUV
(d)
(e)
(f)

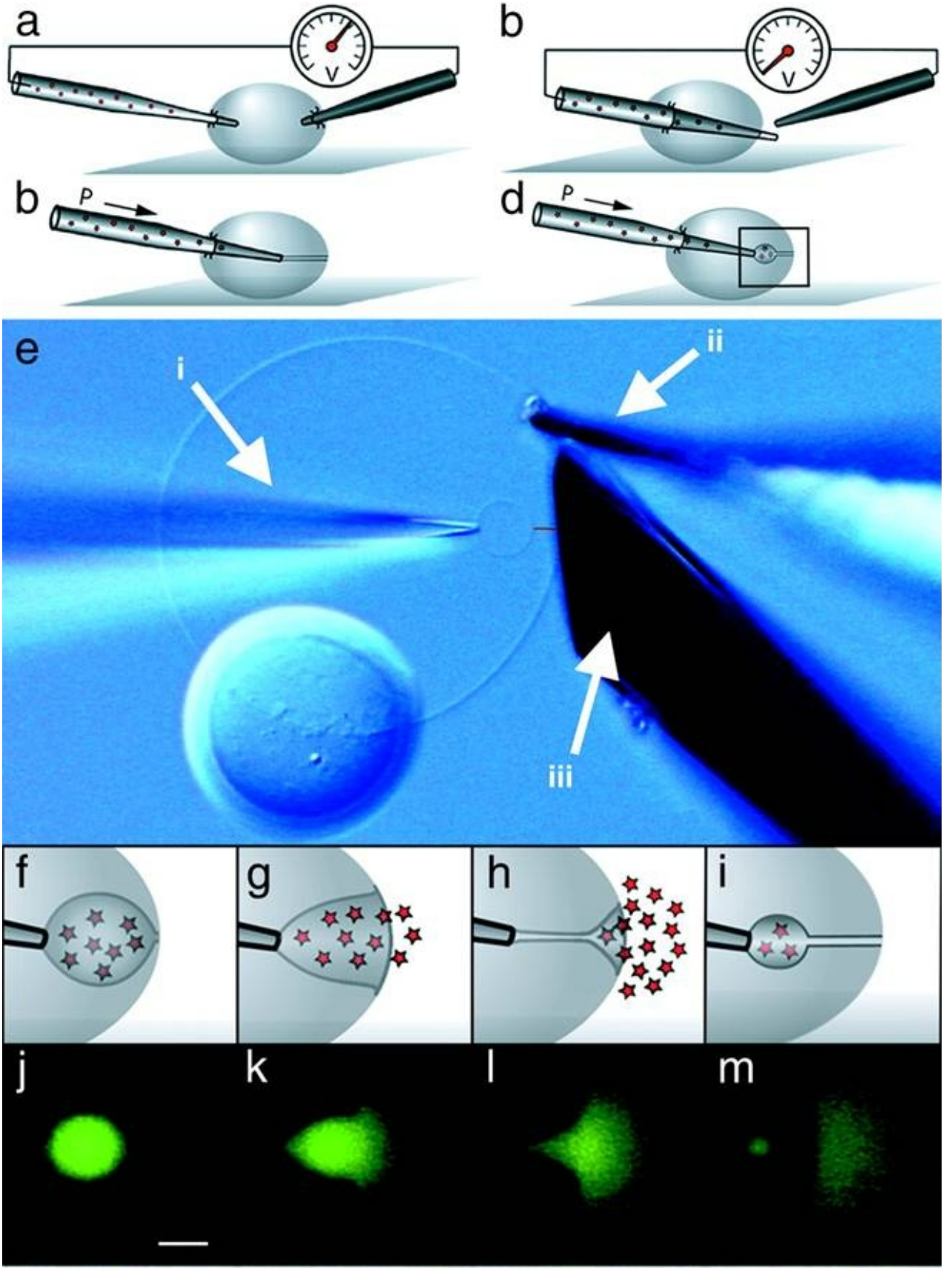
a
V
b
b
P
d
P
e
i
ii
iii
f
g
h
i
j
k
l
m

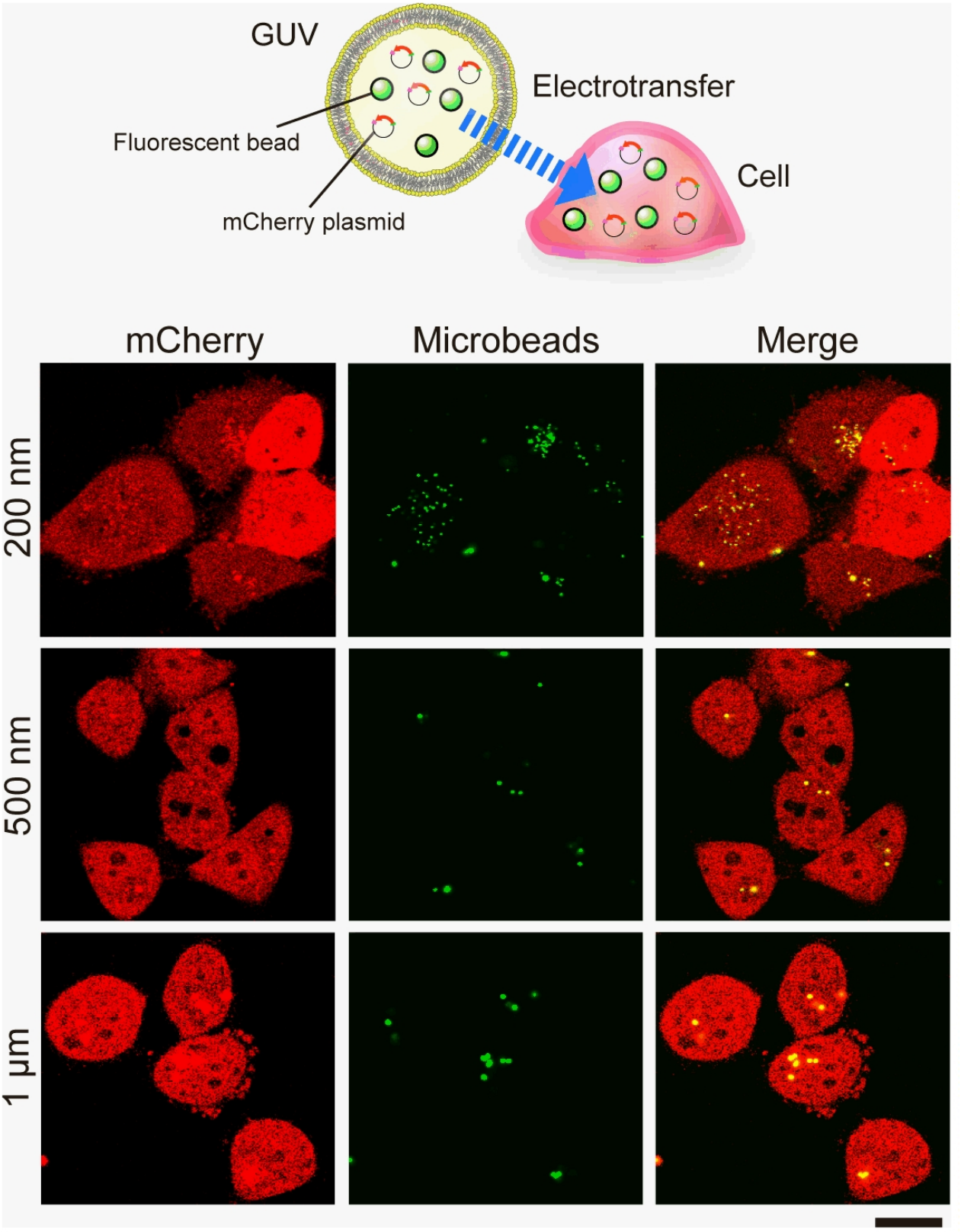
GUV
Fluorescent bead
mCherry plasmid
Electrotransfer
Cell
mCherry
Microbeads
Merge
200 nm
500 nm
1 µm

1) Culture cells on a glass coverslip in cell culture medium

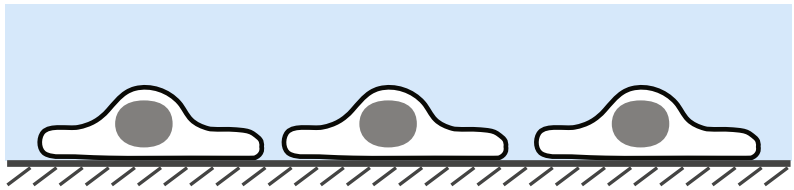

2) Preincubate in serum free medium supplemented with PEG

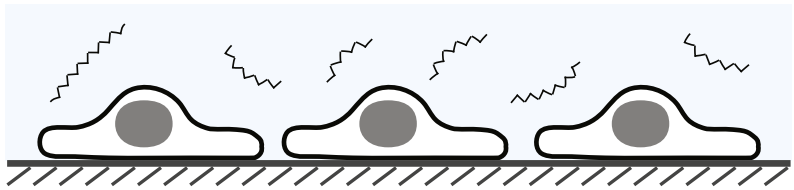

3) Add GUVs made from lipids & labeled lipids

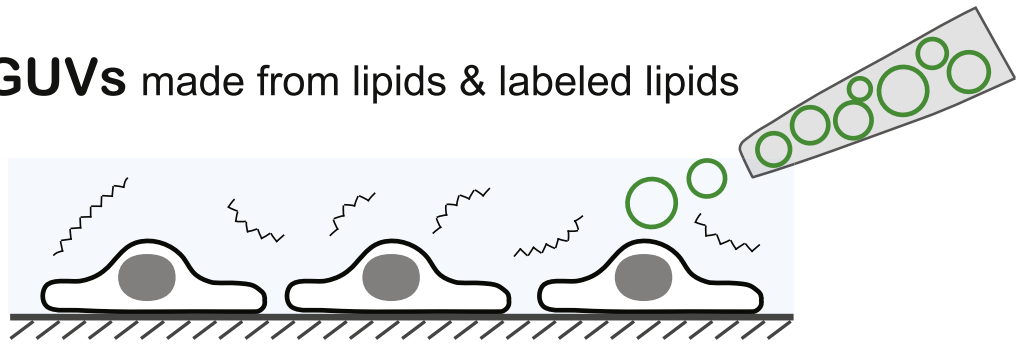

4) Incubate with GUVs (allow GUVs to settle on cells)

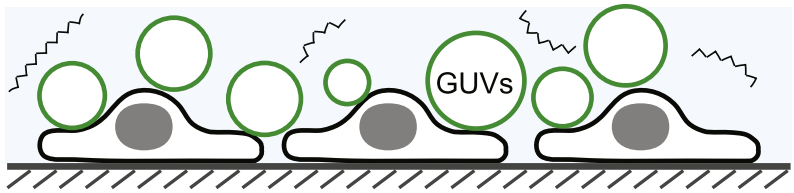

5) Electroporate on coverslip

6) Wash with cell culture medium

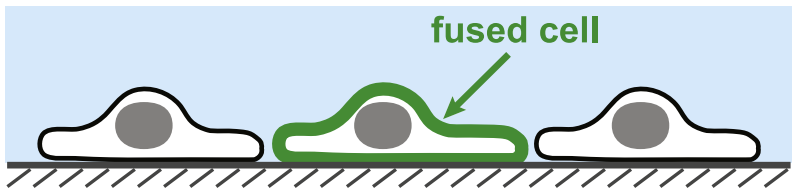

assay for incorporation of labelled lipids

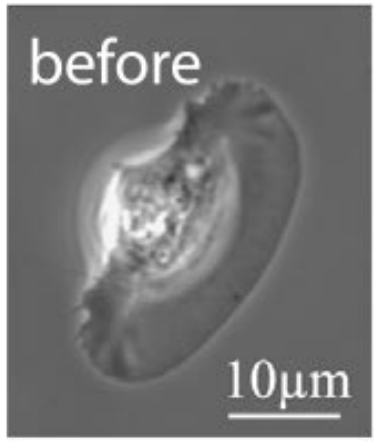

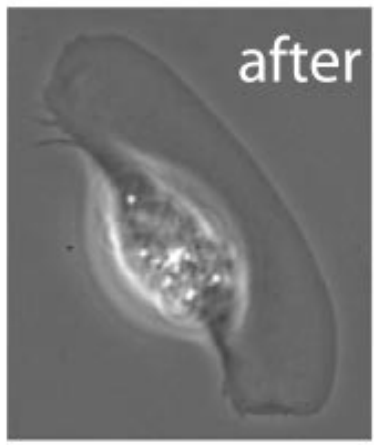

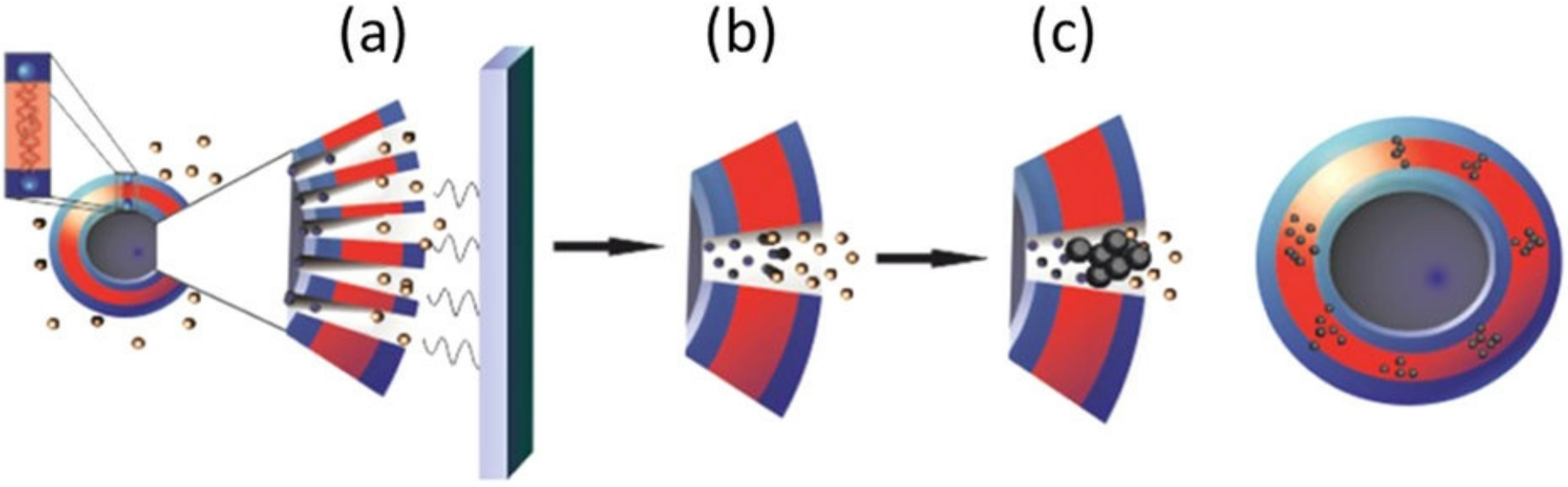
(a)
(b)
(c)

Highlights

- Lipid vesicle is an important model for studying biological cells in electric field.
- The intriguing responses of vesicles to electric pulses are discussed.
- There is a need to increase the complexity of vesicles as model cell systems.
- Electric field is a versatile method for manipulating lipid vesicles.
- Overview of vesicle electroporation in biomedical application is provided.